Theory Dependence in Sensitivity Studies of Dark Pion Searches at the LHCb

Ploeg, Marco van der

Theory Dependence in Sensitivity Studies of Dark Pion Searches at the LHCb

Theory Dependence in Sensitivity Studies of Dark Pion Searches at the LHCb

Marco van der Ploeg

Instituut-Lorentz, Leiden University
P.O. Box 9500, 2300 RA Leiden, The Netherlands

January 23, 2024

Abstract

One of the greatest remaining puzzles in physics is what particle dark matter consists of. For this project, the theory of dark pions is considered, a Hidden Valley model that extends the Standard Model with new, dark particles and a new force, dark QCD. A sensitivity study is performed to determine how many dark pions are expected to be in acceptance of the LHCb detector for Run 2 conditions; the LHCb is well-suited to search for particles in the considered $\mathcal{O}(1)$ GeV mass and $\mathcal{O}(1)$ - $\mathcal{O}(100)$ ps lifetime range. Additionally, a framework has been developed to study the dependence of the sensitivity on a number of theoretical parameters of the dark QCD model, namely the probability to form a dark vector meson instead of a dark pion, the number of colours in dark QCD, the dark QCD scale, and the Higgs mass. It is found that $\mathcal{O}(100)$ dark pions are in LHCb acceptance for different track categories, and that the considered theoretical parameters do not drastically change the number of expected particles (with some small caveats), staying within a difference of about 20%. This is acceptable given the expected experimental uncertainty, showing theory independent searches for dark pions are possible.

Contents

Chapter 1

Introduction

One of the largest unsolved problems in physics is the identity of dark matter (DM): what particle is dark matter made of? The existence of DM particles is hardly up for debate anymore; there are plenty of independent astrophysical observations pointing towards a new particle that needs to be added to the Standard Model (SM). Chief among these are firstly the bullet cluster [5], where a discrepancy is found between the location of visible matter (based on emitted X-ray measurements) and the location of gravitating matter (based on gravitational lensing measurements); and secondly the formation of cosmic structures, which would not be possible, within the amount of time in which it happened, without dark matter forming the gravitational wells that attract visible matter and allowed the visible matter to start forming structure (see [18] chapter 27). Other observations include rotation curves (of both starts in galaxies and galaxies in clusters) and measurements of the cosmic microwave background anisotropies.

To explain the astrophysical observations, the DM particle needs to be massive, electromagnetically neutral, stable (on cosmological time scales of at least the age of the universe) and must not (or at most very weakly) interact with itself (see [18] chapter 27). The problem is that we don't know what this DM particle is, specifically, as it has never been observed. There are a number of theoretical models, like WIMPS, axions, dark photons and sterile neutrinos (see [18] chapter 27). In this thesis, we will consider yet another model, namely the theory of the dark pion ($\hat{\pi}$) [4]. Here the SM is extended by a so-called dark sector with new particles. The nice thing about this theory is that it can be tested, by making use of its different portals, through which the dark particles can mix with the SM particles. One interesting portal is the Higgs portal, through which the Higgs boson can oscillate into a dark Higgs boson. This is of interest because the measured branching ratio of the Higgs boson to invisible particles has an

upper bound of 18% at the 95% confidence level [6], while the expected branching ratio for this from the SM is only about 0.1%, from the decay $H \rightarrow ZZ^* \rightarrow 4\nu$ [17]. Thus, possibly, some Higgs bosons have turned into dark Higgs bosons, explaining where those missing ones went. Then after the dark pion is formed through some dark process, it can decay back into SM particles through the same Higgs portal, making it possible to detect its signature.

There is a possibility that this signature can be found using the LHCb detector, at the LHC at CERN. This is mainly because the LHCb was originally designed to detect long-lived hadrons containing *b* and *c* quarks (hence its name). Now the dark pion, among other exotic beyond the SM particles, is considered to be a Long-Lived Particle (LLP). An LLP is a particle with a relatively long lifetime, which in the context of collider physics means that the particle is able to travel a measurable distance, of at least the order of millimetres, before decaying. Thus due to its design, the LHCb is also able to detect LLPs in a similar range of lifetime and mass as the long-lived hadrons [10].

In this thesis, the first goal is to do a sensitivity study at the generator level, of how many dark pions can be expected to be found with the LHCb detector, for a range of dark pion masses and lifetimes. This is done using simulations of the dark pion model, starting at the decay of the dark Higgs boson. In this model a number of different theoretical parameters have to be set. The second goal of this thesis is then to determine how much the expected number of dark pions changes when these parameters are varied, and by extent, whether it is possible to perform an analysis of real data independently of the values of these parameters. The parameters that will be varied are the probability to form a dark vector meson (instead of a dark scalar meson), the number of colours in dark QCD, the dark QCD scale $\tilde{\Lambda}_{QCD}$, and the Higgs mass. These will be discussed in more detail in the theory section.

We will start by going through the theory behind dark pions and our dark QCD model in more detail, as well as why the LHCb is well-suited to search for the dark pion, in Chapter 2. Then the methods used in this project, including simulation details, applying cuts, finding expected Run 2 values, making comparisons, and reweighting, are described in Chapter 3. The results of this are shown in Chapter 4 and discussed in Chapter 5, where we also give an outlook. Finally we conclude in Chapter 6.

Chapter 2

Theory

In this chapter the theory of Hidden Valley models, and of dark pions specifically, is discussed, as well as the parameters used in the dark pion theory for this project. The capabilities of the LHCb detector that make it useful for searching for dark pions are also shown.

2.1 Hidden Valley models

The theory of dark pions is part of a larger class of models, known as Hidden Valley (HV) models [22]. In these models, the SM is extended by a number of new light particles (called v-particles, with v for valley). These are charged under a new force, represented by a new non-abelian gauge group G_v which is added to the SM gauge group. At high energies, interactions between the SM particles and v-particles may be allowed when there is for instance a new particle that is charged under both the new and SM charges. Additionally, the v-particles may form (G_v neutral) "v-hadrons". These could then either be stable, making them a DM candidate, or decay with short or long lifetimes.

In order to simulate a dark sector, we use Pythia code, and specifically the Hidden Valley module, which simulates a general model described in [3]. This model allows for different portals, of which we will use the SM mediator gauge boson scenario, with the Higgs boson as mediator (motivated by the invisible Higgs decays mentioned before), as well as a "Higgs-like" boson mediated scenario, where another massive (undiscovered) boson, that is equivalent to the Higgs but has a different mass, couples to both SM and dark sector particles. To access the dark sector, the Higgs(-like) boson oscillates to its dark equivalent, denoted $\hat{h}$. The mediator particle then decays to 2 dark quarks (equivalent to the general v-particles), denoted q_v, which only carry the dark charge. The dark

quarks may emit dark gluons, denoted g_v, the gauge bosons of the G_v group. We will only consider scenarios where G_v contains an unbroken $SU(N_c)$ factor, for N_c the number of dark colours, meaning the dark gluon will be massless, giving a dark QCD-like force (hence the names).

Then like SM QCD, the dark quarks can start a dark shower: they will emit dark gluons, and the dark gluons can create q_v pairs or split into g_v pairs, which can then repeat this process. So in the end, many dark quarks are formed out of one dark Higgs(-like) boson. Now eventually the dark quarks will hadronise into dark hadrons.We only consider dark QCD with $N_f = 1$ flavour, with a single spin $\frac{1}{2}$ dark quark. With these the possible dark hadrons we consider are two mesons, one with spin 0 which is the dark pion, denoted $\hat{\pi}$, and one with spin 1 which is the dark rho, $\hat{\rho}$. The dark rho then exclusively decays into a pair of dark pions, but only if it has a large enough mass, so if $m(\hat{\rho}) \geq 2m(\hat{\pi})$. In the end we thus have many dark pions originating from a single dark Higgs(-like) boson. These are created in two jets, one for each initial dark quark, because of the QCD-like force. A sketch of the dark shower, from the Higgs boson to the dark pions, can be seen in figure 2.1.
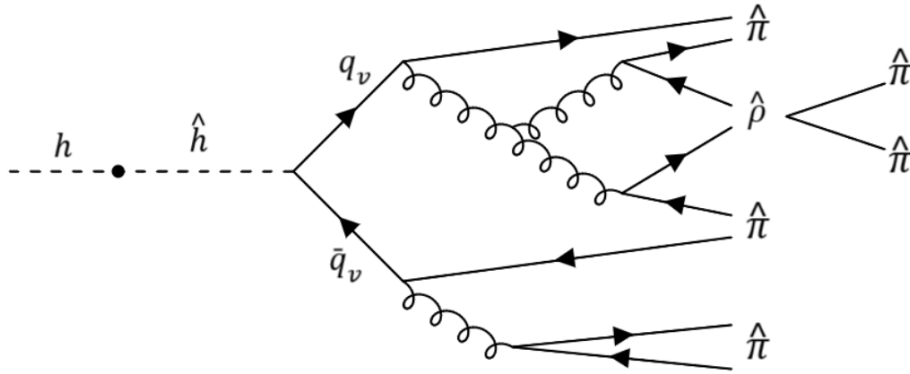
Figure 2.1: *A sketch of the dark shower as considered in this thesis. First the dark sector is accessed by a Higgs boson oscillating into a dark Higgs boson, which then decays to two dark quarks. These emit dark gluons, which split into more gluons or form new quarks pairs; this process continues until hadronisation into dark pions or dark rho's. The dark rho decays into two dark pions, so that only dark pions are left in the end.*

Finally, the dark pion is able to decay back into SM particles. It leaves the dark sector with the same Higgs(-like) dark mediator[*]. The possible decay modes are described in the dark pion theory, in the next section.

---

[*]Technically this decay is not allowed since the Higgs is heavier than the dark pion, but it can happen here through a tunnelling process. The details of this are beyond the scope of the project, but it is a suppressed process, leading to the dark pion being long-lived.

2.2   The theory of dark pions

Let us now look at the theory of dark pions specifically, as described in [4], to see how they decay back to the SM. In this paper, the dark pion exists due to chiral symmetry breaking of the flavour symmetry group $SU(N_f)_L \times SU(N_f)_R$, which is expected when $N_f \geq 2$ (and $N_f \lesssim 4N_c$ to remain below the conformal window so quarks can be confined), giving rise to $N_f^2 - 1$ pseudo-Nambu-Goldstone bosons (pNGB's)[†]. Analogous to the SM where pions are pNGB's, the pNGB's created here are dark pions.

Then we have the decay of the dark pion to SM particles. The specific branching ratio (BR) of each decay mode of the dark pions depends on its mass. A plot of the BR's of dark pions can be seen in figure 2.2.

From all of these, we will specifically consider the decay

$$\hat{\pi} \to K_S^0 + K^- + \pi^+, \tag{2.1}$$

(and its anti-channel) followed by

$$K_S^0 \to \pi^+ + \pi^-. \tag{2.2}$$

As can be seen in figure 2.2, the BR for the first decay is about 0.1 for masses above 1.5 GeV. The BR for the second decay is 0.692, and the mean lifetime of K_S^0 is 89.54 ps (see [18] Meson summary table, page 40). This decay mode was chosen because the BR is relatively flat in the mass range above 1.5 GeV (which we will consider), simplifying calculations. Additionally, this is the decay mode with (by far) the highest BR of which all final particles are charged (the π^0 in the most dominant decay mode decays primarily to photons); we want them to be charged because these are more easily detectable. There is also no problem in having both kaons and pions as final particles, since the LHCb detector is able to distinguish these quite well (which will be discussed more in section 2.4).

[†]Assuming the reader is familiar with Nambu-Goldstone bosons (or simply Goldstone bosons), which appear when spontaneous symmetry breaking occurs, the pseudo boson is created similarly but is massive instead of massless. This happens when the symmetry in question is not only broken spontaneously but also explicitly; that is, a term (often a mass term) is added to the equations describing the system so that the equations themselves are no longer symmetric either.

Figure 2.2: *The branching ratio of the dark pion as a function of its mass, for various decay modes, as predicted by the theory of dark pions. Figure taken from [4].*

One note to this section is that only the $N_f = 1$ case is considered in this thesis, while the dark pion paper performs calculations for $N_f \geq 2$. This does not matter too much however. For us, the $\hat{\pi}$ exists due to a broken $U(1)$ flavour symmetry group. Regarding the decay mode and its BR, it is expected that the same hierarchy of BR's holds for $N_f = 1$, and that the BR is of the same order of magnitude, so that they can still be used here.

2.3   Parameters of the dark pion theory

Within the Hidden Valley module of Pythia, there are a number of parameters that can be set. In this section, we will discuss the important ones for this project, and what their physical meaning is. The documentation of the code which shows all parameters can be found in [20]. Specific settings of parameters in our simulations and how certain parameters will be varied is discussed in section 3.1.

To start, we set the mass and the decay mode of the dark Higgs boson. As discussed, the dark Higgs decays to two dark quarks, with a 100% BR. To consider scenarios with a different Higgs-like mediator, the Higgs mass is changed; this mediator thus acts in the same way as a Higgs boson would, but has a different mass.

Next, one may set the number of flavours of the dark QCD model. We will

use $N_f = 1$ flavour, which is the simplest case, as adding more dark quarks allows many more hadrons to be formed and so quickly complicates things. Additionally, the dark quark is set to be its own antiparticle.

Next for hadronisation, we can set the probability for the dark quarks to form a $\hat{\rho}$ instead of a $\hat{\pi}$. For both these mesons the mass, lifetime and decay modes have to be set. Since the q_v is its own antiparticle, so are the $\hat{\pi}$ and $\hat{\rho}$.

The dark QCD interaction strength depends on the coupling strength, which we can change with the final state radiation coupling α_{FSR}. This determines how likely interactions like the dark quark emitting a dark gluon and the dark gluon splitting are: as α_{FSR} increases, so does the probability of interaction. Note that α_{FSR} does not give the full coupling strength, denoted by α_v, as this also depends on the order at which α_v runs; only for zeroth order $\alpha_v = \alpha_{\text{FSR}}$.

The influence of the number of colours N_c is on the interactions as well. The charge C_F of the dark quarks is set to be 1 if $N_c = 1$, and $C_F(N_c) = \frac{N_c^2 - 1}{2N_c}$ otherwise. Shower branchings such as $q_v \to q_v + g_v$ have this factor of C_F enhancing their coupling constant (so it is proportional to $C_F \alpha_v$). Additionally, the $g_v \to g_v + g_v$ branching has a factor of N_c enhancing its coupling constant (so it is proportional to $N_c \alpha_v$). These factors represent that it is easier for radiation to interact if there are more colours.

Lastly, the dark QCD scale $\tilde{\Lambda}_{\text{QCD}}$ can be set. Physically, it is the energy scale around which quarks are able to confine into hadrons. It is thus one of the things that influences when hadronisation can start at the end of the dark shower. It is also used to calculate the coupling strength for the case of a running α_v.

2.4 Finding dark pions with the LHCb detector

At the LHC, the dark pion may be found by investigating the decays of the Higgs bosons that are created in the proton-proton (pp) collisions. It is here that the measurements of the invisible branching fraction of the Higgs were performed, so there could have formed dark Higgs bosons, and subsequently dark pions and their detectable SM decay products may be present.

We will consider the conditions from Run 2 of the LHC, which ran between 2015 and 2018, where the pp collisions had a center-of-mass energy of $\sqrt{s} = 13$ TeV. Specifically, we investigate using the LHCb detector, a single-arm spectrometer with a cone-like shape in the forward direction which covers a pseudorapidity[‡] range of $2 < \eta < 5$ [7]. The corresponding angular range of the cone

---

[‡]This is essentially a measure of the angle θ a particle's trajectory makes with the beamline, $\eta = -\ln(\tan(\theta/2))$.

is $0.77° < \theta < 15°$. The layout of the detector can be seen in figure 2.3. From all the data it collected, it has a total integrated luminosity[§] of 5.7 fb^{-1} [7].

There are a number of advantages to using the LHCb detector, which are unique to this detector. Firstly, it is able to measure masses with a resolution of order 1 to 100 MeV, depending on the decaying particle and decay channel (see [7]). Secondly, it can precisely reconstruct the tracks and momenta of charged particles, using the VErtex LOcator (VELO), Tracker Turicensis (TT), Inner Tracker (IT) and Outer Tracker (OT) detectors in combination with the magnet [9]. The IT and OT consist of three parts which are located in the three components T1, T2 and T3 in figure 2.3; here the IT is placed close to the beam while the OT is further away. Collectively, these are called the T stations. Thirdly, it has two ring-imaging Cherenkov (RICH) detectors that can be used for particle identification (PID) [9], which we use to distinguish pions from kaons. These measure the Cherenkov radiation emitted by the particles, from which one can determine their velocity; combining this with momenta measurements allows one to identify different particles by their masses. Because of this detector, LHCb is able to distinguish between protons, pions and kaons, unlike other LHC detectors like ATLAS and CMS.

Finally, there is the additional benefit for LLPs, such as the dark pion, as mentioned in the introduction, making LHCb perfect for searches for these particles with masses of the order of 1 GeV. The LHCb can detect LLPs because it is a forward detector, with all of its detectors placed on one side of the pp collision vertex (unlike other LHC detectors like ATLAS and CMS, which are shaped like barrels around the collision vertex). So if an LLP flies into the right direction and enters the detector, it will remain inside of it before it decays as well, allowing for its detection. A disadvantage is that large number of LLPs won't fly into the right direction, meaning those can never be detected.

The combination of these properties makes the LHCb detector capable of precisely measuring the properties of the kaons and pions that result from the dark pion decay, making it possible to search for them.

[§]In scattering physics, the luminosity is understood to be the number of particles detected within a certain amount of time divided by the cross-section. The integrated luminosity is this quantity integrated over the total measuring time. The relation between the total detected amount of particles N_i of species i with cross-section σ_i and integrated luminosity L_{int} is thus $N_i = L_{\text{int}} \sigma_i$.
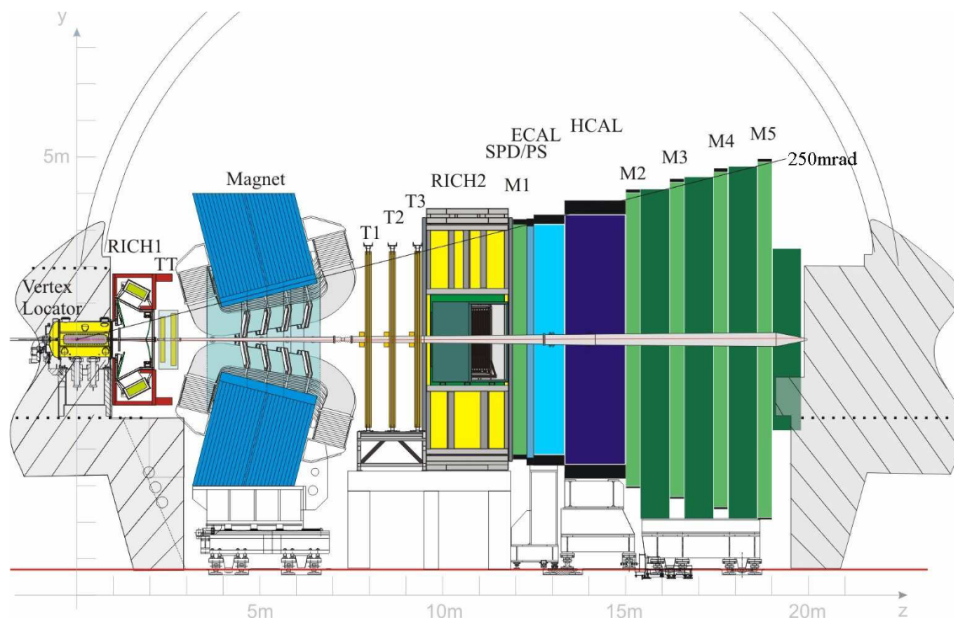
Figure 2.3: *A view of the LHCb detector in Run 2. Figure taken from [9].*

Chapter 3

Methods

In this chapter, the simulations and code used to obtain the data, as well as specific parameters that are kept constant and varied, are presented. We also discuss the various steps of the analysis: applying cuts, rescaling to expected Run 2 values, comparing different scenarios with the baseline and reweighting lifetimes. Additionally, a way of indicating the total sensitivity of the LHCb is presented.

The code used to implement these methods and obtain the result can be found in the Gitlab repository of this dark pion study.

All of the methods described in this chapter have been automated into one framework, organised with a Snakemake pipeline [15]. This can be used to generate the results for any set of input parameters, so that any model can be tested easily.

3.1 Simulation details

To start, the decays under consideration need to be simulated. This is done using the LHCb simulation framework Gauss version 56r3 [8, 13]. This uses the Hidden Valley module [16, 20] to simulate the dark pion model in Pythia 8 [2], which is used to generate the high-energy-physics pp collision events.

The simulation begins with requesting a number of dark Higgs bosons to be simulated; each of these will be called a unique event. The state of the dark Higgs, like its momentum, is determined from the pp collisions from which they originate. The dark Higgs consequently decays into a number of dark quarks. These then either form a dark pion, or the heavier dark rho which in turn decays to the dark pion. Finally the dark pion decays to kaons and pions as in equations 2.1 and 2.2. In the simulation, the BR of the dark pion decay

([2.1](#)) is set to 1, which saves computational resources. The real BR of 0.1 is applied in the analysis by randomly taking 10% of all produced dark pions. For the K_S^0 decay, the actual BR of approximately 0.69 is used. The number of events to be simulated is set to 100,000. These are split into 40 subsets of 2,500 events, which are each generated with a different random seed, to ensure the generated events are independent. This is done using the Stoomboot computer cluster of Nikhef.

3.1.1 Constant parameters

Different properties of the dark pion are considered, each of which requires its own simulation. Simulations are performed with dark pion lifetimes of 1, 5, 10, 50, 100, 500, 1000, 5000 and 10000 ps, and masses of 1.5, 1.75, 2.0, 2.25, 2.5, 2.75 and 3.0 GeV, giving a total of 63 different simulations.

In the Hidden Valley module, relevant fixed parameters are:

- The number of flavours, which, as noted before, will be set to $N_f = 1$.

- The final state radiation coupling is $\alpha_{\text{FSR}} = 0.7$.

- The dark quark mass is set to 1 GeV.

- In case that the $\hat{\rho}$ is produced, its mass is set to 2.5 times that of the dark pion, $m(\hat{\rho}) = 2.5 m(\hat{\pi})$, and its lifetime is set to 0 so it decays promptly.

All these parameters are the same for each run that has different theory parameters varied.

3.1.2 Varied theory parameters

We will consider different scenarios, each of which varies one parameter relative to a baseline model. In the baseline model, the parameters are as follows:

- The probability to form a $\hat{\rho}$ is zero, all dark quarks hadronise into dark pions.

- The number of dark colours is $N_c = 3$.

- The dark QCD scale is $\tilde{\Lambda}_{\text{QCD}} = 4$ GeV.

- The Higgs mass has its SM value of 125 GeV.

There is no strong motivation to choose these specific parameters as the baseline, but they are also not random. Taking 3 colours is analogous to SM QCD, and the SM Higgs mass can be motivated by the measured invisible BR of the Higgs. The dark rho probability can in the end be absorbed into the BR of the dark pion decay mode, so it is mostly an empirical parameter; taking it to be 0 here and changing it below does allow us to find out its theoretical influence. Other parameters (including fixed ones) are chosen so that the hierarchy of parameters is similar to SM QCD, but the details of this are beyond the scope of this thesis.

Now the different scenarios are the following:

- The dark rho scenario, where the probability to form a $\hat{\rho}$ is changed from zero to one, so all dark quarks hadronise into dark rho's. Varying it like this makes its influence the most visible.

- The dark colour scenario, where the number of dark colours is changed from 3 to 2. It is varied like this because 2 colours is technically simpler than having 3, so it is a natural possibility. It also does not seem reasonable to have many more colours than 3, so a small change like this should allow us to say something about what happens when N_c is increased to e.g. 4 as well.

- The dark QCD scale scenario, where the dark QCD scale is changed from 4 GeV to (1) 2 and (2) 8 GeV. Here a hypothesis of what happens when increasing or decreasing the parameters is hard to make, so we check both. It cannot be varied too much as this would affect hadronisation drastically.

- The Higgs mass scenario, where the mass of the Higgs boson is changed from 125 GeV to (1) 500 GeV, (2) 50 GeV and (3) 1250 GeV. Here the dark mediator becomes a Higgs-like boson. As a Higgs-like boson has not been observed, we consider a large mass range, with the 1250 GeV mass at the edge of what can be detected at the LHC.

3.2   Selection

After the simulation has been run, it is necessary to consider the physical limitations of the LHCb detector: it can only detect particles that have not flown outside of the detector, that have the right pseudorapidity range, and that have a high enough momentum to ensure proper tracking and PID efficiency. To account for this, cuts are applied on the simulation results, to select the particles within LHCb acceptance.

One remark on the chosen cut ranges is that these are not chosen with great precision. If one does want to simulate the detector properly, there is LHCb software available to do so. For this generator-level sensitivity study however, the goal is to find if any dark pions can be expected at all, instead of trying to exactly predict the number of expected particles; for this purpose, the following cutting method should suffice.

3.2.1   Track types

Here we need to consider different track types: particles may follow different paths before hitting a certain detector. All possible track types in LHCb can be seen in figure 3.1. The paths that particles followed are reconstructed using information from all the detectors present in the track type. The ones considered in this thesis are the long track and the downstream track. In order to reconstruct the long track, particles must be detected in the VELO and the T stations; to reconstruct the downstream track, particles must be detected in the TT and the T stations [21]. With these tracks, we look at the following categories, based on which particles follow which track:

- Long category (LLLL), where the $\hat{\pi}$ and its decay products are reconstructed in the long track.

- Partial downstream category (LLDD), where the K_S^0 and its decay products (π^+ and π^-) are reconstructed in the downstream track, while the $\hat{\pi}$ and its other decay products (K^- and π^+) are reconstructed in the long track.

- Full downstream category (DDDD), where the $\hat{\pi}$ and its decay products are reconstructed in the downstream track.

The four letters here are based on where each of the charged particles are reconstructed. It is useful to consider the LLDD category, because the K_S^0 has a lifetime of 89.54 ps, making it a long-lived hadron. It is thus to be expected that there will be cases where the dark pion does decay in VELO, but K_S^0 does not, and so we should try to reconstruct it with the downstream track and its detectors that are placed further back from the VELO.

3.2.2   Cutting ranges

As each track category uses different detectors, the cuts on the positions of particles will differ for each. We will talk about these positions in cylindrical coordinates R and z (due to rotational symmetry θ is irrelevant), with the axis on

the beamline, and $z = 0$ around the pp collision vertex. We look at the position of the particle at the moment it decayed and was created, indicated by 'decay' and 'origin' subscripts. So 'decay' applies to the $\hat{\pi}$ and K_S^0, and 'origin' to all particles involved (for the initial position of the $\hat{\pi}$ it's taken into account that it comes from the Higgs decay).
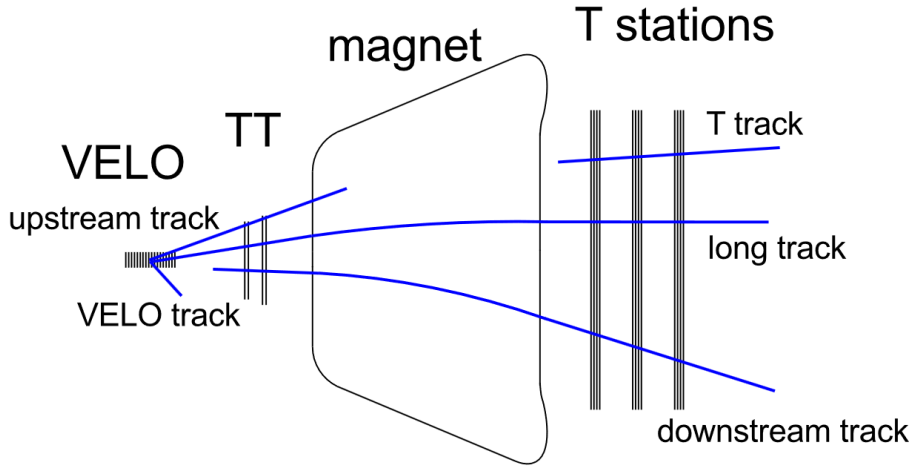
Figure 3.1: *A schematic overview of the different track types in LHCb. Figure taken from [21].*

For the long track, the cuts on the particle's position are chosen to be R_{origin}, $R_{\text{decay}} < 30$ mm, and -100 mm $< z_{\text{decay}} < 600$ mm. The z cut was chosen to be well within the VELO, based on the map of the VELO detector shown in figure 3.2. The R cut was chosen based on where there is good vertex reconstruction efficiency, which has been determined using Monte Carlo simulations of the detector by previous collaborators of this project.

Similarly for the downstream track, the particles need to decay within the TT. The cuts for this are chosen to be R_{origin}, $R_{\text{decay}} < 1300$ mm and 600 mm $< z_{\text{decay}} < 2200$ mm. The lower z bound is based on where the VELO ends, and the upper bound on the location of the TT at $z = 2350$ mm (see table 1 in [14]); we require the particle to decay before going past the TT, and then the decay products fly into it. The R bound is based on the size of the TT's shortest side $R = 1311$ mm (see figure 5.19 in [9]).

Next, the cuts in pseudorapidity and momentum are the same in each track[*]. These are applied to the charged particles that need to be detected, since detection requires these particles to be within the angular acceptance of the de-

---

[*]Actually, there is a small difference in the efficiency for each track so that they require different momentum cuts, but this is negligible for our purposes.

tectors, and requires the momentum to be high enough for proper track reconstruction and PID. As mentioned before, we need $2 < \eta < 5$ for the pseudorapidity [7].
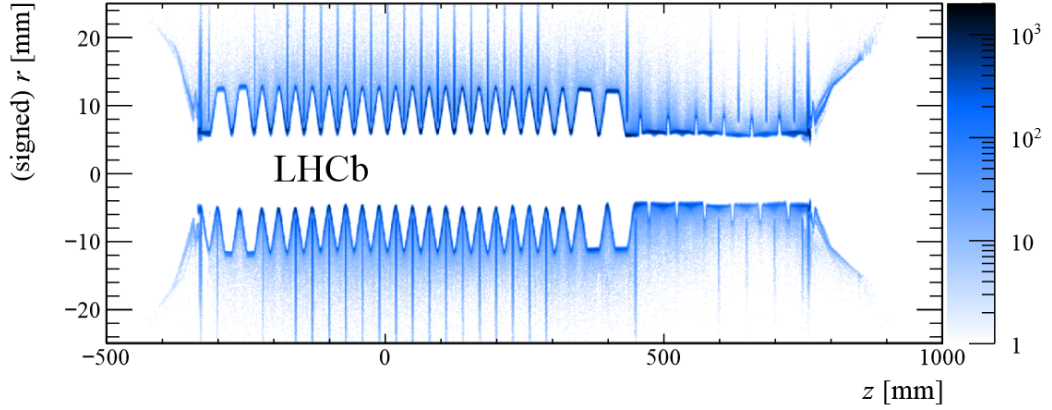
Figure 3.2: *A map showing the size of the VELO. Figure taken from [12].*

For momentum, the cut for PID eficiency is different for the final pions and the kaon, because it is easier to identify the pions with the RICH detector, as they have a lower mass and so a lower momentum threshold to reach a speed high enough for Cherenkov radiation. Based on the PID efficiency as shown in figure 3.3, we take the cut for the kaon to be $5\ \mathrm{GeV} < P_{\mathrm{total}} < 95\ \mathrm{GeV}$, to have a PID efficiency above 80% based on the loose cuts. The loose cut was chosen to retain more signal; the 80% minimum to ensure a large efficiency, while not cutting out all particles which are misidentified, as some of the particles that are cut out with low efficiency will be correctly identified anyway, so we should try to make up for that. For pions, there is no cut needed here.
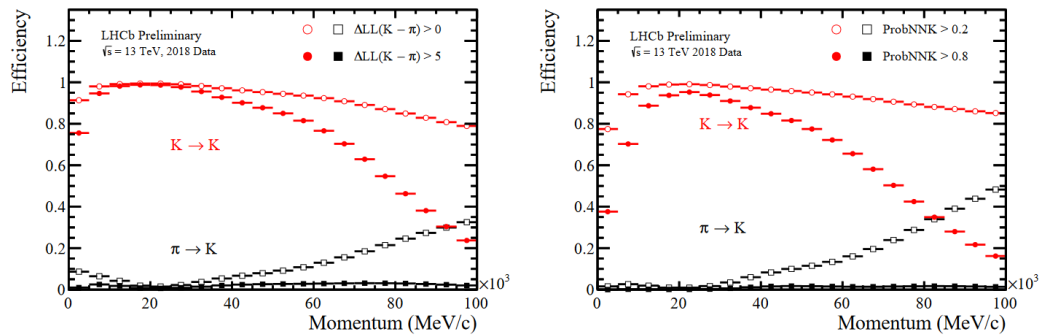
Figure 3.3: *The PID efficiency as a function of total momentum for kaons, with loose and tight cuts, based on 2018 LHCb data. Figure taken from [19], figure 4; see also this paper for the definition of the ΔLL and* `ProbNNK` *variables.*

The cut for tracking efficiency is also different for the pions and kaon, as again the efficiency for the pions does not need to be as large due to the other available methods. For pions, this cut requires $P_T > 250$ MeV and $P_{\text{total}} > 5$ GeV based on figure 3.4 to have an efficiency above 50%, which is deemed good enough for the pions. For the kaon however, we require $P_T > 250$ MeV and $P_{\text{total}} > 10$ GeV, also based on figure 3.4. This way the efficiency for P_{total} is above 80% as well.
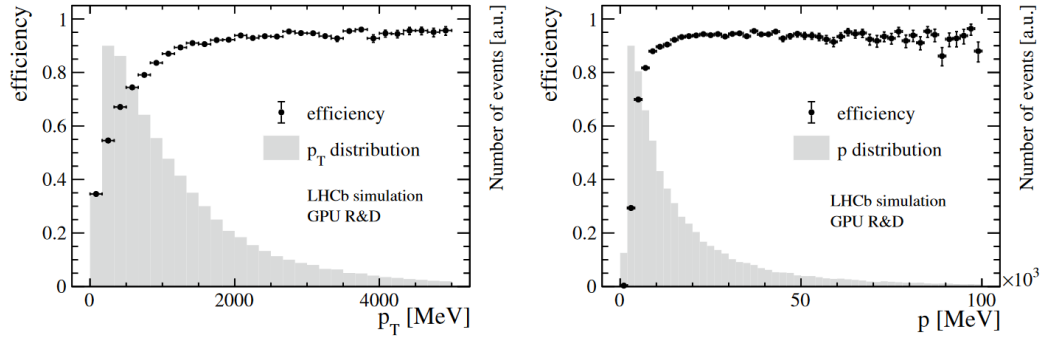
Figure 3.4: *The tracking efficiency (and the momentum distribution) as a function of transverse and total momentum for LHCb. Figure taken from [1] figure 6 (e,f).*

The combination of the momentum cuts for both PID and tracking efficiency gives us the final cuts on momentum that will be used. An overview of all the cuts applied to each particle for each track category can be seen in table 3.1.

To summarise, the cuts are:

- For the long track, $R < 30$ mm and -100 mm $< z < 600$ mm. Applied to decay and origin position of relevant particles.

- For the downstream track, $R < 1300$ mm and 600 mm $< z < 2200$ mm. Applied to decay and origin position of relevant particles.

- For all charged particles, $2 < \eta < 5$ and $P_T > 250$ MeV.

- For the pions, $P_{\text{total}} > 5$ GeV (for 50% efficiency).

- For the kaon, 10 GeV $< P_{\text{total}} < 95$ GeV (for 80% efficiency).

Particle(s)	LLLL	LLDD	DDDD
$\hat{\pi}$	$R_{\text{origin}} < 30$ mm $R_{\text{decay}} < 30$ mm -100 mm $< z_{\text{decay}} < 600$ mm	$R_{\text{origin}} < 30$ mm $R_{\text{decay}} < 30$ mm -100 mm $< z_{\text{decay}} < 600$ mm	$R_{\text{origin}} < 1300$ mm $R_{\text{decay}} < 1300$ mm 600 mm $< z_{\text{decay}} < 2200$ mm
$\hat{\pi}$ child π^+	$2 < \eta < 5$ $P_{\text{total}} > 5$ GeV $P_T > 250$ MeV $R_{\text{origin}} < 30$ mm	$2 < \eta < 5$ $P_{\text{total}} > 5$ GeV $P_T > 250$ MeV $R_{\text{origin}} < 30$ mm	$2 < \eta < 5$ $P_{\text{total}} > 5$ GeV $P_T > 250$ MeV $R_{\text{origin}} < 1300$ mm
$\hat{\pi}$ child K^-	$2 < \eta < 5$ 10 GeV $< P_{\text{total}} < 95$ GeV $P_T > 250$ MeV $R_{\text{origin}} < 30$ mm	$2 < \eta < 5$ 10 GeV $< P_{\text{total}} < 95$ GeV $P_T > 250$ MeV $R_{\text{origin}} < 30$ mm	$2 < \eta < 5$ 10 GeV $< P_{\text{total}} < 95$ GeV $P_T > 250$ MeV $R_{\text{origin}} < 1300$ mm
K_S^0	$R_{\text{origin}} < 30$ mm $R_{\text{decay}} < 30$ mm -100 mm $< z_{\text{decay}} < 600$ mm	$R_{\text{origin}} < 1300$ mm $R_{\text{decay}} < 1300$ mm 600 mm $< z_{\text{decay}} < 2200$ mm	$R_{\text{origin}} < 1300$ mm $R_{\text{decay}} < 1300$ mm 600 mm $< z_{\text{decay}} < 2200$ mm
K_S^0 children $\pi^+ + \pi^-$	$2 < \eta < 5$ $P_{\text{total}} > 5$ GeV $P_T > 250$ MeV $R_{\text{origin}} < 30$ mm	$2 < \eta < 5$ $P_{\text{total}} > 5$ GeV $P_T > 250$ MeV $R_{\text{origin}} < 1300$ mm	$2 < \eta < 5$ $P_{\text{total}} > 5$ GeV $P_T > 250$ MeV $R_{\text{origin}} < 1300$ mm

Table 3.1: *Overview of the cuts applied to each particle for each track category. The R and z are cylindrical coordinates, η is pseudorapidity and P_{total} and P_T are total and transverse momentum, respectively. Note that except in the LLDD track, the cuts on $\hat{\pi}$ and K_S^0 as well as those on the $\hat{\pi}$ and K_S^0 children are the same, except for the difference in P_{total} for pions and the kaon.*

3.3 Rescaling to Run 2

Once the number of dark pions that pass the cuts in the simulation is known, we would like to scale that number to the number of dark pions one would expect in LHCb in Run 2 of the LHC. This can be done by considering the number of dark Higgs bosons passing the cuts, since we can also estimate how many dark Higgs bosons there are in Run 2.

The total amount of Higgs bosons in Run 2 is found using the total integrated luminosity of $L_{\text{int}} = 5.7$ fb^{-1} [7] for LHCb, and the measured cross-section $\sigma_h = 56.9 \pm 3.4$ pb of the Higgs (this result is slightly outdated, but still used by us; the latest is 56 ± 4 pb from [18] p.1185, so it's very close still). Then

$N_{h,\text{Run2}} = L_{\text{int}}\sigma_h$. From this we estimate the number of dark Higgs bosons by using the observed branching ratio of the Higgs into invisible particles of 18% [6], so that

$$N_{\hat{h},\text{Run2}} = 0.18 N_{h,\text{Run2}} \approx 58 \cdot 10^3. \tag{3.1}$$

Note that this is technically an upper bound on the number of dark Higgs bosons, as not all invisible Higgs may end up as their dark counterpart.

Let us then derive the expected number of dark pions after cuts in Run 2. We denote the dark Higgs with $\hat{h}$, dark pion with $\hat{\pi}$, the number resulting from the simulation with 'sim' and in Run 2 with 'Run2', and numbers before cutting with 'uncut' and after cutting with 'cut'. We then have

$$N_{\hat{\pi},\text{Run2}}^{\text{cut}} = \frac{N_{\hat{\pi},\text{Run2}}^{\text{cut}}}{N_{\hat{h},\text{Run2}}^{\text{cut}}} N_{\hat{h},\text{Run2}}^{\text{cut}} = \frac{N_{\hat{\pi},\text{sim}}^{\text{cut}}}{N_{\hat{h},\text{sim}}^{\text{cut}}} N_{\hat{h},\text{Run2}}^{\text{cut}}, \tag{3.2}$$

where the first step is trivial, and in the second step we assume the ratio of dark pions and dark Higgs bosons is the same in the simulation and Run 2. We then also need to rewrite the cut number of dark Higgs in Run 2 to the uncut number that we know, so

$$N_{\hat{h},\text{Run2}}^{\text{cut}} = \frac{N_{\hat{h},\text{Run2}}^{\text{cut}}}{N_{\hat{h},\text{Run2}}^{\text{uncut}}} N_{\hat{h},\text{Run2}}^{\text{uncut}} = \frac{N_{\hat{h},\text{sim}}^{\text{cut}}}{N_{\hat{h},\text{sim}}^{\text{uncut}}} N_{\hat{h},\text{Run2}}^{\text{uncut}}, \tag{3.3}$$

where the first step is again trivial, and in the second step we assume the ratio of dark Higgs bosons after and before cuts is the same in Run 2 and the simulation. Substituting equation 3.3 into 3.2 finally gives

$$N_{\hat{\pi},\text{Run2}}^{\text{cut}} = \frac{N_{\hat{\pi},\text{sim}}^{\text{cut}}}{N_{\hat{h},\text{sim}}^{\text{cut}}} \frac{N_{\hat{h},\text{sim}}^{\text{cut}}}{N_{\hat{h},\text{sim}}^{\text{uncut}}} N_{\hat{h},\text{Run2}}^{\text{uncut}} = \frac{N_{\hat{\pi},\text{sim}}^{\text{cut}}}{N_{\hat{h},\text{sim}}^{\text{uncut}}} N_{\hat{h},\text{Run2}}^{\text{uncut}}. \tag{3.4}$$

All quantities in the final expression can be calculated, and so we can find the expected number of dark pions after cuts in Run 2: $N_{\hat{h},\text{Run2}}^{\text{uncut}}$ is the number in equation 3.1, $N_{\hat{\pi},\text{sim}}^{\text{cut}}$ can be counted after the cuts are applied, and $N_{\hat{h},\text{sim}}^{\text{uncut}}$ is simply the number of events that were simulated.

To calculate the standard deviation of the expected Run 2 number, we use that the error of the number of particles passing in the simulation is given by its square root, because the number of particles is Poisson distributed; that is, $\sigma_{\hat{\pi},\text{sim}} = \sqrt{N_{\hat{\pi},\text{sim}}^{\text{cut}}}$. The other quantities in equation 3.4 do not have an error[†].

[†]There is an experimental error on the Higgs cross-section, but we can neglect this, as it is relatively smaller than the error on the passing number.

Using first order error propagation, the standard deviation of the expected Run 2 number is

$$\sigma_{\hat{\pi},\text{Run2}} = \frac{\sigma_{\hat{\pi},\text{sim}}}{N_{\hat{h},\text{sim}}^{\text{uncut}}} N_{\hat{h},\text{Run2}}^{\text{uncut}} = \sqrt{\frac{N_{\hat{h},\text{Run2}}^{\text{uncut}}}{N_{\hat{h},\text{sim}}^{\text{uncut}}}} \sqrt{N_{\hat{\pi},\text{Run2}}^{\text{cut}}}. \tag{3.5}$$

3.3.1 Note on the Higgs mass scenario

There is one important note for the scenario where the Higgs mass parameter is varied. Here we cannot estimate the number of dark pions as derived above, because we consider the Higgs-like boson. Since it has a different mass, it will not be produced in the same amount as the Higgs boson at the LHC (if it is produced at all, that is). Exactly the fact that this new particle is not detected also means there is no measurement of how many of these are produced, nor of what percentage of them mixes with their dark counterpart. Thus a calculation like above using the Higgs boson is impossible.

Instead we will determine what the number of required Higgs-like particles in Run 2 is if we want a certain number dark pions in Run 2, and from that what the production cross-section of the Higgs-like boson needs to be. This number can then also be calculated in the baseline model, so that comparison is still possible. Using the result of equation 3.4, the required production cross-section σ_{req} is

$$\sigma_{\hat{h}} = \frac{N_{\hat{\pi},\text{Run2}}^{\text{req}}}{L_{\text{int}}} \frac{N_{\hat{h},\text{sim}}^{\text{uncut}}}{N_{\hat{\pi},\text{sim}}^{\text{cut}}}, \tag{3.6}$$

where we want $N_{\hat{\pi},\text{Run2}}^{\text{req}}$ dark pions in Run 2, and the $\hat{h}$ should be considered a Higgs-like boson. We will set $N_{\hat{\pi},\text{Run2}}^{\text{req}} = 50$.

Note that the fraction of Higgs-like bosons that oscillates into a dark Higgs-like boson f is taken along here: $\sigma_{\hat{h}} = f\sigma_h$. This way we do not assume that $f = 0.18$, like the SM Higgs, for each mass.

To calculate the error on the production cross-section, also resulting from the error $\sigma_{\text{sim}} = \sqrt{N_{\hat{\pi},\text{sim}}^{\text{cut}}}$, we again use first order error propagation which gives the standard deviation $\sigma_{(\sigma_{\hat{h}})}$ as

$$\sigma_{(\sigma_{\hat{h}})} = \frac{\sigma_{\hat{h}}}{\sqrt{N_{\hat{\pi},\text{sim}}^{\text{cut}}}}. \tag{3.7}$$

3.4   Comparing different scenarios

As multiple scenarios are considered in this project, each of which has one parameter varied relative to the baseline model, a method of comparing the different scenarios to the baseline is needed. We consider the percentual difference defined as

$$\text{difference} = \frac{N_{\text{scenario}} - N_{\text{base}}}{N_{\text{base}}} \cdot 100\%, \qquad (3.8)$$

where N_{scenario} is the number of expected Run 2 dark pions for a certain scenario and N_{base} is that same number for the baseline model. This will only be calculated for the points where $N_{\text{base}} > 5\sigma$, so where the passing number is larger than 5 times its standard deviation in the baseline model, so that there is at least one particle passing there within the 5σ margin.

For the Higgs mass scenario, the difference calculation is done analogously, but with the required cross-section in that scenario compared to the required cross-section in the baseline model.

The difference is used to determine whether the influence of a varied parameter is small enough to say a search for dark pions can be done independently of that parameter. This is the case if the difference is smaller than about 20%, as this is generally the expected experimental uncertainty, so a theory uncertainty like that would not be visible in the data.

3.5   Reweighting lifetimes

In order to create a fine grained study of the number of expected dark pions in Run 2, one would have to run the simulations at many different dark pion lifetimes and masses. This takes a lot of time, and therefore this alternative method of reweighting is used, which allows us to get results at different lifetimes than those that are simulated. (This same method cannot be applied to the masses, as the influence of the dark pion mass is more complicated than can be captured with what follows.)

Given the simulated lifetimes, the target lifetimes that will be reweighted to are 2, 3, 4, 6, 7, 8 and 9, and their multiples by 10, so the same numbers in the range 20 to 90, 200 to 900, and 2000 to 9000.

3.5.1   Weight formula

To get more results at different lifetimes, we make use of the decay times of all dark pions that are determined with the simulation, which depend on the

known (input) lifetime. Essentially, the idea is then to divide out the generated lifetime curve and multiply by the desired lifetime curve, which are both of the form $e^{-t/\tau}$. In order to do this, equation 3.9 is used, which gives a weight w_i to each simulated dark pion i based on its (proper) decay time t_i, the lifetime that was used to generate the simulation τ_{gen} and the target lifetime we want to get, τ_{target}:

$$w_i = \frac{\tau_{gen}}{\tau_{target}} \frac{e^{-t_i/\tau_{target}}}{e^{-t_i/\tau_{gen}}}. \tag{3.9}$$

Here the factor $\frac{\tau_{gen}}{\tau_{target}}$ ensures that the number of particles before and after reweighting is the same. An example of a reweighted set of decay times is shown in figure 3.5. Here we reweighted to a lifetime that is also simulated, from 10 ps to 5 ps. The reweighted result is well-behaved and lines up quite well with the simulated result.
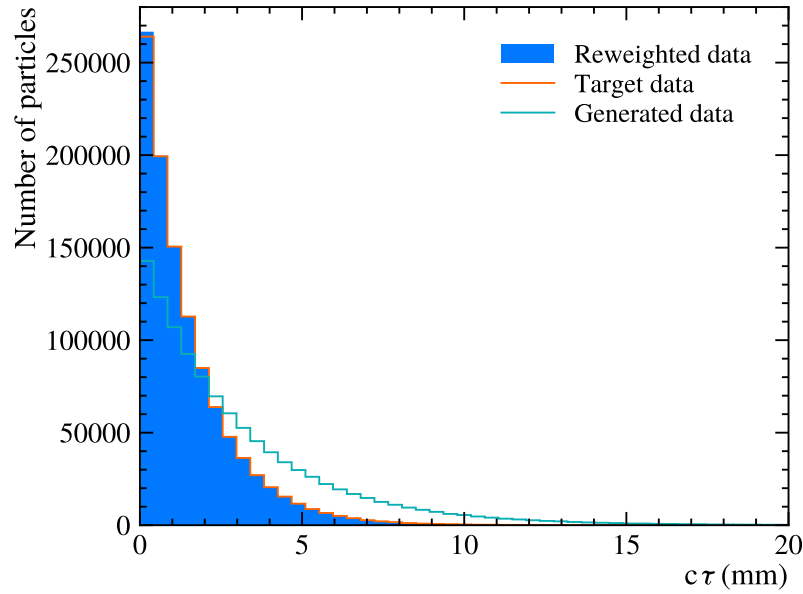
Figure 3.5: *An example of a reweighted set of decay times, from 10 to 5 ps. Note that here the 'Target data' has also been simulated, and has the lifetime that is the target for the 'Reweighted data'. The decay curves are plotted for the decay times multiplied by the speed of light, $c\tau$.*

Apart from the distribution of decay times of the dark pions, other distributions that depend on the decay time will also change due to the reweighting. These are the decayradius R_{decay} of all particles, including the dark pion, in the decay chain, as well as the originradius R_{origin} of all particles originating from the dark pion. The same holds for z_{decay} and z_{origin}. Distributions

of other quantities like momentum are unaffected. These were checked and well-behaved like the distribution of the decay times themselves. The cuts are on these positions, so the reweighting method works because the positions are rescaled as much as the decay times themselves; this is the case because a specific particle has the same velocity before and after reweighting.

3.5.2   Reweighting from above and below

Given a certain target lifetime, we will reweight to that target using the generated datasets with both the larger and smaller lifetime closest to the target. Doing this increases the available data for this statistical trick and should thus improve the results. To combine them, each reweighted set is given an additional weight, namely the maximum weight of that set:

$$w_i \rightarrow w_i' = \frac{w_i}{\max\left(\{w_i\}_{i=1}^N\right)}. \tag{3.10}$$

Note that doing this will cause the number of particles to change, which will be taken into account later. The result of this extra weight is related to the tail of the exponential distribution, where it is possible to have spiking bin counts as there are not a lot of particles in that region to do statistics with. These spikes are shrunk to a value closer to zero by dividing the maximum weight, decreasing their disruptive effect on the distribution as a whole.

   Once the reweighting procedure has been done and the combined weights from the datasets with lifetimes directly above and below the target are obtained, the number of dark pions expected in Run 2 can again be calculated, with the key difference that the numbers from the simulation are now those after reweighting.

   To find the number of dark pions after reweighting, one simply sums the weights, since each passing particle no longer counts as a single particle, but instead as one time its weight. The way to find the number of dark Higgs bosons after reweighting is not obvious however, as the weights are assigned to dark pions, not to the Higgs. It can be derived by requiring that the number of Higgs stays the same before and after reweighting (like the number of dark pions), and starting from an ansatz of the form $w_{\text{event}} = \alpha \sum_{j=1}^{N_{\hat{\pi},\text{event}}} w_j$ for a constant α to be determined, where w_j is the dark pion weight, and $N_{\hat{\pi},\text{event}}$ is the amount of dark pions in that event (originating from the single Higgs).

   The resulting weight for each Higgs/event is

$$w_{\text{event}} = \frac{N_{\hat{h}}}{N_{\hat{\pi}}} \sum_{j=1}^{N_{\hat{\pi},\text{event}}} w_j, \tag{3.11}$$

where $N_{\hat{h}}$ and $N_{\hat{\pi}}$ are the number of dark Higgs and dark pions before reweighting.

Then to find the Run 2 numbers after the reweighting procedure, the combined weights from both the above and below sets are used to calculate the number of dark pions and dark Higgs using the above methods. Using the weights including the maximum weight factor w_i', let $N_{\hat{\pi},\text{sim,below}}^{\text{cut}}$ be the number of dark pions passing from the below set and $N_{\hat{\pi},\text{sim,above}}^{\text{cut}}$ from the above set, and let $N_{\hat{h},\text{sim,below}}^{\text{uncut}}$ and $N_{\hat{h},\text{sim,above}}^{\text{uncut}}$ be the number of dark Higgs, then

$$N_{\hat{\pi},\text{Run2}}^{\text{cut}} = \frac{N_{\hat{\pi},\text{sim,below}}^{\text{cut}} + N_{\hat{\pi},\text{sim,above}}^{\text{cut}}}{N_{\hat{h},\text{sim,below}}^{\text{uncut}} + N_{\hat{h},\text{sim,above}}^{\text{uncut}}} N_{\hat{h},\text{Run2}}^{\text{uncut}}. \tag{3.12}$$

As this only depends on the ratio of numbers of particles, the factor of inverse maximum weight essentially drops out, so that a number similar to one without dividing the weights by their maximum is found, as one would expect.

Note that the reweighting procedure will be skipped for the Higgs mass scenario, although it could also be applied there, by calculating the required cross-section with the reweighted number of dark pions passing from the simulation.

Given the weights (of either the dark pions or dark Higgs), and that their sum is the passing number, $N = \sum_i w_i$, the standard deviation of this passing number is given by

$$\sigma_{\text{sim}} = \sqrt{\sum_i w_i^2}. \tag{3.13}$$

This is taken into account for both the number of dark pions and dark Higgs after reweighting. With these errors on the combined passing number $N = N_{\text{below}} + N_{\text{above}}$, with which equation 3.12 becomes the same as equation 3.4, the standard deviation of the expected number of dark pions in Run 2 after reweighting can be derived using first-order error propagation, giving

$$\sigma_{\hat{\pi},\text{Run2}} = \frac{N_{\hat{h},\text{Run2}}^{\text{uncut}}}{N_{\hat{h},\text{sim}}^{\text{uncut}}} \sqrt{\sigma_{\hat{\pi},\text{sim}}^2 + \left(\frac{N_{\hat{\pi},\text{sim}}^{\text{cut}}}{N_{\hat{h},\text{sim}}^{\text{uncut}}} \sigma_{\hat{h},\text{sim}} \right)^2}. \tag{3.14}$$

3.5.3 Check of proper reweighting

As a check of whether the reweighting worked properly, the results for a certain target lifetime will be fitted to an exponential decay curve. This is especially necessary because some problems can occur when reweighting to a larger target lifetime, as the data from the smaller generated lifetime does not cover the same decay time range as a larger lifetime would, which can cause relatively

large irregularities in the tail of the distribution. (Although as explained before, this is reduced by the maximum weight method.)

The fit is done using the fitting library zfit [11]. Based on the resulting fitted lifetime τ_{fit} and error σ of this fit, a reweighted result will only be accepted if it satisfies the following two statistical criteria:

1. The target lifetime is within the uncertainty of the fit result, so $|\tau_{\text{fit}} - \tau_{\text{target}}| < 5\sigma$.

2. The error is not too large, which we choose to be the case when $\sigma < \tau_{\text{fit}}/10$.

Note that this check will be done using the full simulation result, before any cuts are applied, since this is meant to create another simulated dataset (without actually doing the simulation).

3.6   Indication of total sensitivity

For the sensitivity study it is nice to also consider what the total sensitivity of the LHCb detector would be, when all three categories we consider are combined. So to determine this, we sum the expected number of particles of each category together.

Note that this result is useless for an actual analysis, as there the categories have to be considered separately. It does allow use to see the different lifetimes and masses that an analysis of all three categories can cover.

This result will be shown and discussed in appendix B, as it is not directly relevant to the main goals of this thesis.

4 Chapter

Results

In this chapter the results of calculating the number of expected dark pions in Run 2 will be discussed, after cuts are applied, both before and after reweighting, for each set of simulated parameters. In these plots, points where the expected number of particles is less than 5 times its standard deviation are left white, as there it is not certain whether any dark pions are expected. (Also for the Higgs mass scenario, using the number of particles passing from the simulation.) For the different scenarios the percentual difference with the baseline model will be plotted as well. To keep things concise, the plots of expected Run 2 numbers are shown only for the LLDD category here, while those for the LLLL and DDDD categories can be found in appendix A. The LLDD category is chosen because it performs the best, having the largest expected number of dark pions overall. Additionally, for each scenario the number of dark pions that is produced, so before any cuts are applied, are listed for each mass, as this will turn out to be useful information later. (This number is about the same for each lifetime, since of course the mechanism producing dark pions has nothing to do with their lifetime.)

4.1 Baseline model

We start with the baseline model results. Firstly, the number of dark pions produced here, from lowest to highest mass, is around: 107k, 96k, 87k, 80k, 74k, 70k, 65k.

The resulting expected number of dark pions in Run 2 can be seen in figure 4.1, with the exact passing number and its standard deviation printed in each cell. A large dependence on lifetime is visible, as the passing number steadily decreases as lifetime increases, with the most dark pions passing at the

33

shortest lifetime of 1 ps and effectively none at the white spaces of 1000 ps and above. Additionally, it can be seen that the passing number decreases as mass increases at lifetimes of 1, 5, 10 and 50 ps, although the ratio of the passing number between the masses of 3 GeV and 1.5 GeV becomes smaller as lifetime increases. For the highest lifetimes of 100 and 500 ps the decrease is not clearly visible anymore, as the passing number is mostly constant at different masses. There is a peak in passing number at the smallest lifetime and mass and from there it decreases, except for some small hiccups. Most notably there is an increase at 2.0 GeV mass and 5 ps lifetime. There are also some smaller increases and decreases at larger lifetimes. Additionally, the change in passing number from 10 ps to 50 ps lifetime, from 50 ps to 100 ps lifetime and from 100 ps to 500 ps lifetime is quite large compared to the ones at the other lifetimes. Especially from 100 to 500 ps there is a decrease of roughly a factor 4.

The result after reweighting is shown in figure 4.2. In the plot it can be seen the reweighted results are well-behaved, as they do not show any large sudden changes compared to the generated data or other reweighted data; the entire figure looks quite smooth. Indeed the notable changes in passing number from 10 to 50 ps, 50 to 100 ps and 100 to 500 ps seen before reweighting are not as sharp anymore. The standard deviation of the expected number after reweighting is not printed here as to not make the figure too busy, but were found to be of the same order as the errors on the passing numbers of the generated datasets close to the reweighted data. Interestingly, the slight increase in expected number at a mass of 2.0 GeV and 5 ps seen before reweighting is still present here, as the reweighted data between 1 and 5 ps also gives a larger passing number at 2.0 GeV than at 1.75 and 2.25 GeV. Yet between 5 and 10 ps, this does not happen. Additionally, all reweighted data between 1 and 5 ps at 1.5 GeV mass shows a large passing number, enlarging the region of the maximal expected particles. Above the lifetime of 5 ps there is also an increase visible.

Looking at the figures for the LLLL and DDDD categories in the appendix A, similar things can be said.

Starting with the simulation results of LLLL in figure A.1, the first thing to note is that the overall number of dark pions is a lot smaller than for the LLDD result. Additionally, the plot seems less smooth than for LLDD: there only one dip in an otherwise smoothly decreasing plot could be seen, while here there are a number of increases and decreases. The dependence on lifetime is very close to that of LLDD, with the passing number decreasing as lifetime increases, although there are already barely any dark pions left at a lifetime of 500 ps, and so this region is also left white in the plot. There is now one sharp drop in passing number between 10 ps and 50 ps lifetimes, decreasing it by about a factor 3 for the smallest mass. The dependence on mass is also similar to LLDD, as the expected number of particles decreases as mass increases, but this change becomes smaller as one looks at larger lifetimes.

The reweighting results for LLLL in figure A.2 again smooth out the figure over the lifetime axis, but the fluctuations over the mass axis remain visible (which is to be expected as the reweigthing is based on lifetime). There are no large sudden changes introduced by the reweighted data however, so it is still well-behaved.

Then looking at the simulation results of DDDD in figure A.3, there are again less expected dark pions overall compared to LLDD, but slightly more than in the LLLL category. The most obvious difference with the former two categories is that the passing number is no longer largest at the smallest lifetime and then decreases with increasing lifetime, but instead is large in the region of 50 and 100 ps, and decreases as the lifetime increases and decreases from there. Looking at the mass dependence, this is similar again, with the number of dark pions decreasing as mass increases for lifetimes of 50 and 100 ps, but at the other lifetimes the mass has seemingly no influence as the passing number stays constant within their standard deviation at each mass.

The reweighting results for DDDD in figure A.4 again mostly smooth out the figure as in the previous categories. There is an interesting increase at 2 GeV mass between 100 and 500 ps.
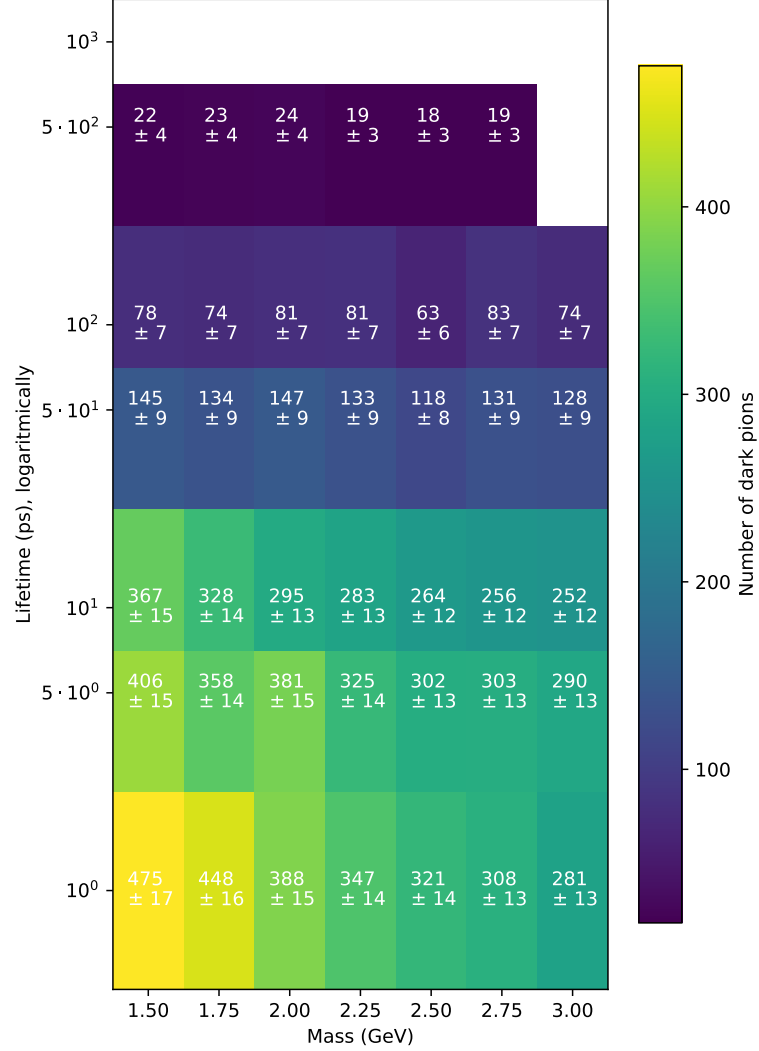
Figure 4.1: *The expected number of dark pions in Run 2 passing the cuts in the LLDD category, for the baseline model. The white cells have less particles passing than 5 times their standard deviation. A large dependence on lifetime is visible, as well as a dependence on mass that becomes smaller with increasing lifetime.*
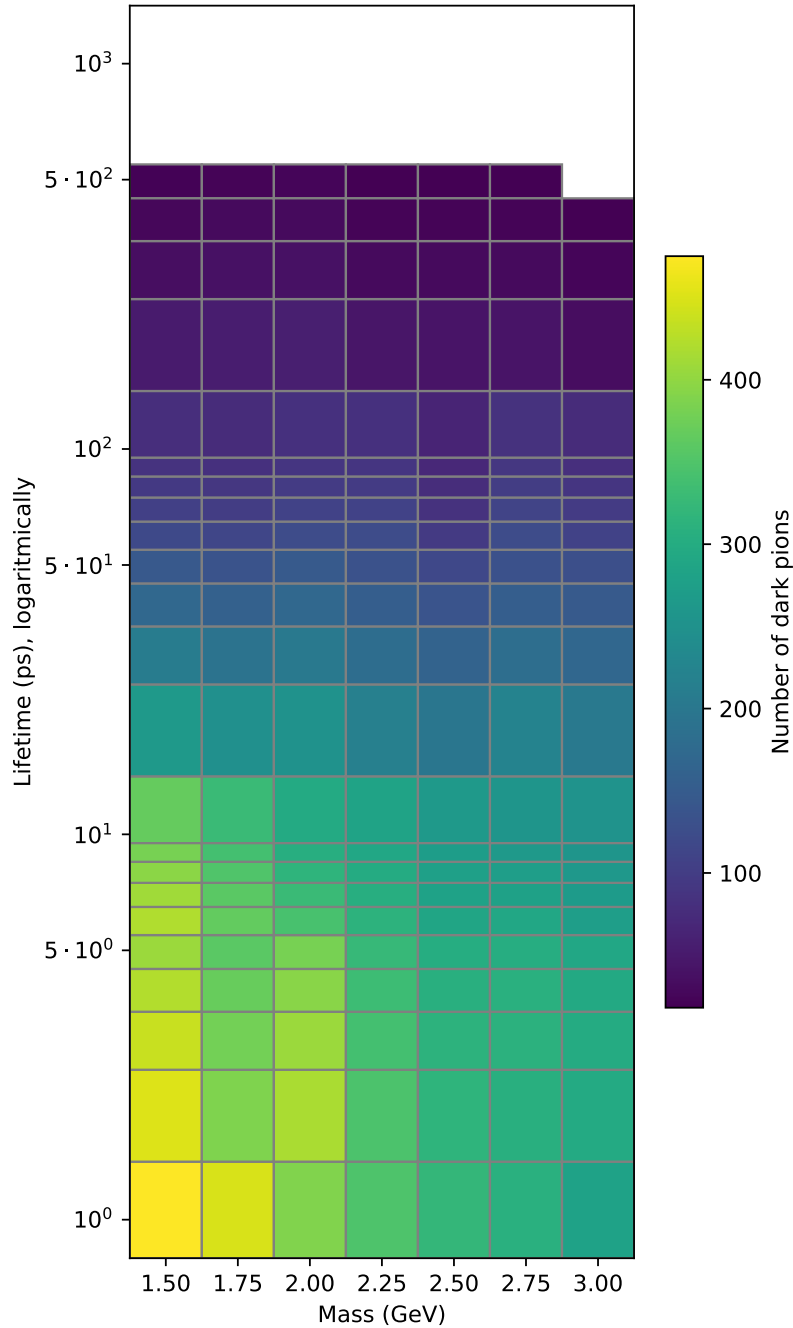
Figure 4.2: *The expected number of dark pions in Run 2 passing the cuts in the LLDD category, after reweighting, for the baseline model. The white cells did not pass the statistical criteria, or have less particles passing than 5 times their standard deviation. It can be seen that the reweighting produces a smoother plot.*

4.2 Dark rho scenario

Now we consider the dark rho scenario. Firstly, the number of dark pions produced in this scenario, from lowest to highest mass, is around: 67k, 34k, 17k, 8k, 1500, 600. This is notably a lot less than in the baseline model.

However, something else happened as well: the number of events we got from the simulation, which should be 100k, actually turns out to be around (from lowest to highest mass): 58k, 33k, 18k, 9k, 4k, 1800, 750. Why this happened is discussed in the Discussion chapter, but it is important to keep in mind as we cannot calculate the expected Run 2 number using the supposed number of events of 100k, but have to use these numbers instead. Additionally, the number of dark pions per dark Higgs is not so much smaller as would be the case if we had 100k events, but actually somewhat similar.

Moving on, the resulting expected number of dark pions in Run 2 can be seen in figure 4.3. It looks fairly similar to the baseline model results, but only at smaller masses. At the larger masses, there are large fluctuations; e.g. 682 dark pions at 3.0 GeV and 10 ps is quite a sudden spike. The same lifetime dependence as in baseline seems to be present, but this is only clear when looking at the 1.5 and 1.75 GeV masses. There also seems to be a decrease with mass still, but this is hard to see due to the fluctuations.

All this is also visualised in the plot of the percentual difference of this scenario with the baseline model, which can be seen in figure 4.4. Mostly at large masses we see strong deviations from the baseline results, with very large percentages. But at smaller masses, the differences are generally small with percentages between -10% and 30%.

The result after reweighting is shown in figure 4.5. Most notably, there are quite a lot of rejected points visible here, especially at larger masses, but also at the largest lifetimes for each mass. In the points that were accepted, we do see that the reweighting is well-behaved still. But the large fluctuations are still visible in the reweighted points as well, so that the figure does not look very smooth.

Let us also shortly consider the results for the LLLL and DDDD categories in the appendix A. With the discussion of the differences between LLDD and the other categories for the baseline model in mind, as well as the effect of the dark rho scenario for LLDD, there is not much to add.

For the simulation results in figures A.5 and A.8, the same happens as for LLDD, where we have similar results but very large fluctuations at mostly the larger masses. This is also confirmed by the percentual difference plot in figures A.6 and A.9. The reweighting also acts the same, as seen in figures A.7 and A.10, with many rejected points at larger masses, but overall well-behaved accepted points although the fluctuations remain visible in them.

Number of expected dark pions in Run 2 in the LLDD category.
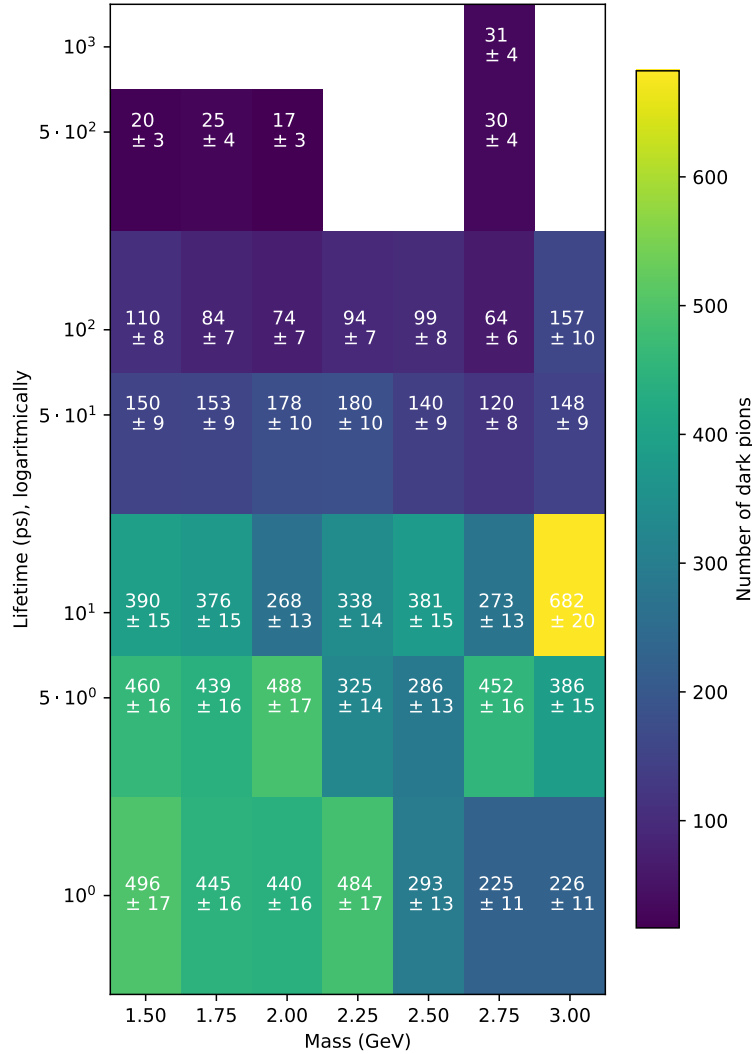
Figure 4.3: *The expected number of dark pions in Run 2 passing the cuts in the LLDD category, for the dark rho scenario. The white cells have less particles passing than 5 times their standard deviation. This result looks similar to the baseline model, but has very strong fluctuations at large masses.*

Percentage of the difference in expected dark pions in the LLDD category.
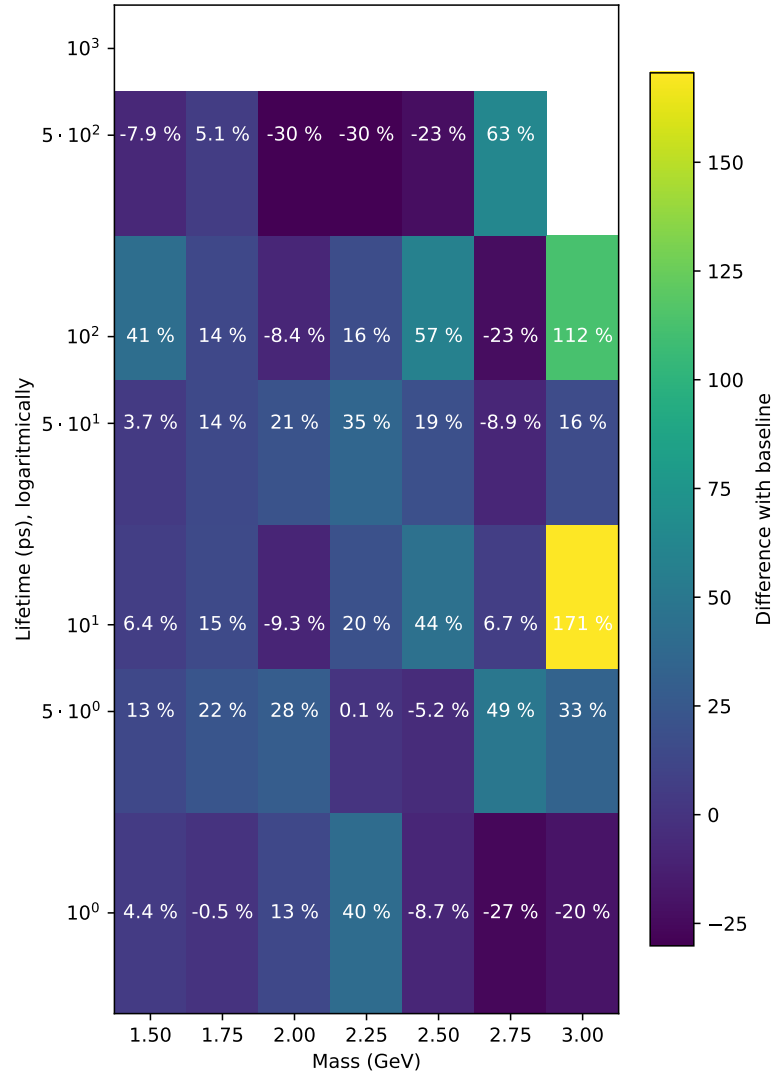
Figure 4.4: *The percentual difference for the dark rho scenario in the LLDD category. The whitespaces indicate the points left out because there the number of expected dark pions is less than 5 times its error in the baseline model. The large fluctuations at larger masses is visible here, as well as the small difference with baseline at smaller masses.*

Number of expected dark pions in Run 2 in the LLDD category.
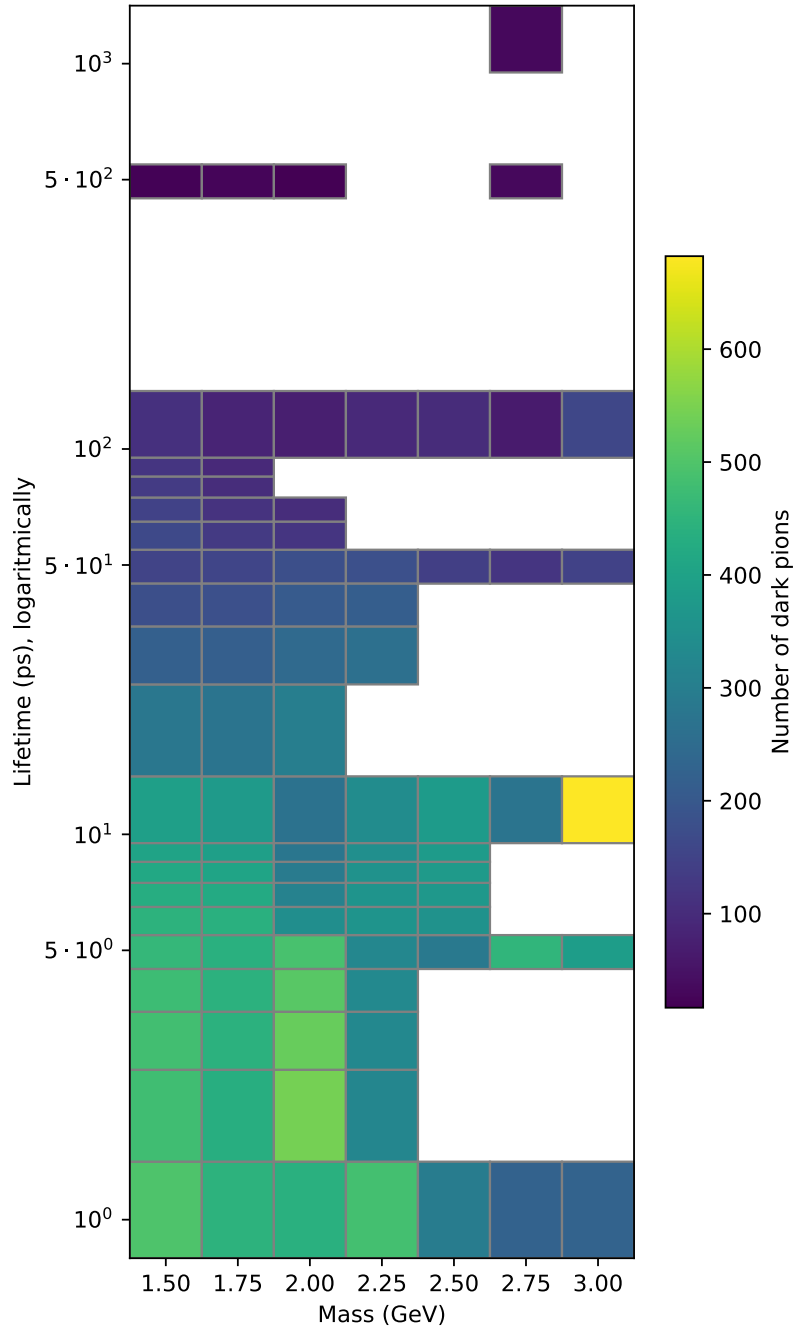
Figure 4.5: *The expected number of dark pions in Run 2 passing the cuts in the LLDD category, after reweighting, for the dark rho scenario. The white cells did not pass the statistical criteria, or have less particles passing than 5 times their standard deviation. We see that quite a large number of reweighted datapoints have been rejected, especially at larger masses. The accepted ones are well-behaved though.*

4.3 Dark colour scenario

We now consider the dark colour scenario. To start, the number of dark pions produced in this scenario, from lowest to highest mass, is around: 105k, 94k, 86k, 79k, 73k, 68k, 64k. These are about 98% of the baseline numbers, so very close.

The resulting expected number of dark pions in Run 2 is shown in figure 4.6. Just looking at this plot, it is almost indistinguishable from the baseline result, with the same mass and lifetime dependence, as well as nearly the same passing numbers. Of course the random variations do not occur in the exact same points, but like in the baseline model, there are no large hiccups in the plot here, and it decreases smoothly from the 1.5 GeV mass and 1 ps lifetime maximum. There are also the same large changes in passing number from 10 ps to 50 ps lifetime, from 50 ps to 100 ps lifetime and from 100 ps to 500 ps lifetime.

The similarity is confirmed by the percentual difference plot in figure 4.7. Most points either have a small increase or decrease compared to the baseline model. There is no dependence on either mass or lifetime visible. Overall most percentages lie between +20% and -20%, and the average seems to be around 0; a full calculation gives $-3.7 \pm 1.8\%$.

Finally, the result after reweighting can be seen in figure 4.8. The reweighted results are well-behaved, mostly smoothing out the plot like in the baseline model. The large changes from 10 ps to 50 ps lifetime, from 50 ps to 100 ps lifetime and from 100 ps to 500 ps lifetime are again made less sharp. We do also see that slight hiccups in the generated results often are still visible in reweighted results, as was also the case in the baseline model.

We may also consider the LLLL and DDDD result in appendix A. Both their results for the expected Run 2 numbers, in figures A.11 and A.14, look very similar to their baseline equivalents. This is again confirmed by the percentual difference plots in figures A.12 and A.15, which both show random variations independent of lifetime or mass. However, while the LLDD results showed equally large increases and decreases of at most 20%, in both LLLL and DDDD the decreases seem slightly larger than the increases; LLLL has most values between about 10% and -30%, and DDDD has most values between about 10% and -20%. So it seems like there may be a slight decrease in overall passing number. Calculating the averages gives $-7.3 \pm 2.7\%$ for LLLL and $-5.0 \pm 2.5\%$ for DDDD.

Lastly the results after reweighting in figures A.13 and A.16 mostly smooth out the plots; there is little to add here that is not a repetition of the baseline results.

Number of expected dark pions in Run 2 in the LLDD category.
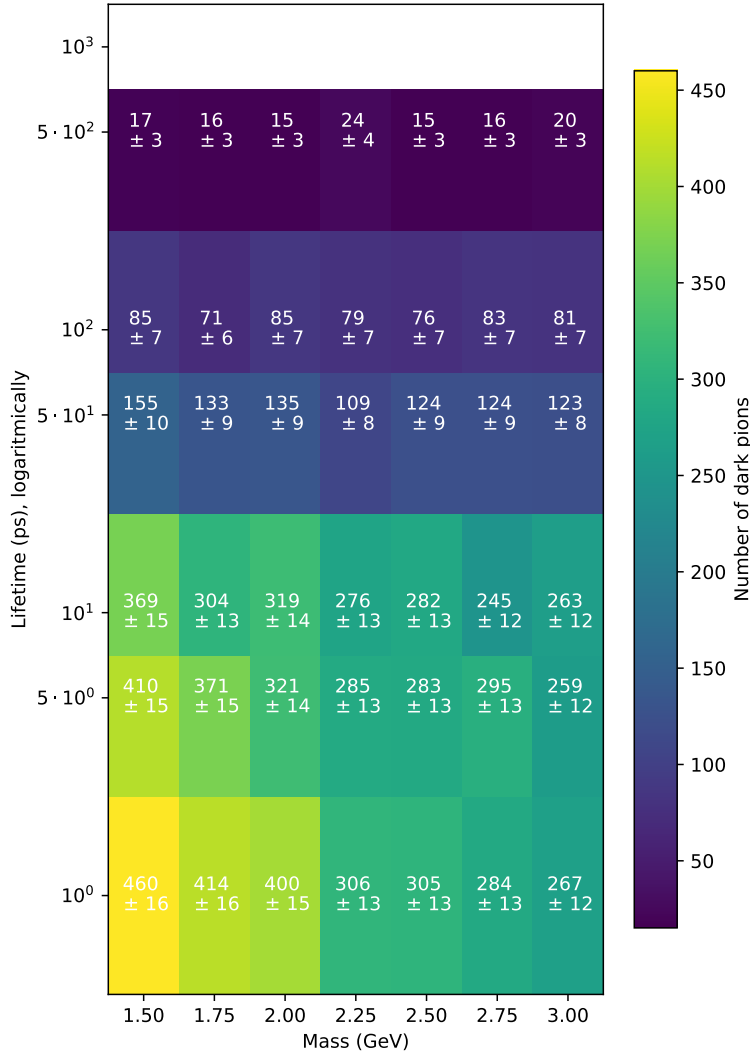
Figure 4.6: *The expected number of dark pions in Run 2 passing the cuts in the LLDD category, for the dark colour scenario. The white cells have less particles passing than 5 times their standard deviation. These results are almost indistinguishable from the baseline results.*

Percentage of the difference in expected dark pions in the LLDD category.
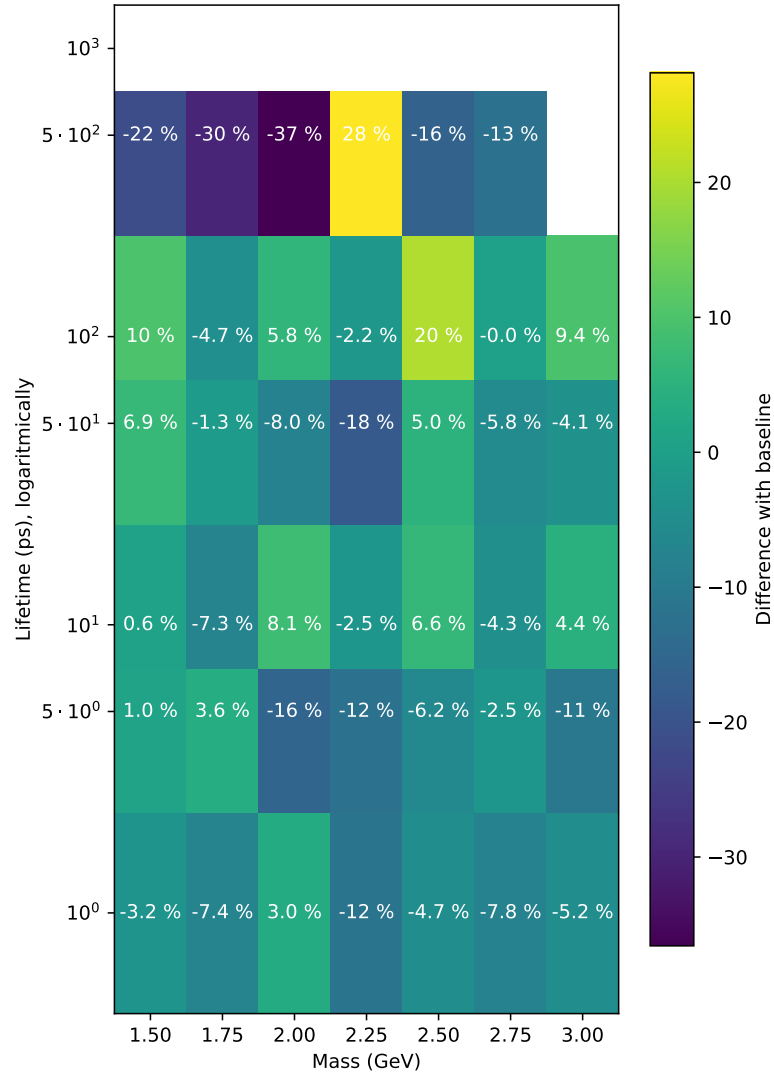
Figure 4.7: *The percentual difference for the dark colour scenario in the LLDD category. The whitespaces indicate the points left out because there the number of expected dark pions is less than 5 times its error in the baseline model. There are mostly small variations around the baseline result, with an average around 0.*

Number of expected dark pions in Run 2 in the LLDD category.
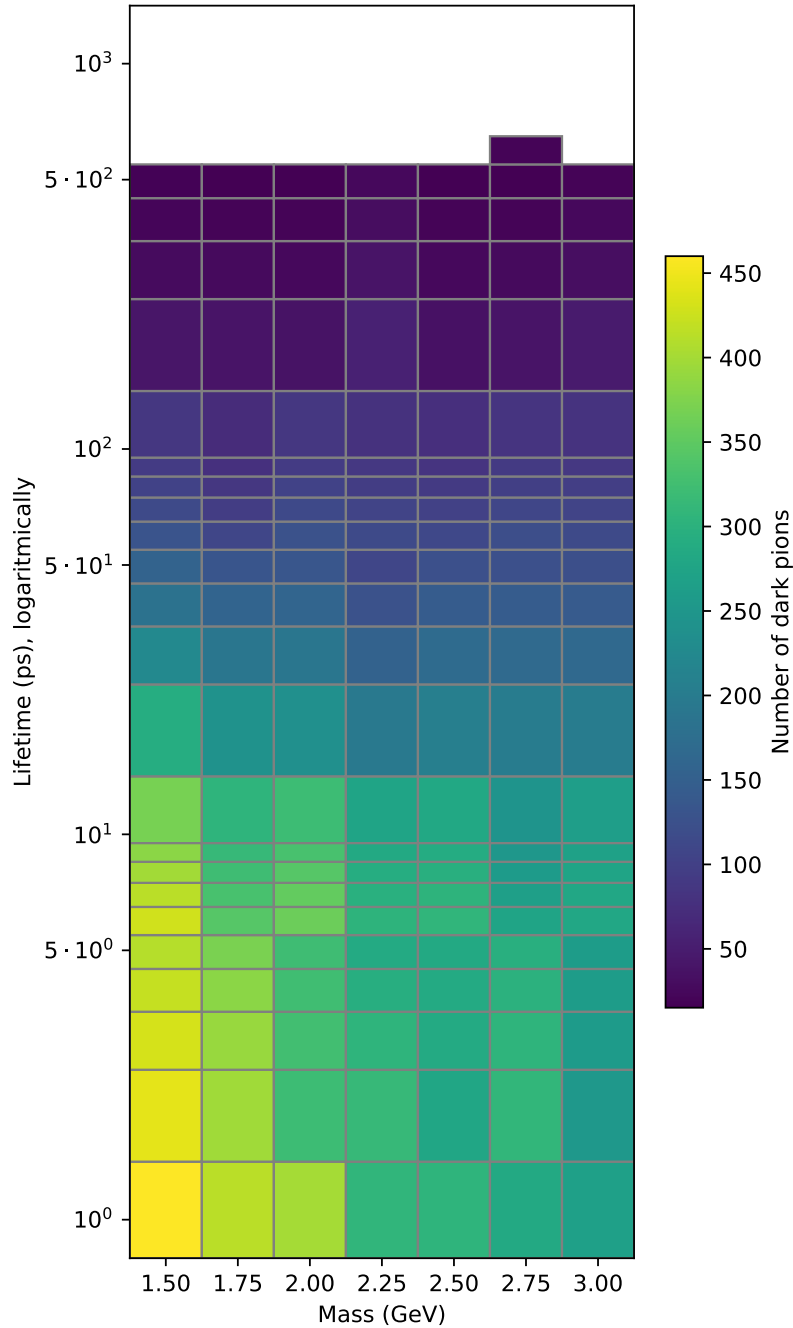
Figure 4.8: *The expected number of dark pions in Run 2 passing the cuts in the LLDD category, after reweighting, for the dark colour scenario. The white cells did not pass the statistical criteria, or have less particles passing than 5 times their standard deviation. The reweighted results are well-behaved and produce a smoother plot.*

4.4   Dark QCD scale scenario

Next is the dark QCD scale scenario, where we change the dark QCD scale $\tilde{\Lambda}_{\text{QCD}}$ from 4 GeV to first 8 and then 2 GeV.

To start with the 8 GeV scale, the number of dark pions produced in this scenario, from lowest to highest mass, is around: 96k, 86k, 79k, 73k, 67k, 63k, 60k. These are about 90% of the baseline numbers, so quite close.

The expected number of dark pions in Run2 for this scenario can be seen in figure 4.9. Just like for the dark colour scenario, there is no change clearly visible here compared to the baseline model. Looking at the percentual difference plot in figure 4.10, there indeed seems to be mostly random variation here, with no mass or lifetime dependence. We do see that overall, there seems to be a decrease in passing number. The percentages vary mostly between -20% and about 6%; the average is $-5.5 \pm 1.8\%$.

Additionally, the reweighted result in figure 4.11 does not display any new behaviour either. It is well-behaved just like for the baseline model.

Let us also look at the LLLL and DDDD results in appendix A. Just like for LLDD, the expected number in figures A.17 and A.20 look very similar to the baseline results, and the percentual difference plots (figures A.18 and A.21) show a small decrease; the averages are $-8.7 \pm 2.6\%$ for LLLL and $-7.8 \pm 2.4\%$ for DDDD. The reweighted results are still well-behaved, as visible in figures A.19 and A.22.

Next we have the results for the 2 GeV scale. Here, the number of dark pions produced, from lowest to highest mass, is around: 107k, 96k, 87k, 80k, 74k, 69k, 65k. These are almost the exact same as the baseline numbers.

The expected number of dark pions in Run 2 are shown in figure 4.12. Yet again, this result is indistinguishable from the baseline result. This is confirmed by the percentual difference plot of figure 4.13, which is mostly random variation again, without any mass or lifetime dependence. The average seems to be around zero again though, unlike the 8 GeV case. The average here is indeed smaller, $-3.0 \pm 1.7\%$.

For the reweighted result in figure 4.14, we just see it is well-behaved again, like the baseline model. One interesting thing is that the point at 600 ps and 1.5 GeV is accepted here, while all points below it up to 100 ps are not.

The LLLL and DDDD results, in appendix A, behave very similar to LLDD here as well: the expected number in figures A.23 and A.26 look the same as in baseline. The percentual difference plots in figures A.24 and A.27 show an average even closer to 0 than LLDD, with $-1.5 \pm 2.8\%$ for LLLL and $-0.7 \pm 2.6\%$ for DDDD. The reweighted results in figures A.25 and A.28 are still well-behaved too.
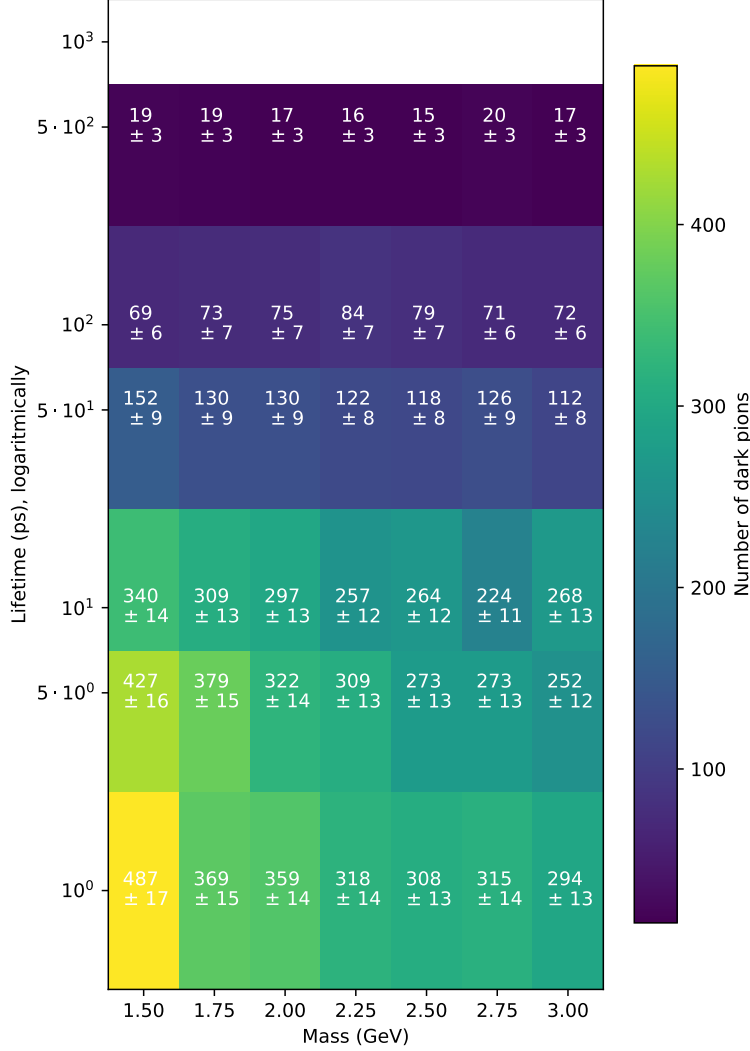
Figure 4.9: *The expected number of dark pions in Run 2 passing the cuts in the LLDD category, for $\tilde{\Lambda}_{\mathrm{QCD}} = 8$ GeV. The white cells have less particles passing than 5 times their standard deviation. These results are very similar to the baseline model.*

Percentage of the difference in expected dark pions in the LLDD category.
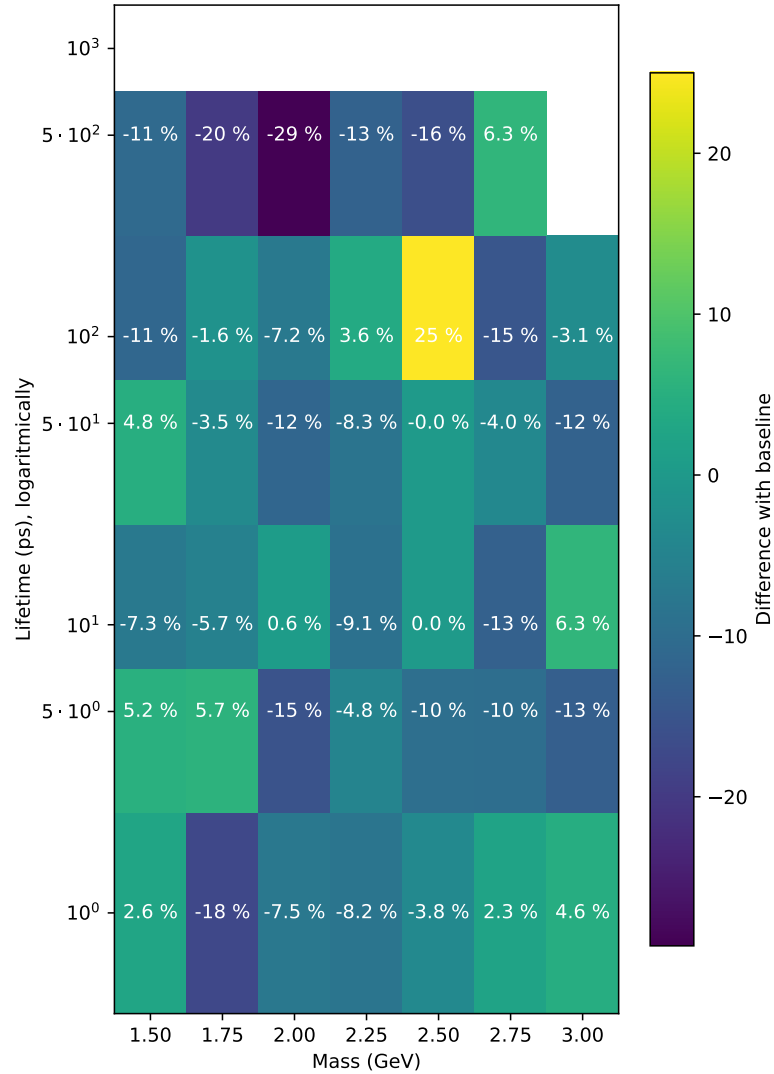
Figure 4.10: *The percentual difference for $\tilde{\Lambda}_{\text{QCD}} = 8$ GeV in the LLDD category. The whitespaces indicate the points left out because there the number of expected dark pions is less than 5 times its error in the baseline model. We see random variations, but on average there is a small decrease.*

Number of expected dark pions in Run 2 in the LLDD category.
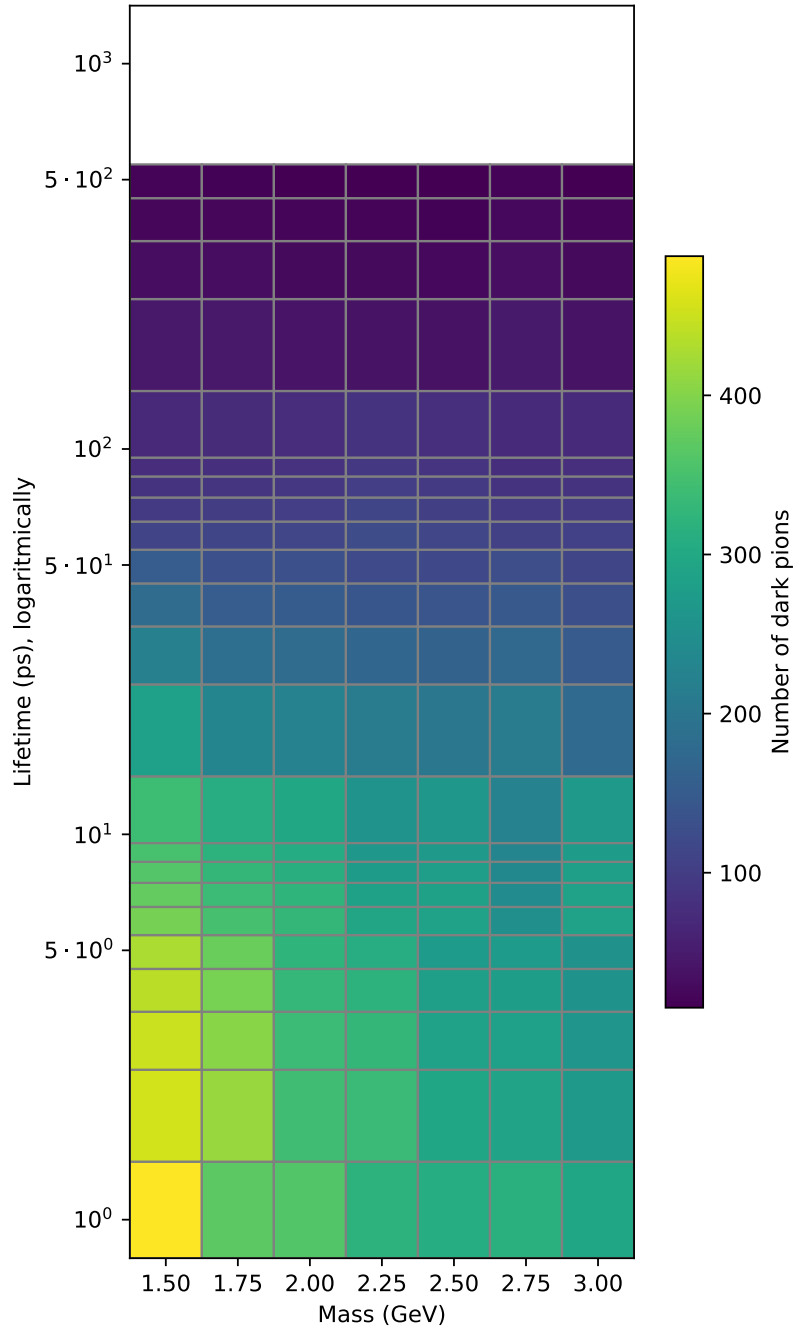
Figure 4.11: *The expected number of dark pions in Run 2 passing the cuts in the LLDD category, after reweighting, for* $\tilde{\Lambda}_{\mathrm{QCD}} = 8$ *GeV. The white cells did not pass the statistical criteria, or have less particles passing than 5 times their standard deviation. These results are well-behaved and similar to the baseline model.*

Number of expected dark pions in Run 2 in the LLDD category.
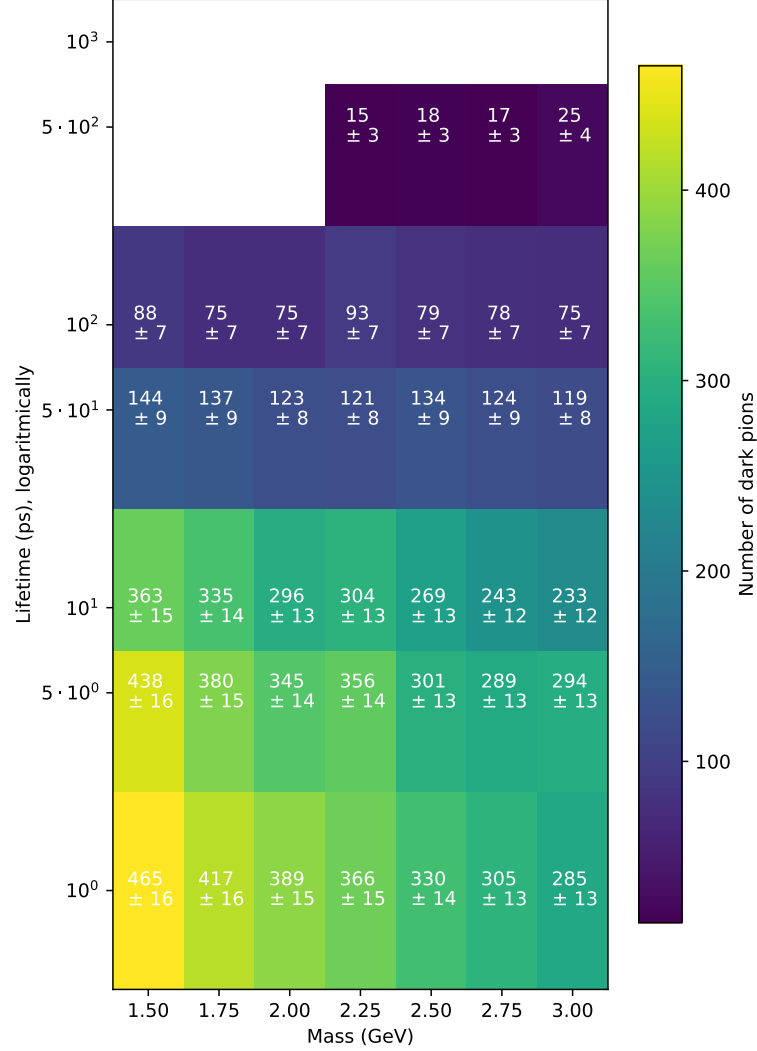
Figure 4.12: *The expected number of dark pions in Run 2 passing the cuts in the LLDD category, for $\tilde{\Lambda}_{\text{QCD}} = 2$ GeV. The white cells have less particles passing than 5 times their standard deviation. These results are very similar to the baseline model.*

Percentage of the difference in expected dark pions in the LLDD category.
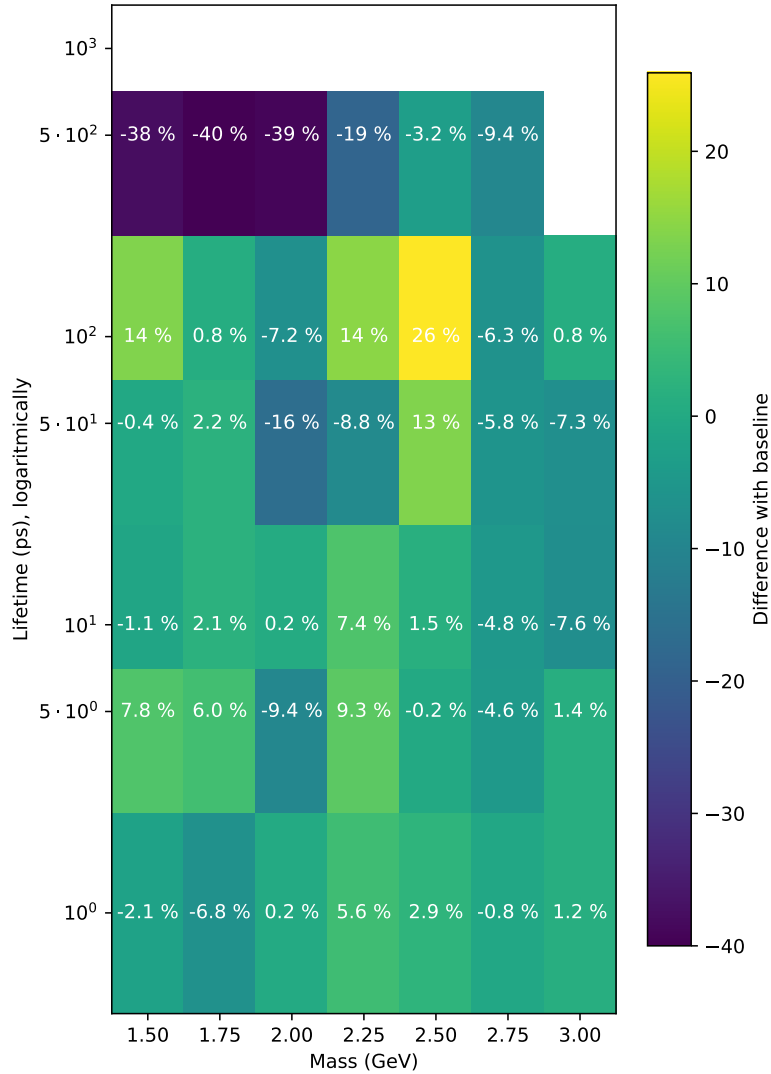
Figure 4.13: *The percentual difference for $\tilde{\Lambda}_{\mathrm{QCD}} = 2$ GeV in the LLDD category. The whitespaces indicate the points left out because there the number of expected dark pions is less than 5 times its error in the baseline model. We see random variations, but on average there is a small decrease.*

Number of expected dark pions in Run 2 in the LLDD category.
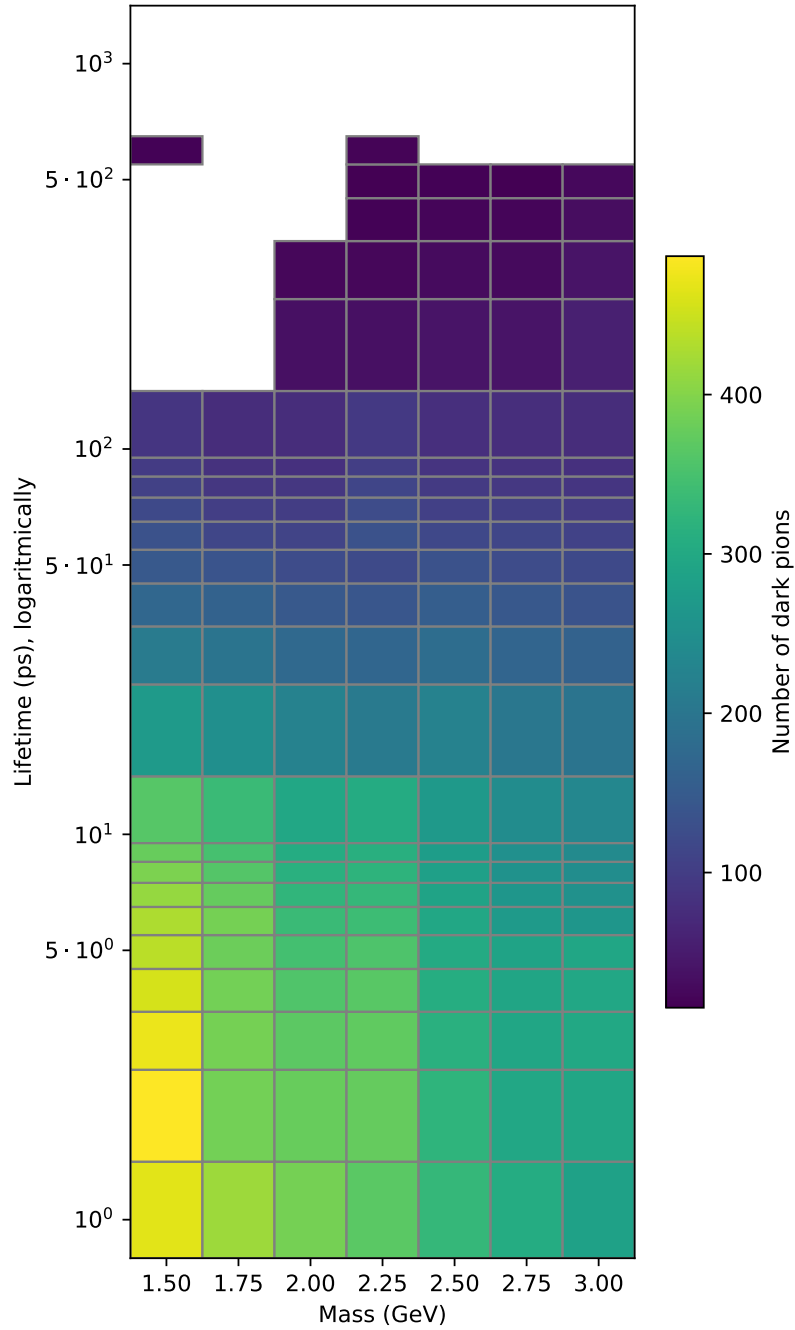
Figure 4.14: *The expected number of dark pions in Run 2 passing the cuts in the LLDD category, after reweighting, for $\tilde{\Lambda}_{\mathrm{QCD}} = 2$ GeV. The white cells did not pass the statistical criteria, or have less particles passing than 5 times their standard deviation. These results are well-behaved and similar to the baseline model.*

4.5   Higgs mass scenario

Finally, there is the Higgs mass scenario, in which the mass of the Higgs boson (and its dark counterpart) is changed from its measured SM value of 125 GeV to 500 GeV, to 50 GeV and to 1250 GeV. The dark mediator is then no longer the Higgs boson but rather a Higgs-like boson.

For the 500 GeV Higgs mass, the number of dark pions produced in this scenario, from lowest to highest mass, is around: 213k, 190k, 173k, 158k, 146k, 136k, 128k. This is about twice as many as in the baseline model.

The resulting required cross-section can be seen in figure 4.15. A shape similar (but in reverse) of the expected number plots of the baseline model can be seen, where a larger cross-section is needed as lifetime increases, with relatively large jumps between the 10 and 50 ps, and the 50 and 100 ps lifetimes (also between 100 and 500 ps, but we only have 1 mass column to look at here). The dependence on the mass is also similar, as the cross-section increases with mass, but this increase is smaller than the one due to changing lifetime.

The difference with the required cross-section in the baseline model is shown in figure 4.16. From this it is clear that there is a larger cross-section required for the 500 GeV Higgs mass in all points, i.e. less particles are produced for a 500 GeV mass than in the baseline model. Additionally, it seems like there is some dependence on lifetime, as the difference generally increases with lifetime; percentages of about 40% and higher only appear for the 50, 100 and 500 ps lifetimes, while almost all points at 1 and 5 ps are below 20%. Additionally, there are two large spiking increases at 500 ps for 1.75 GeV and 2.5 GeV mass.

Now let us look at the results for the LLLL and DDDD categories in appendix A. For LLLL, in figure A.29, the mass and lifetime dependence is very similar to that of LLDD. The same holds for DDDD, in figure A.31, but with the lowest required cross-section at larger lifetimes, as familiar from the baseline model.

Looking at the difference plot for LLLL in figure A.30, there is also an increase of cross-section in each point. There is a large peak at 50 ps lifetime and 2.25 and 2.5 GeV mass, which might be the effect of less statistics for the 500 GeV mass scenario here (the 2.5 GeV point has an error too large to be plotted in figure A.29). Otherwise, the increase is larger here than for LLDD, where most points lay between 10% and 40%, while here most are between 20% and 90%. The lifetime dependence observed for LLDD is not clearly visible here, as both the larger and smaller percentages appear for all lifetimes.

Lastly there is the difference plot for DDDD in figure A.32, which not only shows increases of cross-section but also multiple points where it stays about the same or even slightly decreases. Most points lay between 0% and 30%, again different from LLDD. The lifetime dependence seen for LLDD is certainly not present here, as the greatest decreases actually occur for the larger lifetimes;

simultaneously, the largest increases are there too, but both of these seem like statistical outliers.
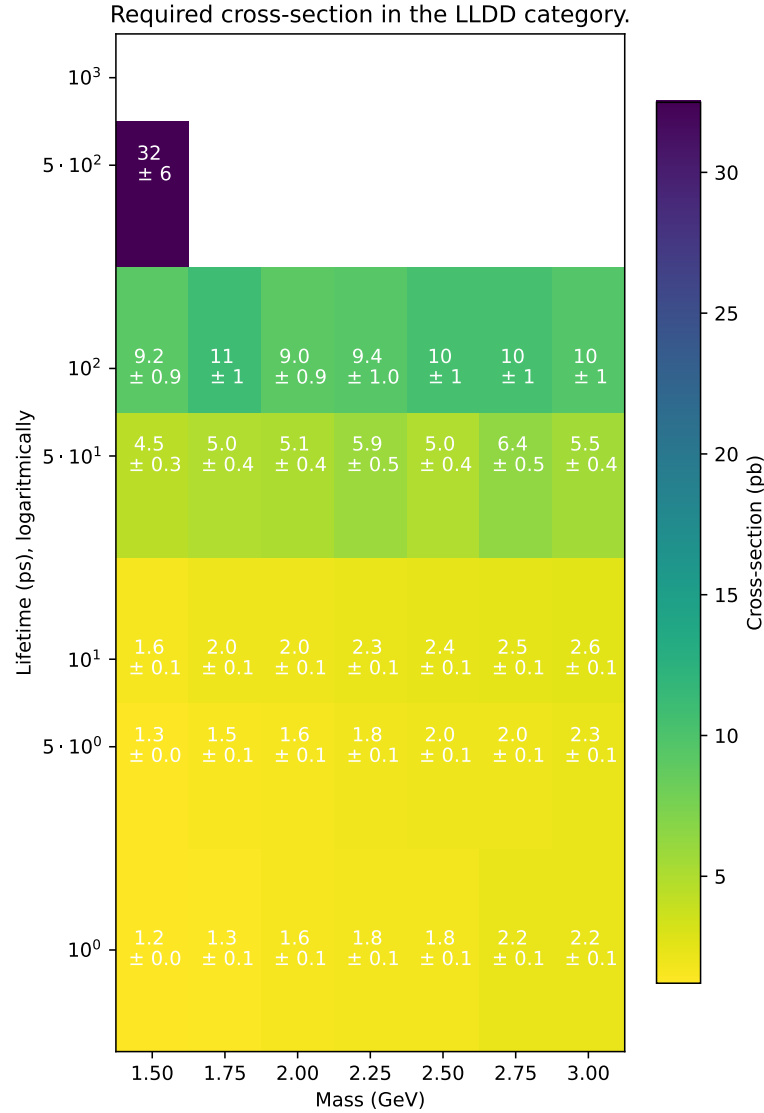
Figure 4.15: *The required cross-section of the Higgs-like boson to have 50 dark pions in Run 2 for the 500 GeV Higgsmass scenario in the LLDD category. The white cells are left out because there the number of dark pions passing from the simulation is less than 5 times its error. The dependence on lifetime and mass is similar to the expected number plots, but in reverse.*

Percentage of the difference in cross-section in the LLDD category.
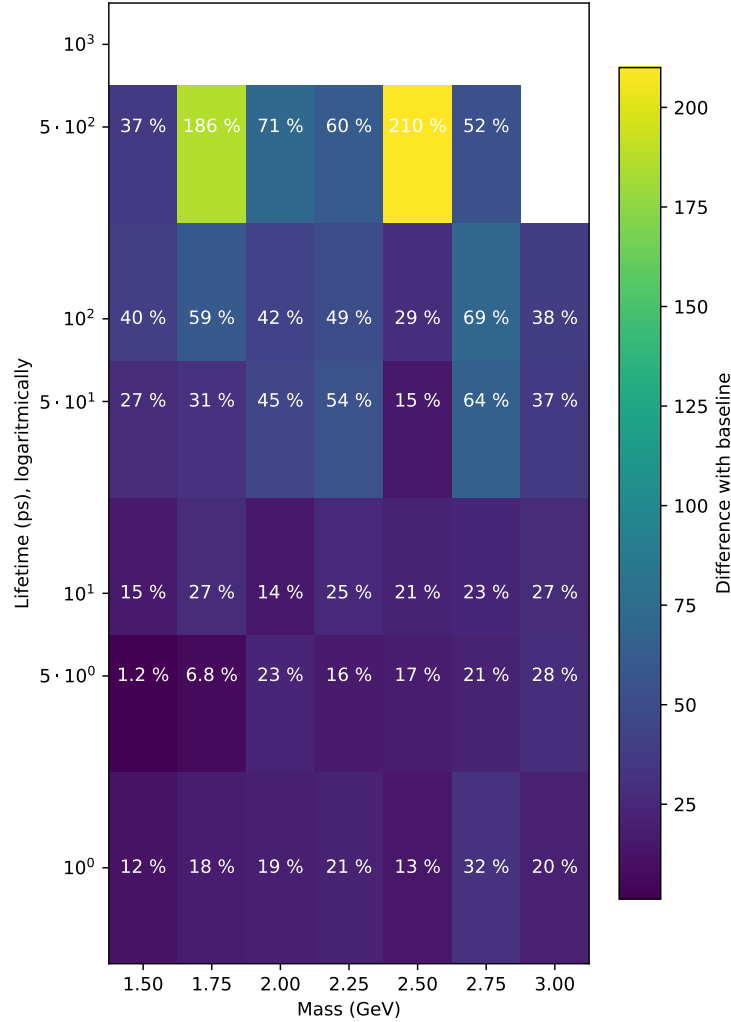
Figure 4.16: *The percentual difference for the 500 GeV Higgs mass scenario in the LLDD category. The whitespaces indicate the points left out because there the number of dark pions passing from the simulation is less than 5 times its error in the baseline model. Generally we see an increase of required cross-section in this scenario, with some dependence on lifetime.*

Next for the 50 GeV Higgs mass, the number of dark pions produced in this scenario, from lowest to highest mass, is around: 62k, 56k, 51k, 47k, 44k, 42k, 39k. This is about 60% of the baseline model.

The resulting required cross-section can be seen in figure 4.17. The same story as for the 500 GeV applies here: a shape similar (but in reverse) of the expected number plots of the baseline model can be seen, where a larger cross-section is needed as lifetime increases, with relatively large jumps between the 10 and 50 ps, and the 50 and 100 ps lifetimes; the large jump from 100 to 500 ps is however also visible here, unlike in the 500 GeV case. The dependence on the mass is also similar, as the cross-section increases with mass, but this increase is smaller than the one due to changing lifetime. Interestingly, there is a stronger mass dependence visible for the 500 ps lifetime here as well.

The difference between the two masses does become visible when looking at the percentual difference with the baseline model in figure 4.18. There is now a decrease of required cross-section at the largest lifetimes, which turns into an increase again as you move to smaller lifetimes. So where there was a growing increase with lifetime in the 500 GeV mass case, there is now a shrinking increase that even turns into a decrease. There does seem to be a small increase in cross-section overall. An exception to the lifetime dependence is visible at 500 ps, where there suddenly is a large increase at 1.5, 1.75 and 2.0 GeV that then decreases with mass.

Then considering the results for LLLL and DDDD in appendix A, there is essentially nothing new compared to the 500 GeV mass. Both LLLL, in figure A.33, and DDDD, in figure A.35, show the lifetime and mass dependence as familiar from the 500 GeV mass scenario.

Looking at the difference plot for LLLL in figure A.34, the only difference with the 500 GeV mass is that most percentages fall in a slightly smaller range from -20% to 5%; compared to LLDD there seems to be a small decrease in cross-section overall. It is still not clear to see if there is also a lifetime dependence for the difference here, like there is in LLDD; the points look as random as in the 500 GeV result.

Lastly there is the difference plot for DDDD in figure A.36, which compared with the 500 GeV mass actually has most percentages fall in the same range from 0% to 30%, but with smaller outliers. Compared to LLDD there are only increases in cross-section here, no large decreases. The lifetime dependence of LLDD is again not visible here, like for the 500 GeV result.
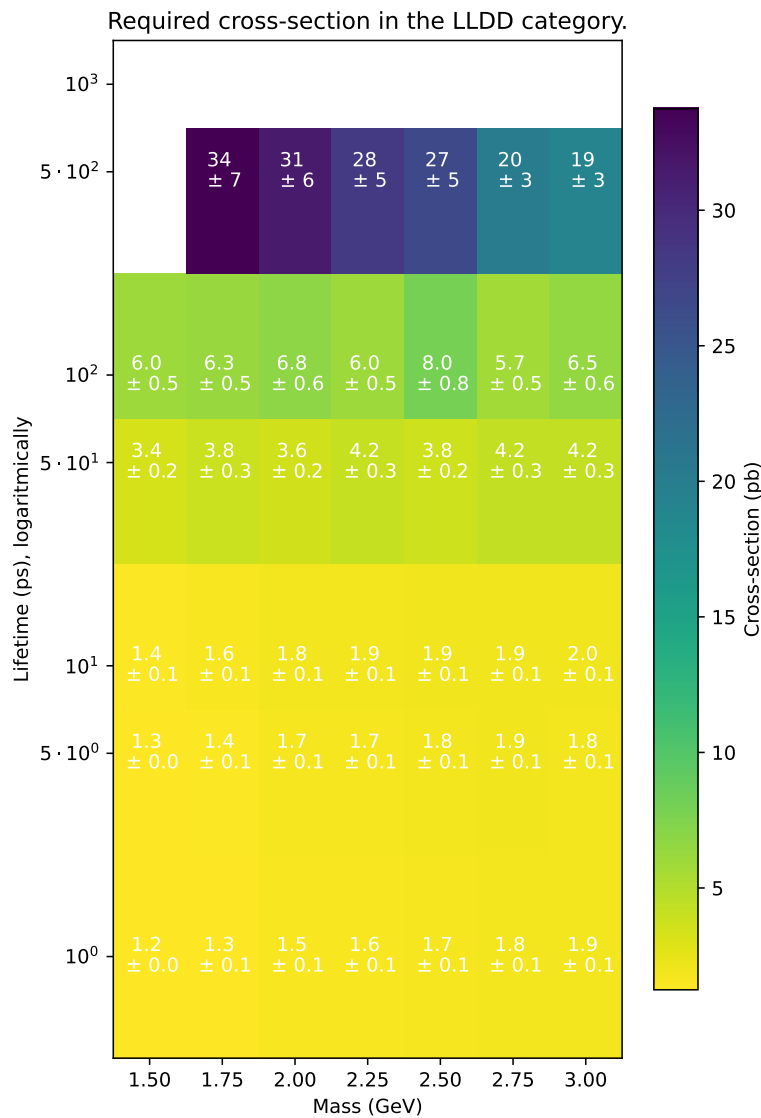
Figure 4.17: *The required cross-section of the Higgs-like boson to have 50 dark pions in Run 2 for the 50 GeV Higgsmass scenario in the LLDD category. The white cells are left out because there the number of dark pions passing from the simulation is less than 5 times its error. A similar but reverse shape to the baseline expected number of dark pions plot is visible here, like for the 500 GeV Higgs mass.*

Percentage of the difference in cross-section in the LLDD category.
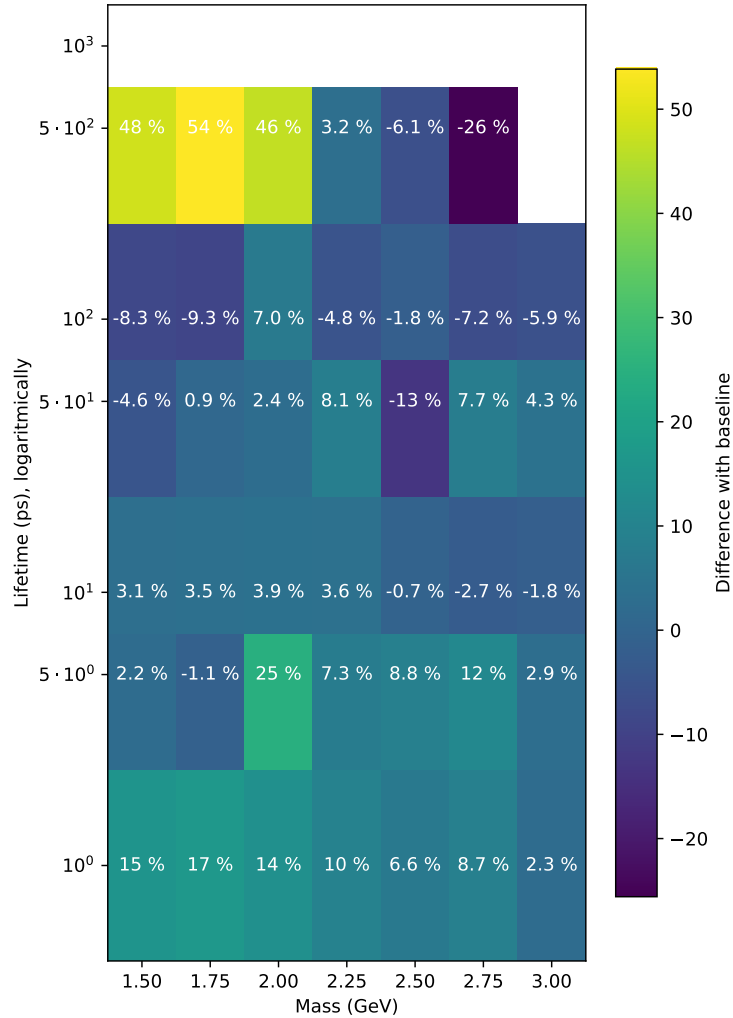
Figure 4.18: *The percentual difference for the 50 GeV Higgs mass scenario in the LLDD category. The whitespaces indicate the points left out because there the number of dark pions passing from the simulation is less than 5 times its error in the baseline model. There is a decrease of required cross-section at the largest lifetimes, but an increase at the smallest lifetimes; this is the opposite of what happened for the 500 GeV mass case.*

Finally, we consider the 1250 GeV Higgs mass scenario (which is a mass 10 times that of the SM Higgs mass).

The number of dark pions produced in this scenario, from lowest to highest mass, is around: 257k, 229k, 208k, 190k, 176k, 163k, 153k. This is about 2.4 times as much as in the baseline model.

The resulting required cross-section can be seen in figure 4.19. Like for 500 GeV and 50 GeV mass, the same mass and lifetime dependence as in the baseline model is visible here. Here we have clear jumps in passing number between 10 and 50 ps and 50 and 100 ps as well.

Looking at the percentual difference with the baseline in figure 4.20, it is quite similar to the differences for the 500 GeV mass. There is an overall increase in required cross-section, as almost every percentage is higher for 1250 GeV mass than for 500 GeV. The same lifetime dependence is also visible, namely a larger increase for larger lifetimes. This increase seems slightly stronger than for the 500 GeV mass, reaching around 80% a number of times while this was about 70% for 500 GeV. There are some especially large variations at the 500 ps lifetime, most notably at 2 GeV mass.

For the LLLL and DDDD results in appendix A, the required cross-sections in figures A.37 and A.39 are very similar to the 500 GeV case, so we will not discuss them further. As for the percentual differences in figures A.38 and A.40, the LLLL result is almost the same as well, although the percentages are higher, as was the case for LLDD, here ranging mostly from 30% to 110%; the same holds for the DDDD result which now has most percentages between 20% and 70%.
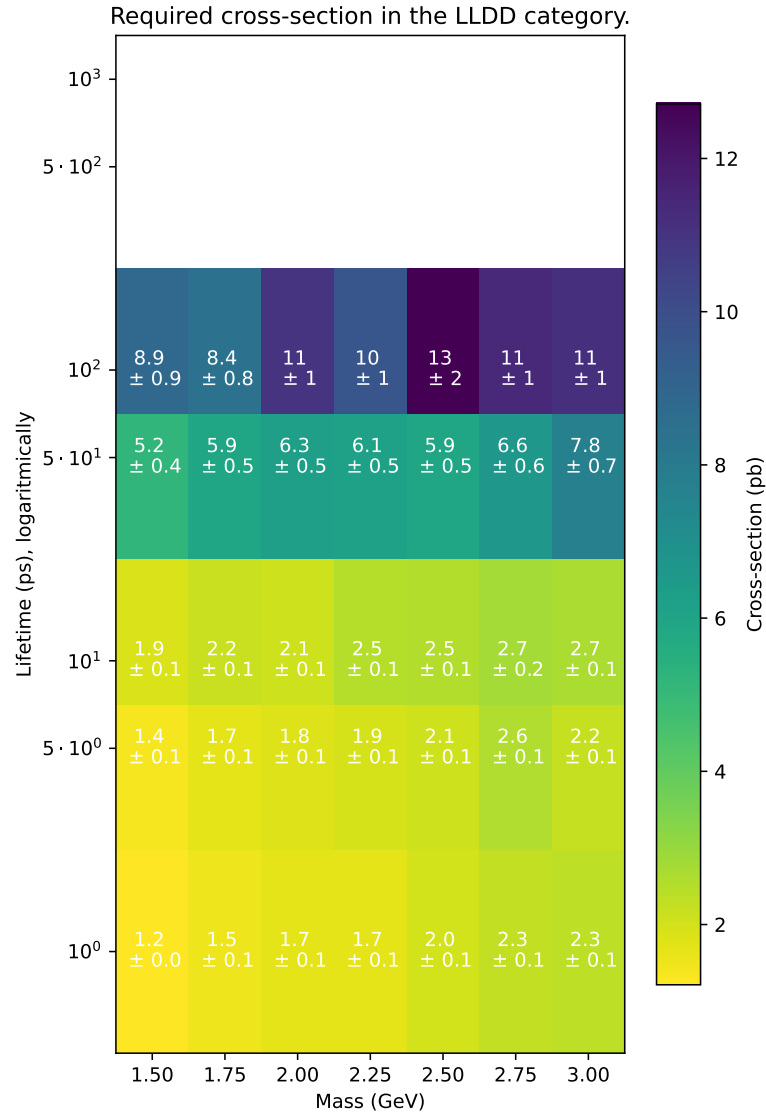
Figure 4.19: *The required cross-section of the Higgs-like boson to have 50 dark pions in Run 2 for the 1250 GeV Higgsmass scenario in the LLDD category. The white cells are left out because there the number of dark pions passing from the simulation is less than 5 times its error. The same similar but reverse shape to the baseline model expected Run 2 number plot is visible, just like for the 500 GeV and 50 GeV masses.*
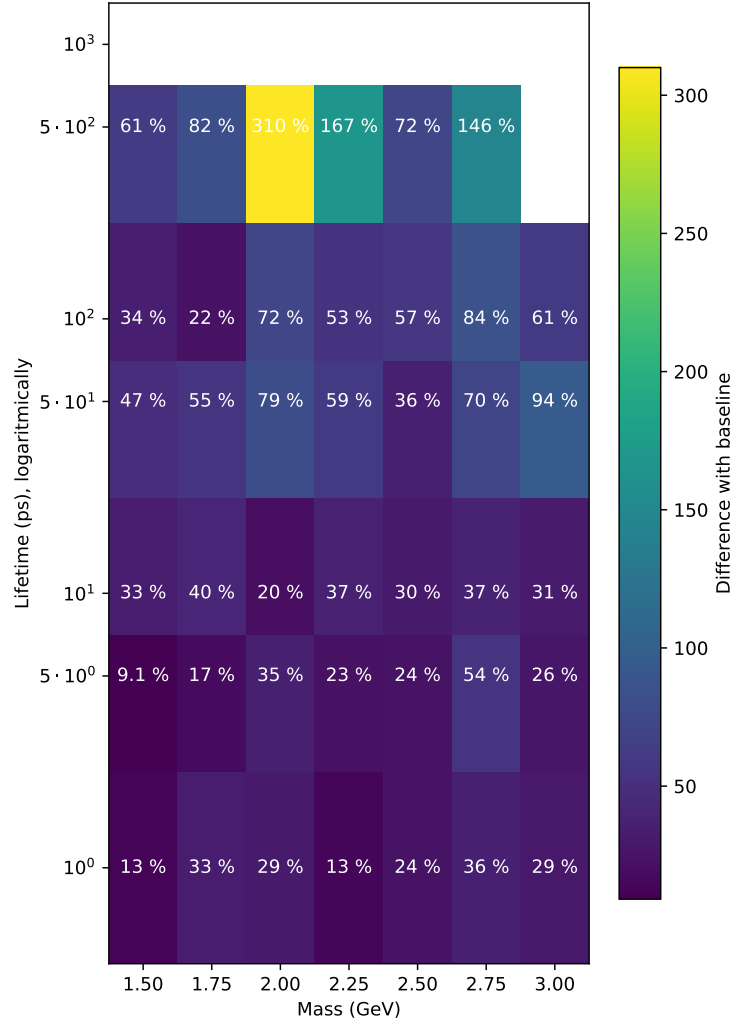
Figure 4.20: *The percentual difference for the 1250 GeV Higgs mass scenario in the LLDD category. The whitespaces indicate the points left out because there the number of dark pions passing from the simulation is less than 5 times its error in the baseline model. An overall increase compared to baseline is visible, as well as a lifetime dependence similar to the 500 GeV case.*

5

Chapter

Discussion

In this chapter, we discuss the results obtained for each scenario. These are interpreted and explained. At the end, an outlook is given for future research.

The results for the LLLL and DDDD categories will not be discussed here, only those for LLDD, but generally the same reasoning can be applied to explain those results. We choose LLDD because this was the best performing category, with overall the most expected dark pions.

5.1   Baseline model

Let us first discuss the very clear dependence of the expected numbers on mass and lifetime as noted in the Results chapter, which returns in every other scenario as well.

5.1.1   Lifetime dependence

The lifetime dependence is a fairly simple consequence of particles needing to decay in the right detector. Of course, a larger lifetime means that the dark pions will (on average) travel a larger distance before decaying. For the LLDD and LLLL categories, which both need the dark pion to decay within the VELO right at the vertex of the pp collision, we thus see that a larger lifetime means the dark pion is more likely to just fly out of the detector; this means it will be cut out. Therefore as lifetime increases, the passing number decreases. The difference between LLLL and LLDD comes from the K_S^0: since it is long-lived it will also travel some distance, making it more likely to decay in the TT than the VELO. Thus LLDD performs better than LLLL. For DDDD, the dark pion needs to decay in the TT, and so it has to travel some distance to get there. This

explains why almost no particles pass at the lowest lifetimes (as the LLLL/LLDD results show, those decay mostly before the TT), and why for larger lifetimes the passing number increases: these particles live long enough to reach the TT. For even larger lifetimes however, the dark pions fly out of the TT as well, and so the passing number reduces again.

We do see that there are extra sharp transitions between the passing number from 10 ps to 50 ps lifetime, from 50 ps to 100 ps lifetime and from 100 ps to 500 ps lifetime. To understand those, we may consider the distributions of the coordinates of the dark pion when it decays, z_{decay} and R_{decay}, shown together in figure 5.1.

One thing to keep in mind here, is that these distributions look different than one would expect given the $\hat{\pi}$ lifetimes: particles travel larger distances than they should, even if they all moved at the speed of light. What happens here is not that they move faster than light, but that the decay times are affected by time dilation due to the particles' relativistic speeds. The effective lifetime is then $\tau_{\text{eff}} = \gamma \tau$ and so the particles indeed have larger decay times and can travel larger distances.

Now for z_{decay} we see there is a large jump around the cut between 100 ps and 500 ps lifetimes, so starting at 500 ps a significant amount of $\hat{\pi}$ are not able to stay within the VELO anymore, which explains the sharp drop in passing number there. For other lifetimes this cut has only a small or no effect.
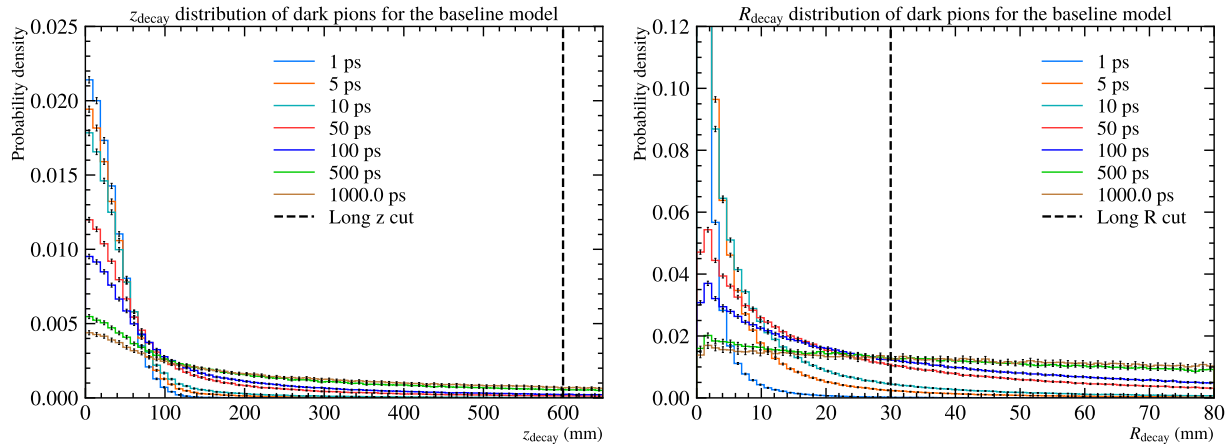
Figure 5.1: *The normalised distribution of z_{decay} and R_{decay} of the dark pion. The upper bounds for each cut are also plotted. We see large changes in the number of particles able to make the cut at 500 ps for z_{decay} and at 50, 100 and 500 ps for R_{decay}.*

For R_{decay} there are already particles not making the cut at 5 and 10 ps (which shows why there is a decrease in passing number there), but between

10 and 50 ps there is a large change visible with relatively a lot more particles above the cutting line, explaining the sharp decrease in passing number between those lifetimes. Then from 50 to 100 ps and 100 to 500 ps similar large changes can be seen, explaining the sharp drops there as well.

The fact that the 100 to 500 ps transition is the largest is likely because both the z_{decay} and R_{decay} cut have an effect there, while for lower lifetimes only the R_{decay} cut has influence.

5.1.2 Mass dependence before cuts

The mass dependence can be explained by looking at the number of dark pions that are produced, so the number we have before any cuts are applied, which as seen in the Results is 107k, 96k, 87k, 80k, 74k, 70k, 65k. Using exact numbers, the factor between next neighbours is, from lowest to highest again: 1.11, 1.10, 1.09, 1.08, 1.07, 1.06 (e.g. 107k/96k = 1.11)[*]. As the error on these is at most 0.006, we can say there is a statistically significant decrease visible for this factor.

Let us explain these numbers first, and then get back to the results after the cut. To do this, consider the distribution of the total energy of the dark pions in figure 5.2, plotted for each mass. (Note that these are from the data with 1 ps lifetime, but there is no difference between the energy distributions at different lifetimes.) Here we see that each distribution peaks slightly above the dark pion mass. This means that most dark quarks that formed a dark pion, had an energy not much larger than the required binding energy to form the dark pion; if it were much larger, the dark pions themselves would have a much greater energy as well. Now the energies of the dark quarks are the same regardless of dark pion mass, as the dark pions have no influence before they are formed. Thus if we increase the dark pion mass, there is actually a significant amount of dark quarks that no longer have enough energy to form a dark pion. As a result, the number of dark pions that are produced decreases with mass, as we saw. On top of this, in the region after the peak up to about 40 GeV, there are still more light than heavy $\hat{\pi}$ produced. This is because for a given energy, there are more momentum states accessible for a lighter $\hat{\pi}$, giving a larger phase space for the final state, and so it is more likely to form this lighter $\hat{\pi}$. At the very largest energies (starting around 40 GeV here) the $\hat{\pi}$ mass becomes irrelevant and there is no difference between the distribution for different masses anymore.

---

[*]There is a decrease visible in this factor, which has to do with the slope after the peak becoming less steep as mass increases; this is irrelevant for now, but will be for the dark rho scenario, so it is discussed there.
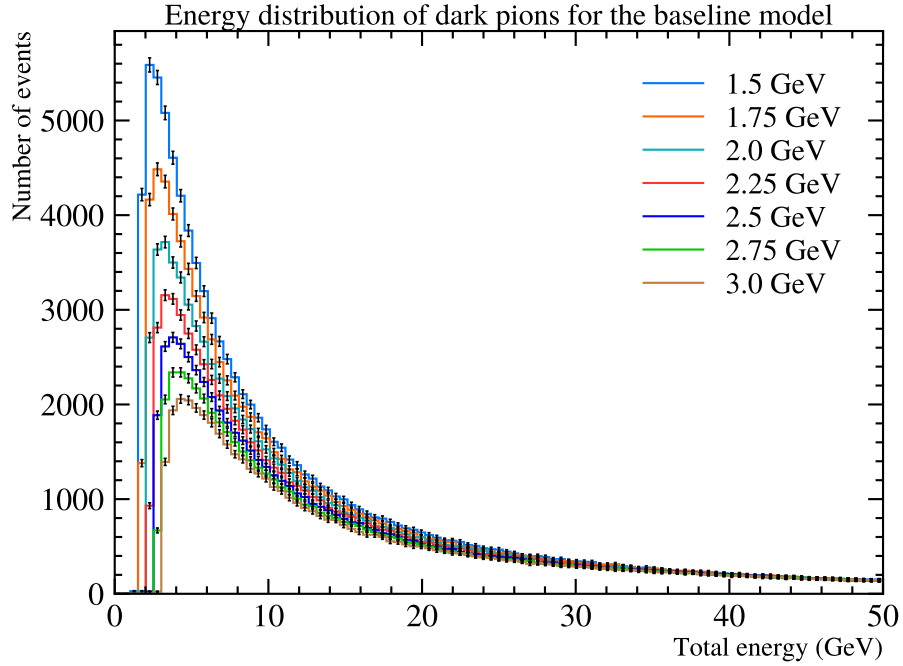
Figure 5.2: *The energy distribution of dark pions at each mass (for a 1 ps lifetime), before applying cuts. Note the energy peaks only just above the dark pion mass for each curve, indicating many dark pions are formed without much extra energy. Starting around 40 GeV, all different mass curves overlap.*

5.1.3 Mass dependence for small lifetimes after cuts

Now returning to results after the cut, the question is whether the cuts change the mass dependence at a given lifetime; that is, does the factor change compared to the one of the produced numbers? Using the 1 ps lifetime row in figure 4.1, the factor between next neighbours is (again lowest to highest) 1.06, 1.15, 1.12, 1.08, 1.04, 1.10. So no decrease is visible in this factor, like there was before doing cuts. However, the error on these is at least 0.07, so we cannot say for sure whether there is a difference between this and the uncut numbers. We can say that the influence of the cuts is similar for each mass; there is no visible mass dependence introduced by the cuts that was not there already.

To explain the apparent indifference of the cuts to mass, at low lifetimes, we may look at the percentage of dark pions cut out (relative to the total amount) by each cut for the 1.5 GeV mass and 3.0 GeV mass, at 1 ps lifetime. This shows that more of the charged particles pass the cut for total and transverse momentum. Most notably the total momentum cut goes from about 20% to about 28% for each charged particle. (The combination of all momentum cuts goes

from 7.6% to 9.0%.) Physically, this happens because a larger $\hat{\pi}$ mass gives the charged particles resulting from its decay more momentum, so that more make the momentum cut. There are no other large changes visible, so based on the increased passing percentage for momentum we may expect the mass dependence to be smaller after the cuts. However, one must consider that a particle that does make the momentum cut, can still be removed by another cut. Because of effects like this, where different cuts overlap, we get the result that the mass dependence from the momentum cuts is negligible compared to the mass dependence induced by the production (within the uncertainty). Let us then find out what the overlap is in this case.

There is an increase in momentum and thus in speed, so we may consider what changes about the travelled distances of the particles, and the positions they reach. The relevant positions are those of the $\hat{\pi}$ and K_S^0 when decaying. The dark pions mostly won't make it out of the detector at 1 ps lifetime, which is confirmed by the 99% passing rate they have for their R_{decay} and z_{decay}. The K_S^0 needs to reach the TT though, so it might seem advantageous if it's given more momentum by a heavier $\hat{\pi}$. But given that it needs to decay into two pions with momenta over 5 GeV to make the cut, and it has a mass of about 0.5 GeV, it will need a momentum of at least about 10 GeV. So the K_S^0 is already relativistic, meaning an increase in momentum will not change its speed much as it's essentially moving at the speed of light already anyway. Then there may still be a way for the K_S^0 to reach the TT if the $\hat{\pi}$ it originates from moves faster, so that it has less distance to travel itself. However, the same reasoning holds for the $\hat{\pi}$, which needs to decay into a 10 GeV K_S^0, a 10 GeV K^- and a 5 GeV π^+, so it needs about 25 GeV itself, making even the heaviest 3 GeV $\hat{\pi}$ relativistic. In the case of dark pions we actually expect a slight decrease in momentum with mass, since they originate from the same dark Higgs, so as more energy is used up for mass, less energy is left as kinetic energy. But this decrease also has no effect on the velocity, as a small decrease won't change the $\hat{\pi}$ from being relativistic.

(We can confirm this by looking at the distribution of the z-components of the velocity of the $\hat{\pi}$ and K_S^0. These are not plotted here, but were checked and show no change with mass.)

There is however another thing to consider besides change in speed, namely the time dilation of the decay times of the K_S^0. In terms of momentum, we can write the Lorentz factor as $\gamma = \sqrt{1 + p^2/m^2}$, so in the limit of large momentum, $p \gg m$, we get $\gamma \to p/m$. Thus an increase in momentum will mean that the K_S^0 decays later, and so it can travel a larger distance. Because of this, more K_S^0 do end up passing the z_{decay} cut as dark pion mass increases; at 1 ps the passing percentage changes from 5.3% for 1.5 GeV to 6.6% for 3.0 GeV.

Another note is that we can also look at the situation differently: a K_S^0 that did make the TT but only produced a pion with (say) 4.5 GeV energy, may end up producing a (say) 5 GeV pion for a larger $\hat{\pi}$ mass, so that it now makes the $P_{\text{total}} > 5$ GeV cut. So there can also be particles that did make the TT but didn't have a large enough momentum, but do now. This would then increase the number of particles passing at larger $\hat{\pi}$ mass. Additionally, the other kaon and pion originating from the dark pion benefit from the extra energy as well, adding more particles passing at larger $\hat{\pi}$ mass.

We can of course check what happens when we combine the z_{decay} cut for K_S^0 and the momentum cut for the pions that originate from it, as well as the momentum cut of the kaon and other pion, at 1 ps lifetime for 1.5 GeV and 3.0 GeV masses. Then we have 1.42% passing at 1.5 Gev and 1.57% passing at 3.0 GeV; there is a factor 1.10 between them. This is quite small still, especially compared to the production factor, which is about 65k/107k ≈ 0.61.

There are also other cuts to take into account, namely those in pseudorapidity. They seem to change less significantly, from about 12.3% (for 1.5 GeV mass) to 12.2% (for 3.0 GeV) for each charged particle. Yet when they are combined for all four charged particles, a larger change appears: from 8.0% to 6.6%, a factor 0.83 between them. Physically, less particles fall in the right η range when $\hat{\pi}$ mass increases because a heavier $\hat{\pi}$ cannot be boosted as much in the z-direction: as more energy is taken up by its mass, less is left for its kinetic energy. As most $\hat{\pi}$ are moving in the forward/backward direction, this means they are less forward/backward boosted. Heavier $\hat{\pi}$ then move slightly more transversely, so that their decay products also move more transversely, and thus they go outside the η cut range.

Now also taking the pseudorapidity cut along with the z_{decay} K_S^0 and the momentum cuts, the overall passing percentage changes from 0.82% to 0.77%, a factor 0.94. So there is actually a small decrease for larger mass when η is taken along. But compared to the production factor of ≈ 0.61, this effect is quite small still. Combined we have $0.61 \cdot 0.94 \approx 0.57$; given the 1 ps, 1.5 GeV passing number we have $0.57 \cdot 475 \approx 270$ which is within 1σ if the 3.0 GeV passing number 281 ± 13. The other cuts may also add some small mass dependence to this, but overall the discussed cuts are able to explain the final results within our uncertainty.

5.1.4 Mass dependence for large lifetimes after cuts

On the other hand, we can see that at higher lifetimes the mass dependence present from the different production number disappears: here the passing number is about the same for each mass. So here the cuts must be taking out more dark pions at low mass than at high mass, to make the final result equal.

Of course, we have just seen that increasing mass increases the momentum as more particles pass that cut. But then the cuts on the relevant positions need to change at larger lifetimes, so that the combination of them does not stay the same like we saw at low lifetimes.

One difference at the larger lifetimes is that more K_S^0 are able to reach the TT. (The main reason the number of particles decreases here is because $\hat{\pi}$ start flying out of the VELO, mostly radially.) The percentage of particles that pass the K_S^0 z_{decay} cut goes from about 6% at 1 ps to 13% at 500 ps. We however no longer see a clear increase here due to the increase in K_S^0 lifetime from time dilation. This is because at this point, they are able to fly out of the TT as well, so that increasing lifetime removes about as many particles as it adds in the required z range. Simultaneously, it is worth reconsidering if the other effect we noted before, that a K_S^0 may have reached the TT already but did not have enough momentum to give to its decay products to make the momentum cut, and does have enough momentum with a larger $\hat{\pi}$ mass, becomes more influential now, since there are roughly twice as many K_S^0 that reach the TT now.

The combination of z_{decay} cut for K_S^0 and the momentum cut for the pions that originate from it, as well as the momentum cut of the kaon and other pion, at 500 ps lifetime for 1.5 GeV and 3.0 GeV masses, gives passing percentages of 0.49% at 1.5 GeV and 0.82% at 3.0 GeV, with a factor 1.67 between them. This is indeed a larger mass dependence than we saw at 1 ps lifetime, where this factor was only 1.10. Even when we combine the η cut with this again, the change in passing percentage becomes 0.20% to 0.28%, a factor 1.41, so it remains significant. This is able to counter the mass dependence from production quite well: $1.41 \cdot 0.61 \approx 0.86$. Thus in the end, there is almost no mass dependence left, or at least none that is visible within the uncertainty, as observed in the final result; doing the same check as before with the results of the 500 ps row, $0.86 \cdot 22 \approx 19$ is well within the uncertainty range.

5.1.5 Fluctuations

In the results we also see some fluctuations, in the form of small hiccups that disrupt the smooth decrease of passing number. There is the increase at 2.0 GeV mass and 5 ps lifetime and some small increases and decreases between different mass results at larger lifetimes.

One only expects a single maximum when looking at different lifetimes, given the detector layout and the fact that dark pions are able to decay outside the VELO for the smallest lifetimes (e.g. for 1 ps, 99.18% of $\hat{\pi}$ pass the z_{decay} cut, but for 5 ps this already starts reducing, to 96.9%). There then exists the possibility for more K_S^0 to reach the TT as $\hat{\pi}$ lifetime increases, depending on where the cut is exactly, so the maximum does not have to be at the lowest lifetime

necessarily, but there would still be only a single maximum passing number. When looking at different masses, there is no reason to expect a maximum at a certain point due to the different momenta of all particles, so we expect a smooth plot.

The variations seem to occur more often in the LLLL and DDDD plots than the LLDD plot, which seems to be the result of less statistics, since less particles pass for LLLL/DDDD than for LLDD. Then the cause of the variations themselves is likely also a statistical effect, where there are simply more or less $\hat{\pi}$ passing randomly. The fluctuations are also not statistically significant, as they disappear within the uncertainty margin of a given point, and could very well be in between the two points around them.

5.1.6 Reweighting

Finally, let's consider the reweighting results. As noted, the reweighting does a decent job at making the plot smoother. Overall it works quite well.

One thing we do see is that if a generated point has more particles passing than expected and disrupts the smooth decrease, this also happens in the reweighted points based on that generated point, but only for the reweighted ones with a smaller lifetime, not a larger one. This is clearest for the 2.0 GeV and 5 ps point, but more examples are visible in the LLLL plot; you can see these sort of columns that are not are not smooth with the points at masses around them, which start at the generated point with the larger lifetime and stops at the lowest reweighted lifetime. It does make sense that if more particles happen to pass in a generated point, more also pass after reweighting as more weights will be counted as passing too. But with the other generated data added in, this effect should be weakened; this does not seem to happen though. Additionally, it is strange that this effect is only visible for reweighted lifetimes below the generated lifetime, and not also above.

So the deviating generated point only affects the smaller lifetimes, which is not countered by the generated point of the lifetime below. It thus seems like the reweighted passing numbers mostly depend on the generated data with a larger lifetime, and not so much on the data with a smaller lifetime.

Upon closer inspection of the weight formula, this is actually to be expected. As in equation 3.9, the exponential has the factor $t_i \left(\frac{1}{\tau_{\text{gen}}} - \frac{1}{\tau_{\text{target}}} \right)$ in it. So when $\tau_{\text{target}} < \tau_{\text{gen}}$, this is negative, giving an exponentially decreasing w_i, while when $\tau_{\text{target}} > \tau_{\text{gen}}$, this is positive and we get an exponentially increasing w_i. Thus the maximum weight that we divide by when combining the above and below generated data will generally be much larger if $\tau_{\text{target}} > \tau_{\text{gen}}$, so for the generated data below the reweighted lifetime. Then when we sum them together, as

in equation 3.12, the passing number of particles from the 'below' set is much smaller, and so the 'above' set dominates, as observed.

If one wanted to prevent this from happening, the $w_{\max}$ part of the method could be avoided all together, although then its beneficial effect on the distribution cannot be used either. Alternatively, a different way of combining the two reweighted sets than equation 3.12 could be used, e.g.

$$N_{\hat{\pi},\mathrm{Run2}}^{\mathrm{cut}} = \frac{1}{2} \left(\frac{N_{\hat{\pi},\mathrm{sim,below}}^{\mathrm{cut}}}{N_{\hat{h},\mathrm{sim,below}}^{\mathrm{uncut}}} + \frac{N_{\hat{\pi},\mathrm{sim,above}}^{\mathrm{cut}}}{N_{\hat{h},\mathrm{sim,above}}^{\mathrm{uncut}}} \right) N_{\hat{h},\mathrm{Run2}}^{\mathrm{uncut}}. \tag{5.1}$$

Then the influence of the individual $w_{\max}$ drops out in the ratio, and the factor 1/2 serves to average the two by an equal amount. They could also be averaged such that the generated set with a lifetime closer to the target counts more strongly.

5.2 Dark rho scenario

Now we consider the results from the dark rho scenario, where the dark quarks can only hadronise into $\hat{\rho}$ instead of $\hat{\pi}$, which have a mass $m(\hat{\rho}) = 2.5m(\hat{\pi})$, so that they decay into 2 dark pions.

The reweighting results for this scenario will not be discussed further, as they act the same as in the baseline model.

5.2.1 Fluctuations

Let us start by commenting on the large fluctuations we see for this scenario, as they are uniquely occurring here. They are the result of the smaller number of events that we have to work with here. As noted in the Results, we don't get 100k events from the simulations, but only between 58k at 1.5 GeV mass and 750 at 3.0 GeV mass. It seems like this happens because Pythia has more difficulty simulating hadronisation for vector particles like the $\hat{\rho}$, and because it is harder to make hadronisation occur for larger mass hadrons. Due to that last problem, the number of events decreases with mass. (Note that we did have 100k events for all other scenarios.)

Now of course when we have less events, we also have less statistics and so the result will naturally be fluctuating a lot more. And because we have less events as $\hat{\pi}$ mass increases, the fluctuations become larger with mass. So only at the smallest three masses we really have reliable results, where more than 10k events are available. To really analyse this scenario properly, it is necessary to fix the problems in Pythia.

The small amount of events also explains why the reweighting is often not accepted at larger masses, because with less events come less dark pions and so less statistics to work with for the fitting. Then the error becomes large and reweighted data will be rejected. It's also often rejected at higher lifetimes. This was visible for baseline too, but only at reweighted lifetimes above 1 ns, so these are not shown in the plots. So it seems like it is more difficult to fit at these large lifetimes, as the particles are distributed over a larger time range, so that they are further apart and small variations become more important. With the smaller amount of events here, the fits will fail sooner, so that even above 100 ps no reweighted samples are accepted.

5.2.2   Similarity of the result

Then about the result itself, we see that the passing number for this scenario is quite similar to the baseline model. To explain this, we can consider how many $\hat{\rho}$ we expect to be produced based on the baseline model results, assuming that the number of produced particles only depends on mass and not on whether it's a $\hat{\pi}$ or $\hat{\rho}$. We saw this factor between next masses decreased from 1.11 to 1.06, with 65k particles for 3.0 GeV mass. If we assume this decrease continues similarly, then at 3.75 GeV mass (which is the $\hat{\rho}$ mass for a 1.5 GeV mass $\hat{\pi}$) we expect $65\text{k}/(1.05 \cdot 1.04 \cdot 1.03) \approx 58\text{k}$ particles. If we take the factor to be constantly 1.05, as it may not continue decreasing as much, then at 3.75 GeV we expect $65\text{k}/(1.05^3) \approx 56\text{k}$. So whether the decrease continues or not, we expect about 56k to 58k particles to be produced. With this many $\hat{\rho}$, the number of $\hat{\pi}$ is just double that amount, so say around 114k. This is actually very close to the 107k $\hat{\pi}$ we got for 1.5 GeV in the baseline model; it turns out that twice the number of dark rho's produced for 2.5 times the dark pion mass is quite close to how many dark pions are produced at that mass; there are even slightly more now.

Let us discuss a bit more why a decrease in this factor is present (as promised in the footnote in the baseline model discussion). For this, we again turn to figure 5.2. For a certain dark pion mass, let us define the 'next mass point' as the energy corresponding to the mass right above the given one. Then in the figure, we see that as mass increases, there are relatively more particles at energies higher than the next mass point than below it; the slope of the distribution becomes less steep. The dark pions below this point are exactly the ones that can no longer be formed when the mass is increased though, and so the number of dark pions that is *not* 'removed' after each mass increase becomes larger relative to the total amount of particles; the ratio of (remaining particles) over (total particles) increases with mass. Now the factor we have been calculating is the total number of dark pions for a given mass over that number of the mass above it; but the total number of particles for the larger mass is just the number that

remains for the lower mass, and so we are really looking at the ratio of (total particles) over (remaining particles) at one mass: the inverse of what we observe to be increasing. And so the factor between each increase decreases.Now it seems reasonable that the energy distribution keeps evolving similarly as mass increases, so that this effect stays present and so the factor keeps decreasing.

As a check, we can look at how many dark pions were produced in this scenario but correct it for the smaller number of events, to see how many we would expect had we gotten 100k events to work with. Then from lower to higher mass we expect 115k, 104k, 95k, 89k, 83k, 80k, 77k dark pions (e.g. 67k · 100k / 58k = 115k). These are consistently slightly larger than how many we got in baseline; taking the ratio of the number here over how many are in baseline we get 1.07, 1.08, 1.09, 1.11, 1.12, 1.14, 1.18. So this actually increases, which makes sense given that the decrease of produced $\hat{\rho}$ with mass probably keeps getting smaller, so that when we double them we end up with more dark pions than for the lower mass.

Unfortunately, it is very hard to see if there actually is this different mass dependence in the results, because we can only really trust the results at smaller masses. Here the slight expected increase in production number is still somewhat visible, as most percentages are larger than zero, but there is no mass dependence visible between the 1.5 and 1.75 or 2.0 GeV masses.

About lifetime dependence, none is visible. Given that we expect slightly more $\hat{\pi}$ to be produced in this scenario, they would also each have less energy on average (as the total energy must be conserved), but this effect is likely too small to be visible, especially with the smaller number of events we have for this scenario.

5.2.3 Model independence of this parameter

It is hard to say what the exact effect of changing the probability to form a $\hat{\rho}$ instead of a $\hat{\pi}$ is, because we have (much) fewer events to work with. At the smaller masses, the difference is quite small, with slightly more particles expected, and no visible lifetime dependence. At the larger masses, we cannot tell because of the small amount of events. Because of this, we cannot say if there is a different mass dependence; the problems in Pythia have to be solved first. We however do expect some mass dependence, if the decrease in factor between the number of produced particles continues.

Overall, we can conclude that the analysis can be done independently of this parameter at small masses, i.e. up to 2.0 GeV, as the overall increase in particles is small: on average it is about 8%, which is well within the $\sim 20\%$ range of expected experimental uncertainty. At masses above 2.0 GeV, it may be possible.

Changing the mass of the $\hat{\rho}$ to something larger than 2.5 times the $\hat{\pi}$ mass may make the effects we expect here stronger, as then the decrease in produced $\hat{\rho}$ with $\hat{\pi}$ mass is likely even smaller. But to be able to test something like that, it is even more important to solve the problems in Pythia first.

We also consider the percentual change in the LLLL and DDDD categories to see if those are model independent. For this scenario, they both show the same changes as LLDD. For masses up to 2.0 GeV, the average difference is about 17% for LLLL and about -2% for DDDD so both are still within the $\sim$ 20% range of expected experimental uncertainty. Thus for LLLL and DDDD the analysis can be done independently of this parameter as well.

5.3   Dark colour scenario

We now consider the dark colour scenario, where we change the number of dark colours in the dark QCD model from $N_c = 3$ to $N_c = 2$.

The reweighting results for this scenario will not be discussed further, as they act the same as in the baseline model.

5.3.1   Similarity of the result

In the Results section it was already clear that there seems to be no significant difference in passing number with the baseline result, or some different mass or lifetime dependence.

Theoretically, what changes with the number of colours are the coupling constants. The three g_v vertex has a factor N_c in it, and the two q_v plus one g_v vertex has a charge factor $C_F(N_c) = \frac{N_c^2 - 1}{2N_c}$ (for $N_c \geq 2$). So by decreasing the number of colours, we make it less likely for these interactions to occur. One may then expect we end up with less dark pions, because it is less likely for radiation to be emitted and to create dark quarks. This is not necessarily the case however, because the dark shower branchings can still occur if there is more time available.

If we look at the production numbers, these are about 98% of the baseline numbers; they are still within 5σ of each other though. When we combine the differences at each mass however, we get an average difference of 1671 ± 153 particles; this is more than 5σ above 0, so on average we do actually have a difference before cuts. (Or in terms of percentages, we have $-2.0 \pm 0.2\%$ difference.) Looking at the average percentual difference after cuts, it is below zero for each category, but only slightly, and within the standard deviation it could be zero still. Therefore we can say that there are significantly less particles produced in this scenario, but it is by a rather small amount so that there is no

significant difference left after cuts.

So we may conclude that there is enough time for the dark shower to take place mostly like it did before, with only a small percentage of particles that actually did not have enough time and did not form dark pions. Consequently, the final result is the same up to random variations (and a small but insignificant decrease). Since the formation process is essentially the same, we also do not expect a different mass or lifetime dependence in this scenario, as observed. Although with slightly less particles produced, the ones that are produced will have slightly larger energies, which would be beneficial for passing the momentum cuts. But with so few less particles, this effect is not visible in the passing percentages.

5.3.2 Fluctuations

The variations in the expected number results for this scenario (figure 4.6) do not look very different from those in the baseline model, so there's not much to add there. We can take a look at where the larger differences in the percentual difference plot (figure 4.7) come from however. For instance at 2.5 GeV and 100 ps there is a fairly large 20% increase. In this same point, the colour result for the expected number of 76 is about the average in its lifetime row (we see no mass dependence here anymore) which is 80, but the baseline result of 63 is relatively far below the average in the row which is 76.3. So because the baseline result is relatively small here (due to some random fluctuation), the difference is relatively large. The fluctuations thus propagate into the percentages from the numbers they are based on, which makes sense.

In the 500 ps lifetime row we see both the largest increases and decreases. This may be due to the small amount of particles passing there for both the baseline and colour scenario, so that we have less statistics giving a more strongly fluctuating result.

5.3.3 Model independence of this parameter

It is clear that decreasing the number of colours to 2 has a very small effect; there is a possibility that there is a tiny decrease in overall expected number, but within the uncertainty there is no difference. Overall the analysis can be done independently of this parameter, as the average difference of -3.7% is well within the $\sim 20\%$ range of expected experimental uncertainty.

Changing N_c to a larger number than 3 likely has a similar result, barely changing anything. If one keeps increasing it this may eventually lead to an increase in produced and expected Run 2 numbers, following the logic above in the other direction, but we cannot say this for sure. Similarly, setting $N_c = 1$ may

show a statistically significant decrease, as this further decreases the coupling constants. Still it likely will not be a large decrease compared to the baseline model.

We also consider the percentual change in the LLLL and DDDD categories to see if those are model independent. For this scenario, they both show the same changes as LLDD. The decrease seems to be slightly larger, but is still not too drastic on average, with -7.3% for LLLL and -5.0% for DDDD, so well within the $\sim 20\%$ range of expected experimental uncertainty like LLDD. So for LLLL and DDDD the analysis can be done independently of this parameter as well.

5.4   Dark QCD scale scenario

Next we have the dark QCD scale scenario, where we change the dark QCD scale $\tilde{\Lambda}_{\text{QCD}}$ from 4 GeV to first 8 and then 2 GeV.

The reweighting results for this scenario will not be discussed further, as they act the same as in the baseline model. Additionally, the fluctuations in the results for this scenario will not be discussed either, as nothing new is visible here that has not been discussed already for either the baseline model or the dark colour scenario.

5.4.1   Similarity of the result

So looking at the result, there is no added mass or lifetime dependence visible. Overall, there might be a small decrease for the 8 GeV scale, since we also see about a 10% decrease in produced dark pions, but this is not significant after cuts; for 2 GeV no significant difference is seen before or after cuts.

So what would we expect to happen when $\tilde{\Lambda}_{\text{QCD}}$ changes? It essentially is part of what determines at what energies hadronisation can start, so when we increase it, the dark quarks will form dark pions earlier and less shower branchings occur; the q_v do not need to emit as much energy anymore before hadronising. So less q_v are formed, and by extent less $\hat{\pi}$, while the ones that do form are left with more energy.

This seems to explain what we see for the increased 8 GeV scale, where less particles are produced. Because of the increased energy, we also expect more particles to pass the momenta cuts. Looking at the combined passing percentage for all momenta, (at 1 ps and 1.5 GeV, but it's about the same for each simulation) this is about 7.6% for baseline and 8.6% for 8 GeV scale, so there is indeed an increase visible. Combined with the production effect we have $\frac{96000}{107000} \cdot \frac{8.6\%}{7.6\%} \approx 1.0$ so this seems to mostly counter the production effect, so that no significant decrease is visible in the results.

However, when we look at the 2 GeV scale, there is the same amount of particles produced and passing, while here we would expect an increase by the same logic. To get a better idea of what causes this, we may look at the energy distributions of the dark pion in this scenario, shown in figure 5.3. (This plot is for the 3.0 GeV mass, which is chosen because it shows the features of the plot more clearly, but the same ones are also present for the other masses.)

Then we see the 2 and 4 (baseline) GeV scale mostly overlap, although the 4 GeV curve increases slightly faster as we move to smaller energies from about 20 GeV and then dives back under the 2 GeV curve at the peak. The 8 GeV curve has less particles at lower energy.

So what we expect to happen in the plot as $\tilde{\Lambda}_{QCD}$ increases is that the number of particles at lower energies decreases while that at larger energies increases, and that the peak shifts to larger energy, since the decrease in particles gets smaller with increasing energy. For 8 GeV scale the decrease is visible, but the increase is not in the energy range of the plot. The shift is not visible either, as the peak only shifts one bin; the change in $\tilde{\Lambda}_{QCD}$ is probably too small for this to effect to appear. This effect is not visible for the smaller 2 GeV scale either of course.
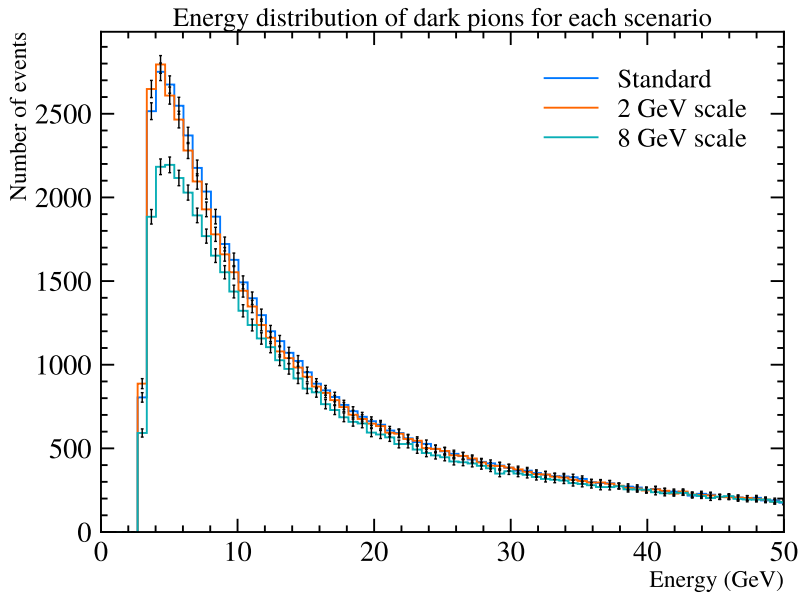
Figure 5.3: *The energy distribution of dark pions, from the 1 ps and 3.0 GeV simulation, for each dark QCD scale scenario. We see the 2 and 4 GeV curves mostly overlap, with only a small change in slope below about 20 GeV. The 8 GeV curve shows less particles at lower energies, as expected.*

What may then be happening here, is that we really expect these effects in the energy distribution of the dark quarks. And that propagates into the dark pion energy distribution, but only if the dark quarks actually form them. We know there is a significant amount of q_v that do not have the required energy to do so from the baseline model discussion. So if any change in the q_v energies only occurs below this required energy, we will not be able to see it in the $\hat{\pi}$ energies.

This can reasonably happen here because the values of the confinement scale are very close to the dark pion mass. But hadronisation is complicated, so it is hard to predict what values of $\tilde{\Lambda}_{QCD}$ will only influence energies below the required energy to form the $\hat{\pi}$. From our results, it seems like this happens at an energy between 4 and 8 GeV.

So just like the 8 GeV scale curve becomes the same as the baseline one at energies of about 30 GeV, the 2 GeV curve is already the same in the entire plot. We do see this small change in slope of the 2 and 4 GeV scale curves, which might be a hint of the 4 GeV curve almost reaching its peak (in the q_v energies). Now in this plot the energy does not abruptly stop and dive to zero once the dark pion mass is reached, as you'd expect when you just cut off the q_v energy, because the q_v that cannot form a $\hat{\pi}$ are not actually created; it is impossible to have such free dark quarks, like for SM quarks, and so these are cancelled in the simulation to give a smoother decrease to zero.

5.4.2 Model independence of this parameter

It is clear that in the end, changing the confinement scale to either 2 or 8 GeV has a very small effect. There is no significant difference with the baseline model. Overall the analysis can be done independently of this parameter, as the average differences of -5.5% for 8 GeV and -3.0% for 2 GeV are well within the $\sim 20\%$ range of expected experimental uncertainty.

Changing $\tilde{\Lambda}_{QCD}$ to an even smaller value likely won't change the result either, as the changes should still be below the relevant energies. Changing to an even larger value might change it, as then the decrease in number of produced dark pions may get larger than the increase in particles passing the momenta cuts. If it is changed too drastically however, hadronisation will play out very differently as well, so this only applies if further changes are not too great, like within one order of magnitude.

We also consider the percentual change in the LLLL and DDDD categories to see if those are model independent. For this scenario, for both the 2 and 8 GeV scale, no significant difference is visible either. For the 8 GeV scale the average difference is smaller, but still not significantly different from 0. At 2 GeV, the average difference is -1.5% for LLLL and -0.7% for DDDD, and for 8

GeV this is -8.7% for LLLL and -7.8% for DDDD, so all within the $\sim 20\%$ range of expected experimental uncertainty. Thus for LLLL and DDDD the analysis can be done independently as well.

5.5 Higgs mass scenario

Finally, there is the Higgs mass scenario, in which the mass of the Higgs boson (and its dark counterpart) is changed from its measured SM value of 125 GeV to 500 GeV, to 50 GeV and to 1250 GeV. The portal is then no longer the Higgs boson but rather a Higgs-like boson.

5.5.1 Overall changes

The first thing to notice for each different Higgs mass is that the number of dark pions that is produced increases with it. In order of increasing Higgs mass, the number of produced 1.5 GeV $\hat{\pi}$ is: 62k for 50 GeV, 107k for 125 GeV, 213k for 500 GeV, and 257k for 1250 GeV. This happens because the simulation starts with a fixed number of dark Higgs(-like) bosons. Since a heavier Higgs(-like) boson will kick off a dark shower with more available energy, more $\hat{\pi}$ will be able to form at the end of it. The extra energy in the simulation is possible because more pp collisions are simulated to create the requested number of Higgs(-like) bosons; in Run 2 conditions, where the number of pp collisions is fixed instead of the number of Higgs(-like) bosons, we thus expect less of them to form as its mass increases. (If you were to calculate the expected Run 2 numbers for a heavier Higgs-like boson, this is accounted for by a lower measured production cross-section.)

Clearly the dependence of produced number on mass is not linear however. This is because the dark pions are formed at the end of the dark shower, and the dynamics there also determine how many are formed. So where a q_v would have reached a low energy and became likely to hadronise before, it may have enough energy for a larger Higgs mass so that it keeps branching and create more q_v. However, this does not happen necessarily, as it is all a matter of probability. It seems like it indeed does not happen for each q_v here, so we do not end up with e.g. twice as many dark pions for a twice as large Higgs mass.

However, these large production differences are not visible in the results after cuts; e.g. the 500 GeV result (figure 4.16) does not have twice as many particles passing than baseline, corresponding to a -100% change in required cross-section, but instead shows increases. To explain this, we may look at the passing percentages again. The most significant change here is in the pseudo-rapidity cut for each charged particle. The combination of all η cuts is around:

11.8% for 50 GeV, 8.0% for 125 GeV, 3.5% for 500 GeV, and 2.7% for 1250 GeV. So the η cut seems to single-handedly make up for most of the difference created by the production. Comparing to baseline, we have $\frac{62000}{107000} \cdot \frac{11.8\%}{8.0\%} \approx 0.85$ for 50 GeV, $\frac{213000}{107000} \cdot \frac{3.5\%}{8.0\%} \approx 0.87$ for 500 GeV, and $\frac{257000}{107000} \cdot \frac{2.7\%}{8.0\%} \approx 0.81$ for 1250 GeV.

The pseudorapidity changes with Higgs mass because early in the process, when the Higgs(-like) bosons are formed from the pp collisions, they will get less kinetic energy if they have a larger mass. So the particles are given less speed and so they are less forward/backward boosted (since anything created from the pp collision is send in the forward/backward direction). Consequently, all particles that are formed from the Higgs, up to the dark pions and the charged particles we apply the cut to, are less boosted for a greater Higgs mass. Thus they cover a larger angular range and are less likely to make the η cut. This can be seen in figure 5.4, showing the distribution of the angle θ the dark pions make with the beamline (which is also representative of the angles the charged particles, on which the cut is actually applied, make). As Higgs mass increases, there clearly are less particles in the forward/backward (around $\theta = 0$ and $\theta = \pi$) region, and more in the transverse region.
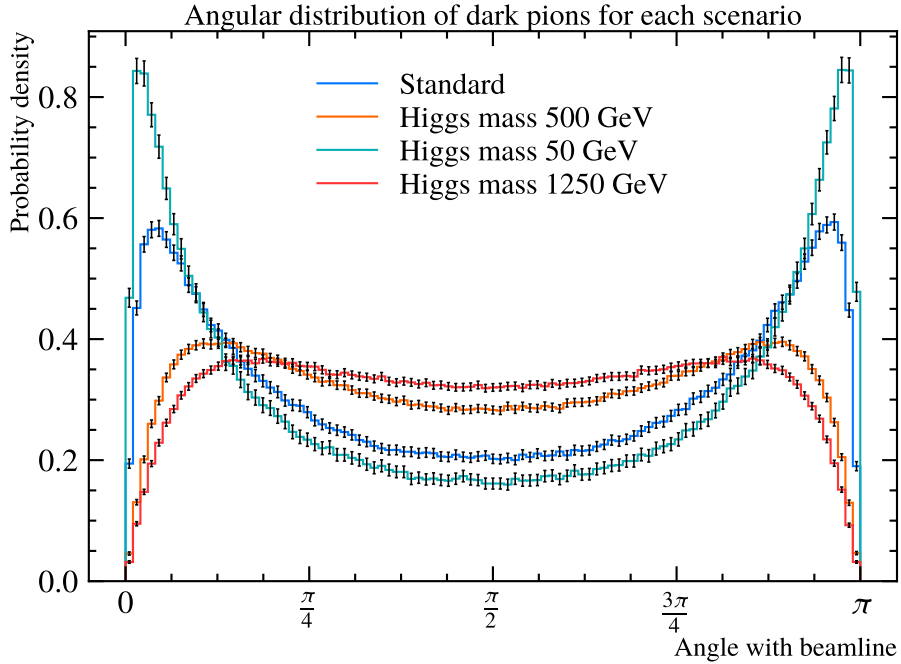
Figure 5.4: *The normalised distribution of the angle the dark pions make with the beamline (from the simulation with 1.5 GeV mass and 1 ps lifetime, but changing these does not change the plot), before applying cuts, for each Higgs mass scenario. We see the particles become less forward/backward as Higgs mass increases.*

Now since the particles only becomes more forward/backward as Higgs mass increases, it may seem unexpected that there is a decrease relative to baseline for the 50 GeV mass. However, recall that there is a lower bound of 0.77° on the angle as well. So as the particles becomes more forward they actually can get below this angle as well, decreasing the number that pass the cut[†].

5.5.2 Lifetime dependence

For the lifetime dependence visible in the results, we first consider what happens at the 1 ps lifetime, and then what happens when we move to larger lifetimes. This is because the average difference in cross-section for each scenario at 1 ps shows an increase with mass: about 10.5% for 50 GeV, 19.3% for 500 GeV, and 25.3% for 1250 GeV.

At small lifetimes

At this 1 ps lifetime the effects of different kinematics for the dark pion cannot be significant, as they decay too quickly, but different kinematics for the K_S^0 can have an effect.

So let us look at the v_z distribution of the K_S^0 for each Higgs mass scenario, in figure 5.5. Here we see there are significantly more particles at high v_z as Higgs mass decreases. This is due to the particles being more forward with lower Higgs mass, as discussed before. With this difference in v_z, it is easier for the K_S^0 to reach the TT as Higgs mass decreases, which we can also see in the cut percentage for z_{decay}: 6.12% for 50 GeV, 5.26% for 125 GeV, 4.74% for 500 GeV, and 4.72% for 1250 GeV. (Additionally, time dilation increases the K_S^0 lifetime for larger velocities which also makes it more likely for them to reach the TT.) Taking these numbers along with the η cut, we get combined passing percentages of 3.7% for 50 GeV, 2.4% for 125 GeV, 1.0% for 500 GeV, and 0.79% for 1250 GeV. Then comparing to baseline we have $\frac{62000}{107000} \cdot \frac{3.7\%}{2.4\%} \approx 0.89$ for 50 GeV, $\frac{213000}{107000} \cdot \frac{1.0\%}{2.4\%} \approx 0.83$ for 500 GeV, and $\frac{257000}{107000} \cdot \frac{0.79\%}{2.4\%} \approx 0.79$ for 1250 GeV. This shows the same mass dependence as the result, with less particles passing (and so cross-section increasing) as Higgs mass increases.

[†]The fact that it's smaller than baseline for both larger and smaller Higgs mass implies the baseline model is at or close to a peak in expected number when the combined effects of production and η for the Higgs mass are considered. As far as I can tell, this is a coincidence.
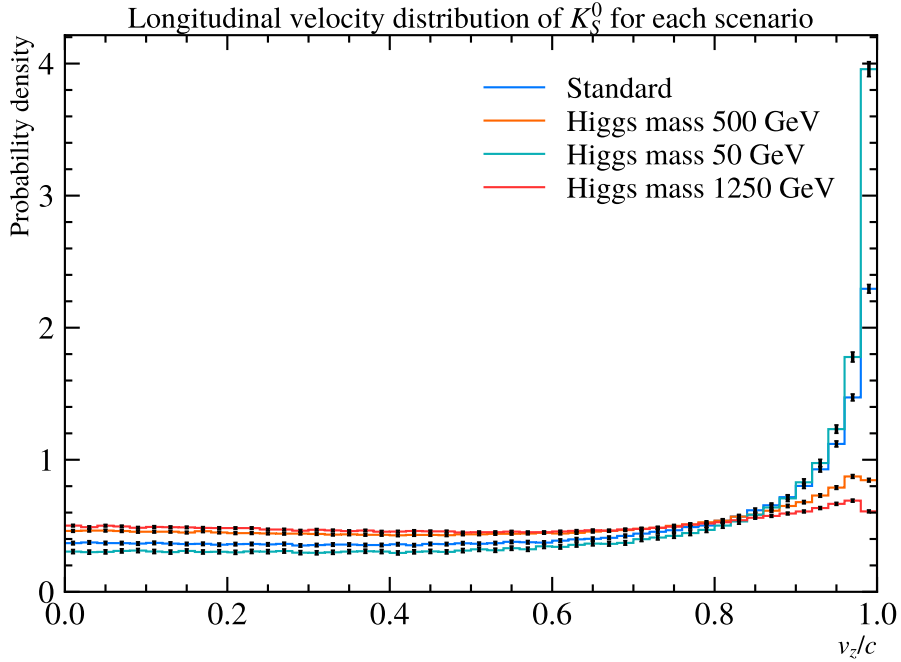
Figure 5.5: *The normalised distribution of the z-component of the velocity of K_S^0 (from the generated set with 1.5 GeV mass and 1 ps lifetime, but these do not change the important features of this plot), before applying cuts, for each Higgs mass scenario. Clearly there are more particles at high v_z for decreasing Higgs mass, which is due to these being more forward boosted.*

Increasing lifetime

Let us then consider what happens when we move to larger lifetimes. Now that we have a noticeable effect of v_z, we expect some lifetime dependence for the percentual difference as well. This can also be seen in the figures 4.16, 4.18 and 4.20: starting at 1 ps, the percentages decrease for 50 GeV, increase for 500 GeV, and increase (a bit more than for 500 GeV) for 1250 GeV.

Now the v_z distribution of dark pions looks similar in shape to that of the K_S^0 in figure 5.5 because the effect of a heavier less boosted Higgs is present here as well. (Due to similarity it's not shown here, but we checked that it looks the same.) If we consider what happens when lifetime increases and the high v_z $\hat{\pi}$ get cut out, we see that relatively more particles get cut as Higgs mass decreases, meaning less particles pass and a larger cross-section is required. However, this is the opposite of what is visible in the plots, so there must be another cut changing the lifetime dependence.

Inspired by the fact that η changes by a large amount due to Higgs mass,

it makes sense to also consider the transverse velocity v_T of the dark pions. However, for the transverse velocity it is quite important to also take the η cut into account, as any high v_T particles will be cut out by that, and so there is quite a large overlap. So the v_T distribution with the η cut applied is shown in figure 5.6. In the high v_T range, and all the way down to about $0.3c$ as well, there are no particles: these have all been removed by the η cut. At lower v_T there are peaks, which shift to higher velocities as Higgs mass increases. This is due to the particles becoming more forward/backward as Higgs mass increases, as we could already see in the θ distribution (figure 5.4)[‡].

Now considering what happens when lifetime increases and the larger v_T $\hat{\pi}$ get cut out, this happens relatively more for the larger Higgs mass, and so less passing particles and a larger required cross-section are expected for larger Higgs mass. This is the opposite of what happens for the z-component, and does agree with the the percentual difference plots. Thus the effect of the transverse velocity dominates over that of the longitudinal velocity. This is to be expected looking at the velocity of the dark pion; the Higgs boson being more or less boosted mostly affects the transverse component.

Looking at cut percentages, we can also see this. We compare the combination of R_{decay} and η cuts with the z_{decay} cut, at 500 ps and 1.5 GeV. For brevity, we only compare with 500 GeV mass, but the others show expected behaviour as well. Then 0.88% make the $\hat{\pi}$ R_{decay} and η cuts in the baseline model, but only 0.33% do for the 500 GeV Higgs mass, so a change of a factor 0.38; for the $\hat{\pi}$ z_{decay} cut this is 41.84% for baseline and 44.39% for 500 GeV mass, so only a change of a factor 1.06. Combining all three of them gives 0.79% for baseline and 0.31% for 500 GeV, so a factor 0.39. Thus there is still a decrease as expected.

Note that the influence of the K_S^0 z_{decay} cut also has an effect here. With more high speed K_S^0 for smaller Higgs mass, as visible in figure 5.5, it is easier for them to reach the TT at the larger lifetimes we consider now as well. However, as the lifetime dependence mostly depends on the things going on in the transverse region, this is not a strong effect. The passing percentage, at 500 ps and 1.5 GeV, is 13.13% for the baseline model and is 12.27% for the 500 GeV mass. Thus only a factor of 0.93; it contributes slightly to the lifetime dependence, but not as much as the $\hat{\pi}$ R_{decay} and η cuts. The combination of cuts on K_S^0 z_{decay}, $\hat{\pi}$ R_{decay} and η gives 0.33% for baseline and 0.12% for 500 GeV, so a factor 0.36, showing the strong decrease still.

[‡]Considering the v_T distribution here, one may wonder if we should also consider it in the baseline model, for the mass dependence observed there; after all, there the η cut changed as well due to the $\hat{\pi}$ mass. Note however that the change in $\hat{\pi}$ mass is much smaller than that in Higgs mass. The effects on the v_T distribution for different $\hat{\pi}$ mass is thus a lot smaller as well. These plots were checked, but no mass dependence is even visible in them, so they don't need to be taken into account.

Transverse velocity distribution of dark pions for each scenario, η cut applied
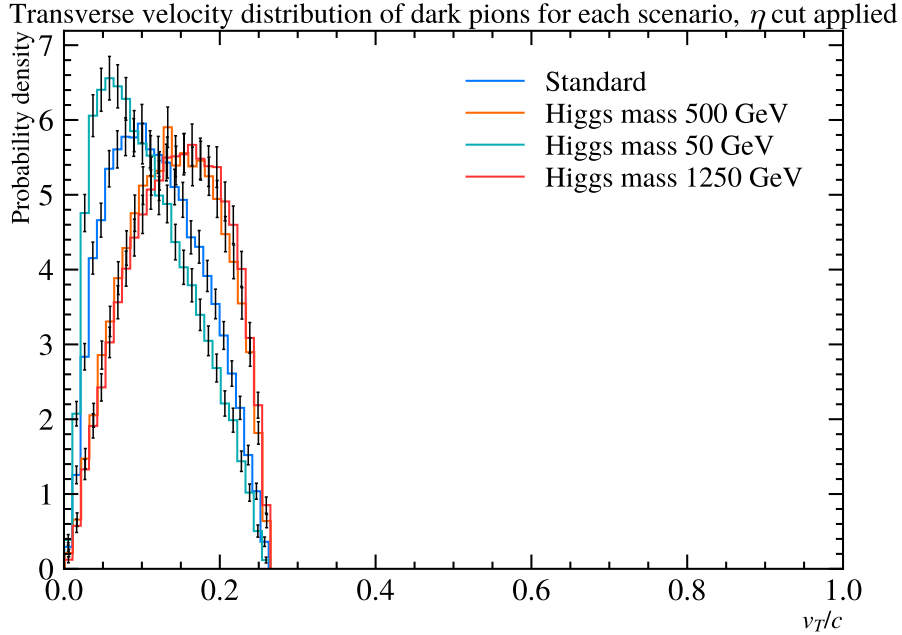
Figure 5.6: *The normalised distribution of the transverse component of the velocity of dark pions (from the generated set with 1.5 GeV mass and 1 ps lifetime, but these do not change the important features of this plot), for each Higgs mass scenario. Here the pseudorapidity cut has been applied as well, since this has a large influence on v_T. We see the peak of each distribution shifts to larger velocities as the Higgs mass increases.*

Note on LLLL and DDDD

In the Results section we saw that the lifetime dependence present for LLDD is not as clear for LLLL and not visible at all for DDDD. Given that a difference in dependence like this uniquely occurs for this scenario, there is this comment.

It seems like this happens because the lifetime dependence is due to the $\hat{\pi}$ R_{decay} cut. For LLLL, this cut is the same, but less particles pass overall which means there is less statistics and so it would become less clear. For DDDD, the cut on the dark pion's decayradius is a lot looser since it needs to decay in the TT. So the $\hat{\pi}$ rarely fly out radially anymore, even at the larger lifetimes, so that the whole effect disappears.

5.5.3   Mass dependence

Having discussed the physics involved in this scenario, we note that there is no different mass dependence, visible in the percentual difference plots. It is hard to say whether we expect this; we see that both the v_z and v_T distribu-

tion change in shape due to the Higgs mass. If the $\hat{\pi}$ become less forward, it may firstly be that a change in p_z due to $\hat{\pi}$ mass does cause a more significant amount of particles to gain more speed in the z-direction, which reduces the mass dependence at small lifetimes. It may secondly be that a change in p_T due to $\hat{\pi}$ mass causes a less significant amount of particles to gain more speed in the transverse direction, which enhances the mass dependence at large lifetimes. We cannot see this however, or at least not within the random variations of the percentual difference. So these effects are probably too small to really change the results.

5.5.4 Fluctuations

In terms of the random fluctuations in the required cross-section, these are not more substantial than we have already seen in the baseline model. There is one thing that stands out, namely that for the 50 GeV Higgs mass, at 500 ps, there seems to be a $\hat{\pi}$ mass dependence visible again: here the required cross-section decreases with mass, meaning more particles pass at larger masses. This is a dependence not seen anywhere else, and also is not gradually appearing in the figure; at 100 ps there is no mass dependence visible, like for the baseline model. The points furthest apart, 34 ± 7 pb at 1.75 GeV and 19 ± 3 pb at 3.0 GeV, are also within 5σ acceptance of each other. Therefore it seems like this is just a statistical effect, where each next mass point has a slightly smaller cross-section than the previous (since the cross-section is the inverse of the passing number, and there are few particles passing at 500 ps, small differences in passing number also look more severe here with different colours than they would in the expected Run 2 number plot). If you look at enough of these plots, something like this is bound to happen eventually.

For the percentual difference plots however, there are some very large percentages visible, as noted in the results. Each occurs at the 500 ps lifetime. The spikes are thus likely the result of the small number of particles passing there, resulting in bad statistics. The reason that such large spiking percentages are not visible in the expected number plots, is because they are exaggerated by the inverse relation of cross-section with passing number. An example is the 500 GeV Higgs mass point at 500 ps and 1.75 GeV: for cross-section the difference is 186%, but for the number of particles passing the simulation (which have the same difference as the expected Run 2 number has if you were to calculate it) it is -65%. This is still an outlier in passing number, as the other percentages are around -30% to -40%, but seems less severe.

This happens because the inverse relation makes the cross-section more sensitive to small changes for a low number of particles passing. Thus it is not true that these spikes in the Higgs mass scenarios show something strange is

happening here that is not present for other scenarios, although it looks like that in the plots; the inverse relation is just more sensitive.

5.5.5   Model independence of this parameter

Overall, the effects from changing the Higgs mass do not cause a large increase or decrease, staying below about ±30%, except at large lifetimes for the 500 and 1250 GeV masses. Still, there is the different lifetime dependence in this scenario. Because of this, it seems like an analysis cannot be done independently of this parameter, except if it were done only for a smaller range of lifetimes (but not for the larger lifetimes for the 500 and 1250 GeV masses, as there the overall change gets too large).

Here it is useful to note that for an analysis with the LLDD category, only a smaller range of lifetimes would actually be used, from 1 ps to 10 or 50 ps, as at larger lifetimes we have more particles passing in the DDDD category (at 50 ps it depends on the mass you look at, so there either category could be used). If we only take the 1 to 10 ps range, the lifetime dependence is quite small for each Higgs mass, and the average difference is about 19% for 500 GeV, 7% for 50 GeV, and 28% for 1250 GeV. So compared to the $\sim 20\%$ expected experimental uncertainty, the 500 GeV and 50 GeV results are fine and the 1250 GeV result is a bit too large, but still quite close; it will likely still be difficult to distinguish. Thus we may carefully say that within this LLDD lifetime range, the difference is acceptable for each Higgs mass and the analysis can be done independently.

Changing the Higgs mass to even larger values than 1250 GeV likely won't change the result much, as we see a fairly small difference between 500 and 1250 GeV already, despite the latter being 2.5 times larger than the former. Changing the Higgs mass to smaller values than 50 GeV may have more influence on the results, as this should make the particles even more forward/backward, but it is hard to predict by how much. Based on the angular distributions (figure 5.4), even more forward/backward is possible. We cannot lower the mass by too much though, as at least 2 GeV is needed to be able to decay to 2 dark quarks in the first place.

We also consider the percentual change in the LLLL and DDDD categories to see if those are model independent. For this scenario, the lifetime dependence as visible for LLDD is harder to see for LLLL, and not really clear for DDDD, as noted before.

For LLLL, the percentual differences are still quite large however. They reach 90% for 500 GeV, and are even quite large when looking only at lifetimes up to 10 ps. The same holds for 1250 GeV, where they even reach 100%. Only for 50 GeV are they within about 20%, and here the lifetime dependence is really not visible. So overall, given a difference of about 20% is acceptable from experi-

mental uncertainty, an analysis cannot be done independently for LLLL either, unless only smaller Higgs masses are considered.

For the DDDD category, the percentual differences are less large. They stay within about 30% for 50 GeV and 500 GeV, but do reach 60 to 70% for 1250 GeV. As there is no lifetime dependence visible here, it may actually be possible to do an analysis independently for DDDD, but likely not for Higgs masses above about 1 TeV, to stay within the about 20% acceptable difference.

5.6 Outlook

There are still other parameters that can be changed in the dark QCD model, namely the final state radiation coupling α_{FSR} and the number of flavours N_f. Additionally, a larger range of parameters than was tested here could be considered as well. Testing these is relatively easy now that the framework for generating results for any set of input parameters, as described in this thesis, exists.

Changing the final state radiation coupling is already studied to an extent here because we varied the number of colours, which also changes the full coupling constant in the end. So varying α_{FSR} would likely have a similarly small effect as varying N_c. Changing the number of flavours would probably have a larger influence however, as the model changes more drastically here since adding another dark quark would allow for many more dark hadrons. All of these will have to be defined, and their masses, lifetimes, decay modes and BR's have to be set. One consequence of this would be that approximately $1/N_f$ of the produced dark mesons can decay back to SM particles [20], thus decreasing the number of expected particles.

Now, from our results it is clear that there are dark pions expected to be in LHCb acceptance. To actually search for these is not easily done however. One thing that will have to be done is to distinguish the signal particles in the dark pion decay mode from background decays, that is, the same signal particles that originate from different decays. A common way of doing this is using machine learning, and this is being worked on for this dark pion study as well. This is done using a boosted decision tree algorithm, which is trained by fully simulating both the dark pion and any relevant background decays (including the LHCb detector in the simulation, so no cuts are applied by hand afterwards). Depending on how well this will separate the signal and background determines if the signal can be found with enough significance. If the signal significance is large enough, it may actually be possible to find the dark pion in the LHCb data (if it's really there).

Chapter 6

Conclusions

For the sensitivity study, it is found that $\mathcal{O}(100)$ particles can be expected in LHCb acceptance for Run 2 conditions in each category in the baseline model, at the right lifetimes. Overall, the LLDD category performed the best with the most expected particles. At larger lifetimes, starting at 100 ps, the DDDD category performs better though. For an analysis, LLDD could be used in the 1 to 50 ps range, and DDDD in the 50 to 1000 ps range (at 50 ps, the better one depends on mass).

For the dependence of the number of expected dark pions on the discussed theoretical parameters, it is found that the difference with the baseline model is generally within the expected experimental uncertainty of about 20%. To summarise the LLDD results:

- For the dark rho scenario, the average difference is about 8% for masses up to 2.0 GeV, so well within experimental uncertainty, although we can only be sure for the smaller masses due to problems in Pythia.

- For the dark colour scenario, the average difference is -3.7%, so well within experimental uncertainty, even with no significant difference with the baseline model.

- For the dark QCD scale scenario, the average difference is -5.5% for 8 GeV and -3.0% for 2 GeV, so both well within experimental uncertainty, and also with no significant difference with the baseline model.

- For the Higgs mass scenario, the average difference for each mass is within $\sim 20\%$ if we consider the lifetime range of 1 to 10 ps, for which the LLDD category would actually be used in analysis. So there the difference is just within the experimental uncertainty. (Overall there is also a lifetime dependence and larger differences however.)

89

The differences for LLLL and DDDD are similar to that of LLDD, so the same conclusions apply. An exception is for the Higgs mass scenario, where there is no lifetime dependence for the DDDD category, so that for the 50 and 500 GeV mass the difference is small at each lifetime.

Overall these results are quite interesting, given that the dark QCD model is complicated; things need not have worked out like this, but it is nice that they do and allow for a theory independent search for dark pions.

Bibliography

[1] R. Aaij et al. Allen: A High-Level Trigger on GPUs for LHCb. *Computing and Software for Big Science*, 4(1), Apr 2020.

[2] Christian Bierlich, Smita Chakraborty, Nishita Desai, Leif Gellersen, Ilkka Helenius, Philip Ilten, Leif Lönnblad, Stephen Mrenna, Stefan Prestel, Christian T. Preuss, Torbjörn Sjöstrand, Peter Skands, Marius Utheim, and Rob Verheyen. A comprehensive guide to the physics and usage of PYTHIA 8.3. *SciPost Phys. Codebases*, page 8, Nov 2022.

[3] Lisa Carloni, Johan Rathsman, and Torbjörn Sjöstrand. Discerning secluded sector gauge structures. *Journal of High Energy Physics*, 2011(4), Apr 2011.

[4] Hsin-Chia Cheng, Lingfeng Li, and Ennio Salvioni. A Theory of Dark Pions. *Journal of High Energy Physics*, 2022(1), Jan 2022.

[5] Douglas Clowe, Anthony Gonzalez, and Maxim Markevitch. Weak-Lensing Mass Reconstruction of the Interacting Cluster 1E 0657-558: Direct Evidence for the Existence of Dark Matter. *The Astrophysical Journal*, 604(2):596–603, Apr 2004.

[6] The CMS Collaboration. Search for invisible decays of the Higgs boson produced via vector boson fusion in proton-proton collisions at $\sqrt{s} =$ 13 TeV. *Phys. Rev. D*, 105:092007, May 2022.

[7] The LHCb Collaboration. Standard set of performance numbers. Available online at https://lhcb.web.cern.ch/speakersbureau/html/PerformanceNumbers.html, last accessed on Oct. 4, 2023.

[8] The LHCb Collaboration. The GAUSS Project. Available online at https://lhcbdoc.web.cern.ch/lhcbdoc/gauss/, last accessed on Dec. 11, 2023.

[9] The LHCb Collaboration. The LHCb Detector at the LHC. *Journal of Instrumentation*, 3(08):S08005, Aug 2008.

[10] Elena Dall'Occo. Searches for long-lived particles with LHCb. In *Proceedings of Science*, Sixth Annual Conference on Large Hadron Collider Physics (LHCP2018), Bologna, Italy, Jun 2018. Available online at `https://cdsweb.cern.ch/record/2667543/files/PoS(LHCP2018)281.pdf`, last accessed on Oct. 21, 2023.

[11] Jonas Eschle, Albert Puig Navarro, Rafael Silva Coutinho, and Nicola Serra. zfit: Scalable pythonic fitting. *SoftwareX*, 11:100508, 2020.

[12] M. Alexander et al. Mapping the material in the LHCb vertex locator using secondary hadronic interactions. *Journal of Instrumentation*, 13(06):P06008, Jun 2018.

[13] I. Belyaev et al. (on behalf of the LHCb Collaboration). Handling of the generation of primary events in Gauss, the LHCb simulation framework. *Journal of Physics: Conference Series*, 331(3):032047, Dec 2011.

[14] J. Gassner, M. Needham, and O. Steinkamp. Layout and Expected Performance of the LHCb TT Station, Apr 2004. Available online at `https://cds.cern.ch/record/728548`, last accessed on Oct. 23, 2023.

[15] K.P. Jablonski et al. Sustainable data analysis with Snakemake [version 1; peer review: 1 approved, 1 approved with reservations]. *F1000Research*, 10(33), 2021.

[16] Simon Knapen, Jessie Shelton, and Dong Xu. Perturbative benchmark models for a dark shower search program. *Phys. Rev. D*, 103:115013, Jun 2021.

[17] LHC Higgs Cross Section Working Group, S. Dittmaier et al. Handbook of LHC Higgs Cross Sections: 1. Inclusive Observables, 2011.

[18] Particle Data Group. Review of Particle Physics. *Progress of Theoretical and Experimental Physics*, 2022(8):083C01, Aug 2022.

[19] Martina Pili. Performance of the LHCb detector in Run 2. In *Proceedings of Science*, 40th International Conference on High Energy physics - ICHEP2020, Prague, Czech Republic (virtual meeting), Jul-Aug 2020. Available online at `https://cds.cern.ch/record/2783948/files/PoS%28ICHEP2020%29767.pdf?version=1`, last accessed on Oct. 23, 2023.

[20] pythia.org. Hidden Valley Processes. Available online at https://pythia.org/latest-manual/HiddenValleyProcesses.html, last accessed on Dec. 11, 2023.

[21] Marian Stahl. Machine learning and parallelism in the reconstruction of LHCb and its upgrade. *Journal of Physics: Conference Series*, 898(4):042042, Oct 2017.

[22] Matthew J. Strassler and Kathryn M. Zurek. Echoes of a Hidden Valley at Hadron Colliders. *Physics Letters B*, 651(5):374–379, Aug 2007.

LLLL and DDDD figures

This appendix contains the figures for the LLLL and DDDD categories. These are the expected number of dark pions in Run 2 both before and after reweighting, and for the different scenarios, the percentual difference. They are discussed in the main Results and Discussion chapters.

A.1 Baseline model

Firstly, the results for the baseline model are shown, before and after reweighting.
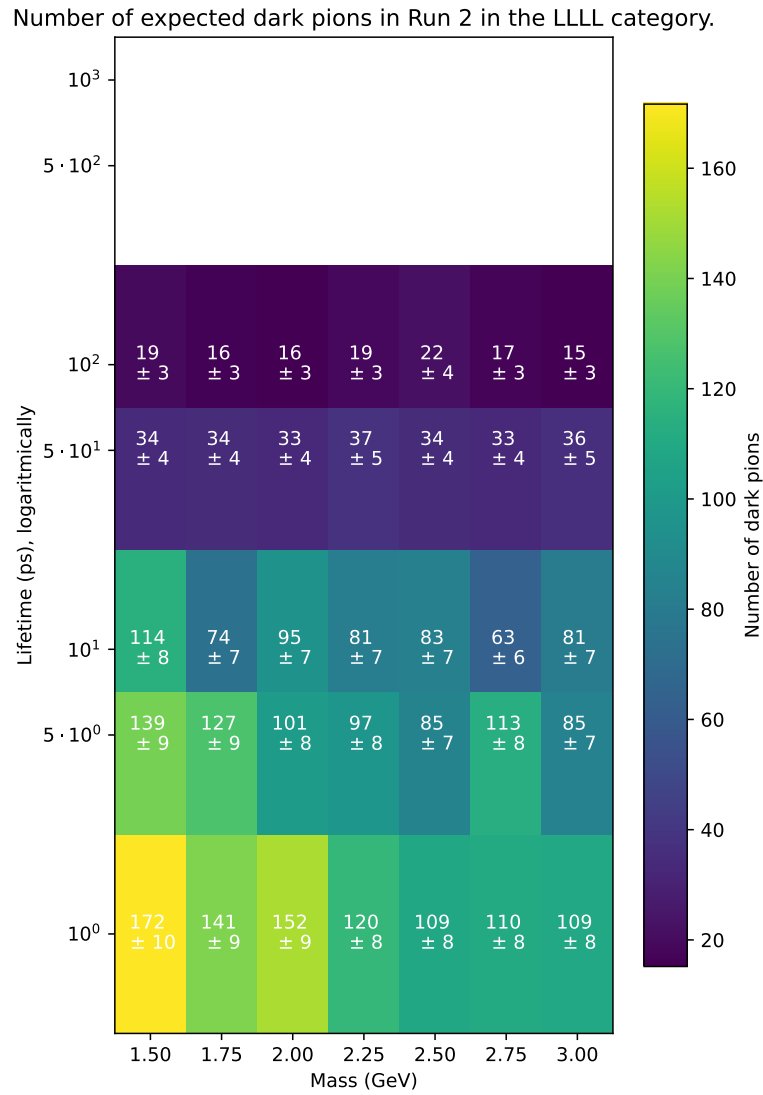
Figure A.1: *The expected number of dark pions in Run 2 passing the cuts in the LLLL category, for the baseline model. The white cells have less particles passing than 5 times their standard deviation. The result is very similar to that in LLDD.*

Number of expected dark pions in Run 2 in the LLLL category.
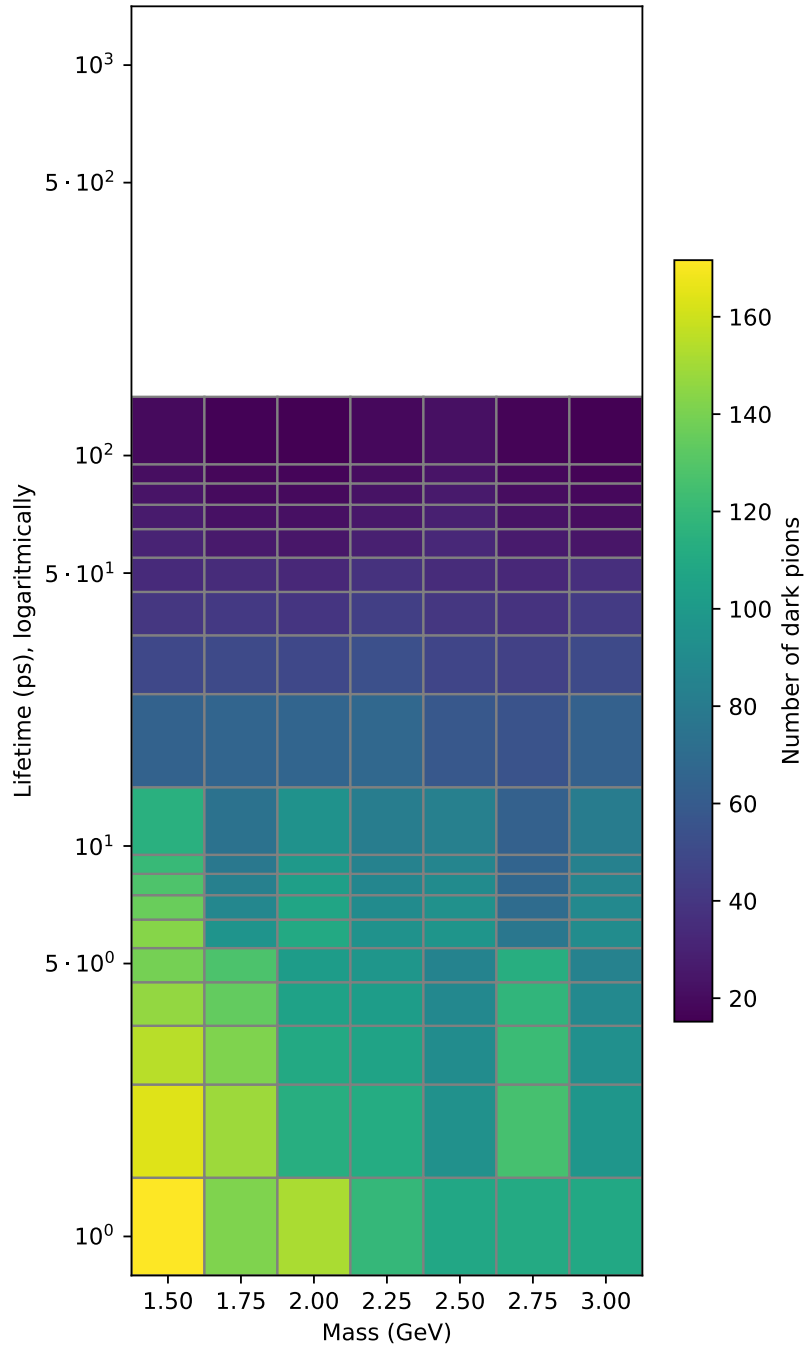
Figure A.2: *The expected number of dark pions in Run 2 passing the cuts in the LLLL category, after reweighting, for the baseline model. The white cells did not pass the statistical criteria, or have less particles passing than 5 times their standard deviation. It can be seen that the reweighting produces a smoother plot, albeit less smooth than for LLDD.*
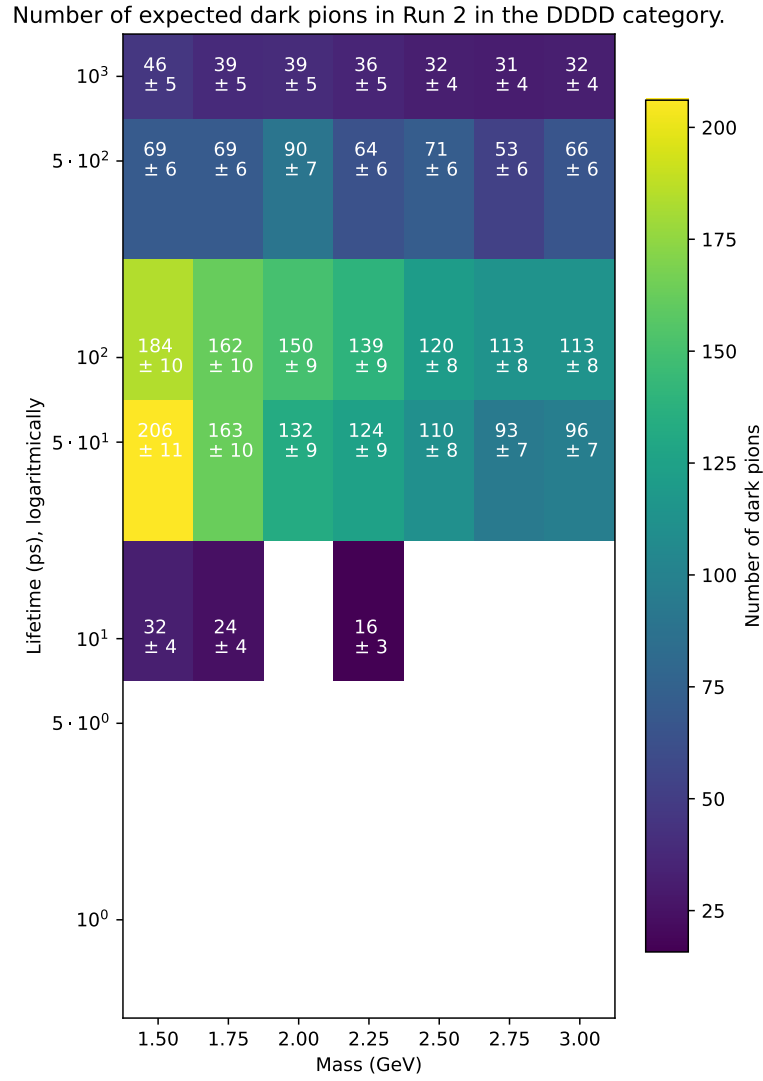
Figure A.3: *The expected number of dark pions in Run 2 passing the cuts in the DDDD category, for the baseline model. The white cells have less particles passing than 5 times their standard deviation. The mass dependence is similar to LLDD, while the lifetime dependence has shifted the peak to a larger lifetime.*

Number of expected dark pions in Run 2 in the DDDD category.
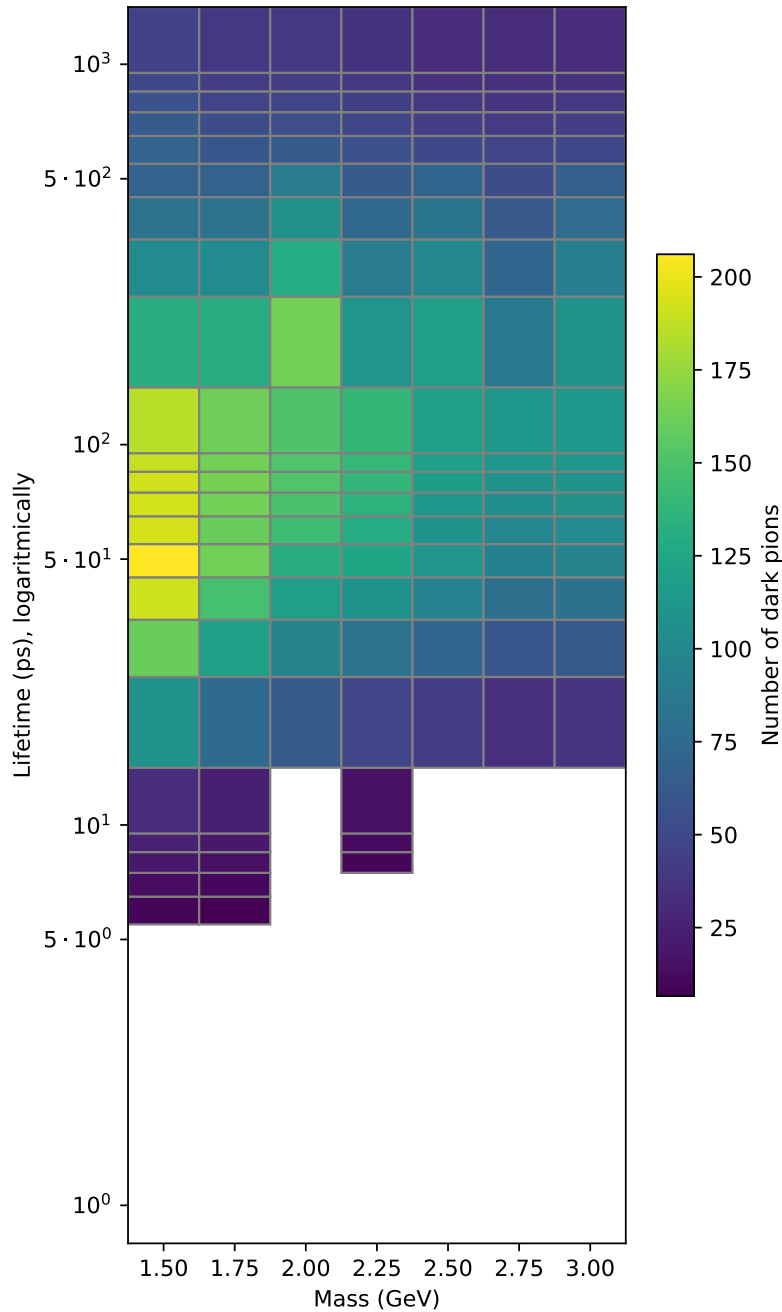
Figure A.4: *The expected number of dark pions in Run 2 passing the cuts in the DDDD category, after reweighting, for the baseline model. The white cells did not pass the statistical criteria, or have less particles passing than 5 times their standard deviation. It can be seen that the reweighting produces a smoother plot.*

A.2 Dark rho scenario

Below follow the results for the dark rho scenario, before and after reweighting. There is also the percentual difference plot.
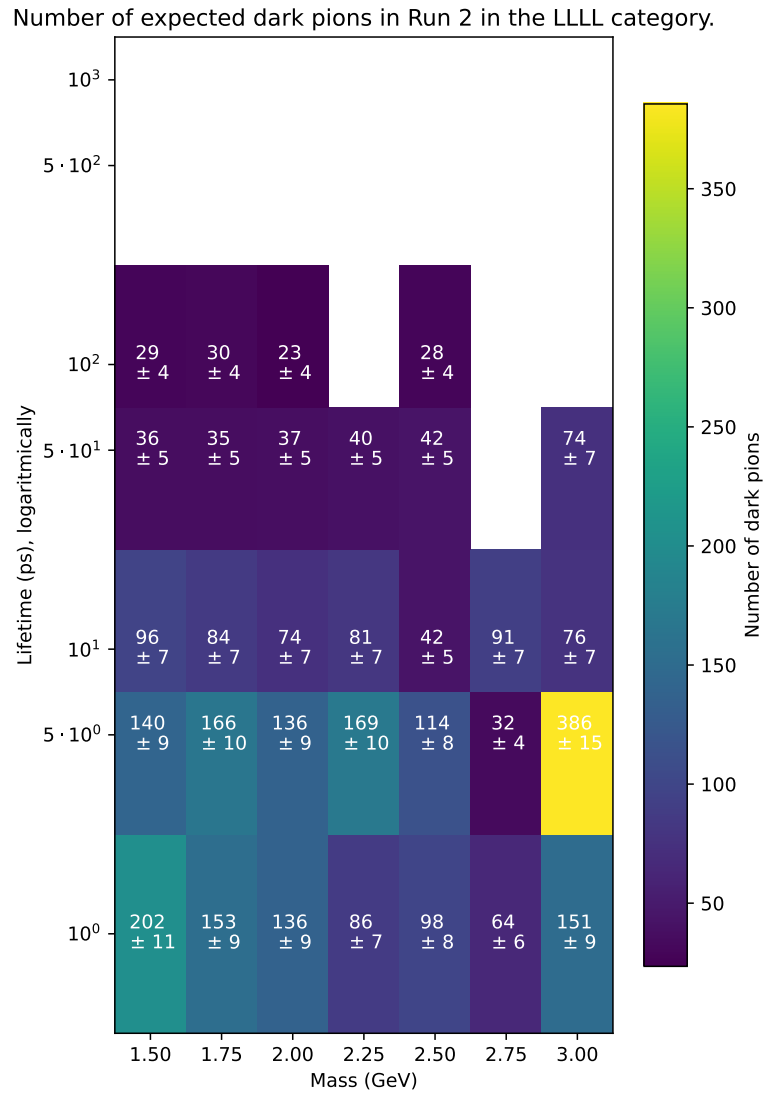
Figure A.5: *The expected number of dark pions in Run 2 passing the cuts in the LLLL category, for the dark rho scenario. The white cells have less particles passing than 5 times their standard deviation. This result acts similarly to LLDD, with similar passing number as baseline but large fluctuations at larger masses.*

Percentage of the difference in expected dark pions in the LLLL category.
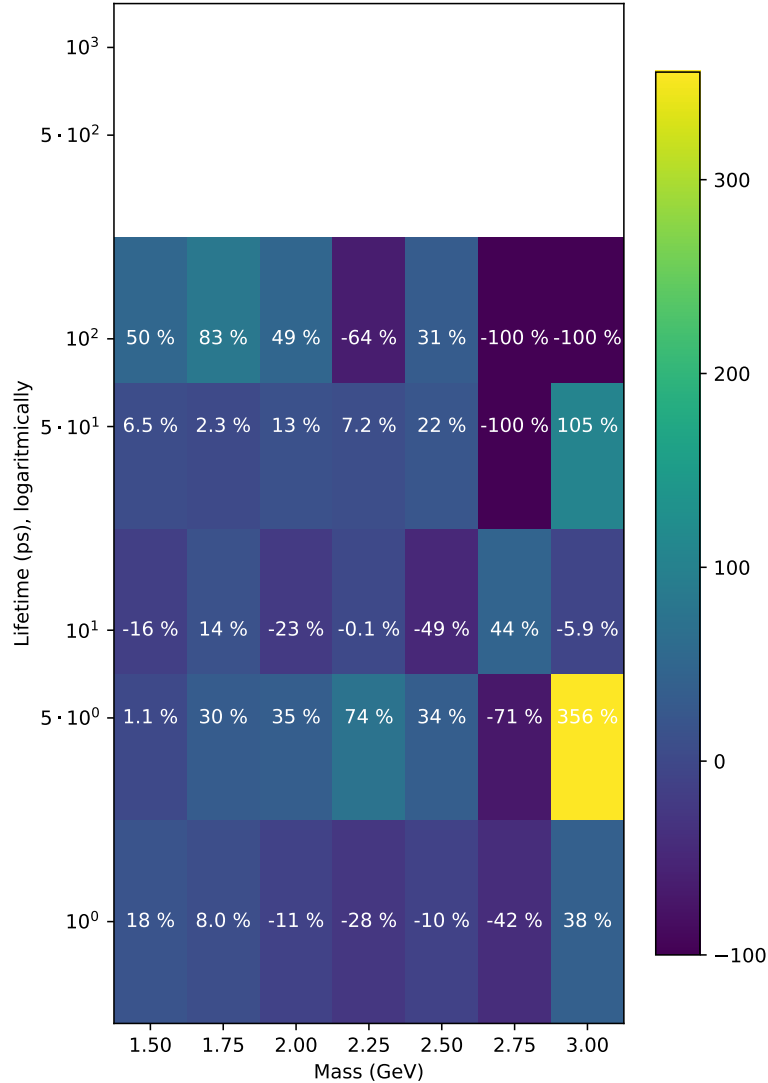
Figure A.6: *The percentual difference for the dark rho scenario in the LLLL category. The whitespaces indicate the points left out because there the number of expected dark pions is less than 5 times its error in the baseline model. Like for LLDD it confirms the similarity with baseline at low mass, but the larger differences at high mass.*

Number of expected dark pions in Run 2 in the LLLL category.
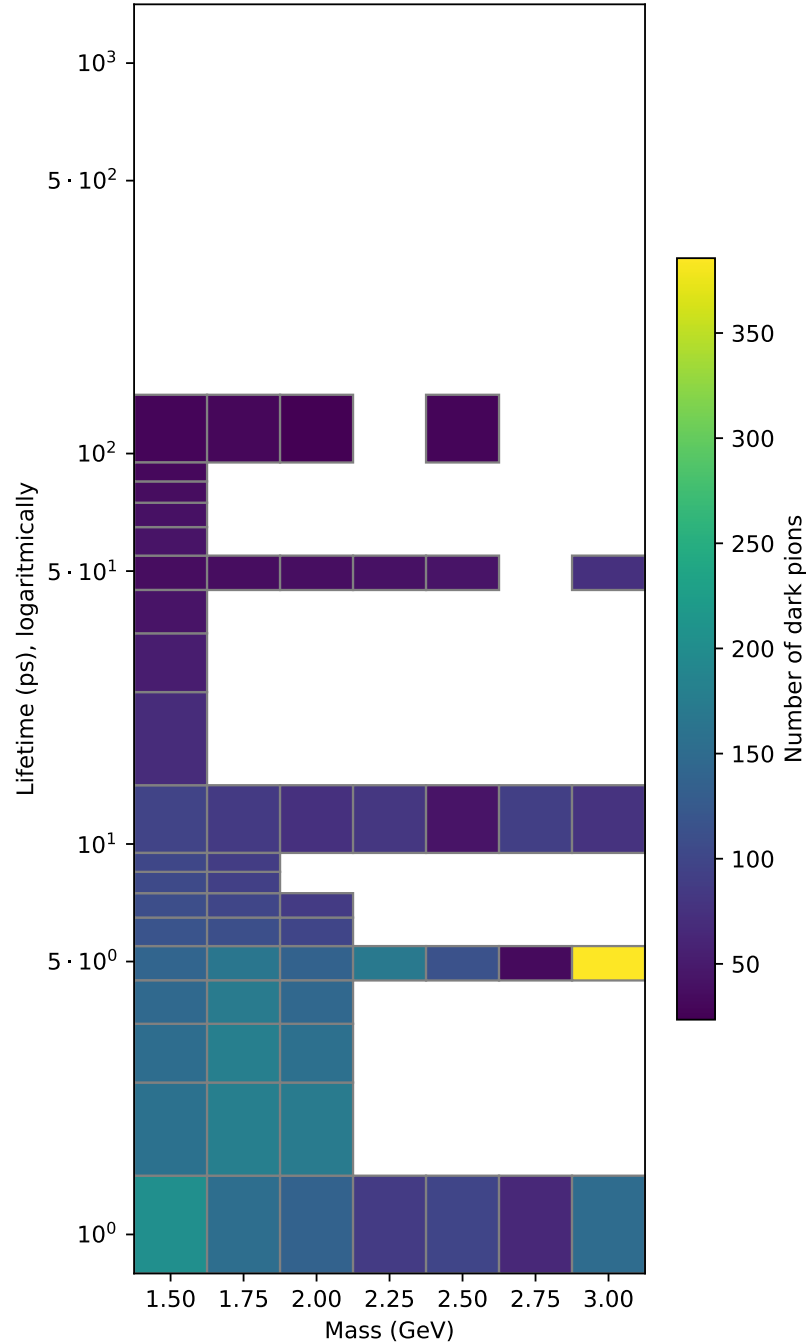
Figure A.7: *The expected number of dark pions in Run 2 passing the cuts in the LLLL category, after reweighting, for the dark rho scenario. The white cells did not pass the statistical criteria, or have less particles passing than 5 times their standard deviation. Like we saw for LLDD there are many rejected points, but the others are well-behaved.*

Number of expected dark pions in Run 2 in the DDDD category.
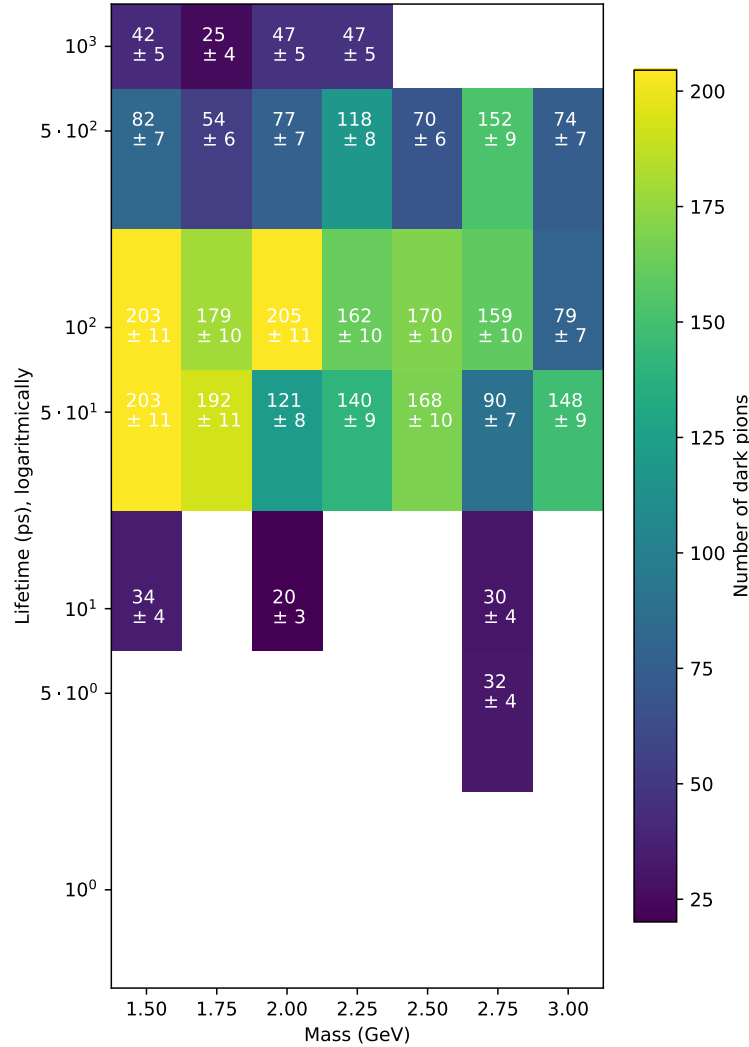
Figure A.8: *The expected number of dark pions in Run 2 passing the cuts in the DDDD category, for the dark rho scenario. The white cells have less particles passing than 5 times their standard deviation. This result acts similarly to LLDD (and LLLL), with similar passing number as baseline but large fluctuations at larger masses.*

Percentage of the difference in expected dark pions in the DDDD category.
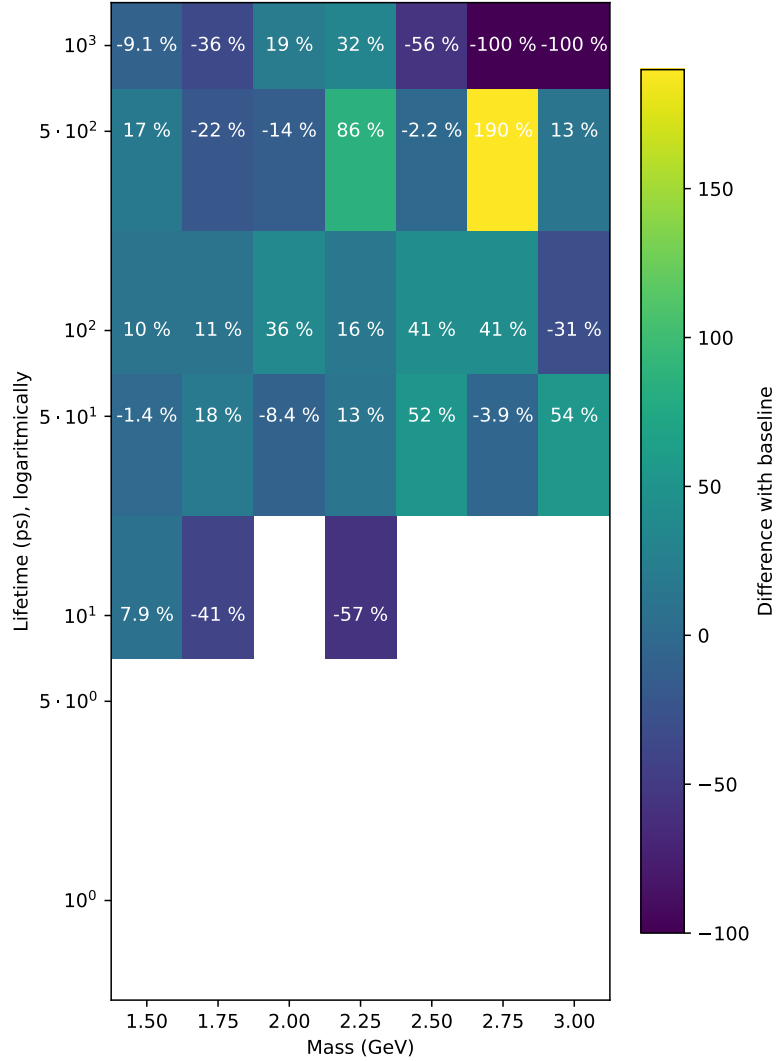
Figure A.9: *The percentual difference for the dark rho scenario in the DDDD category. The whitespaces indicate the points left out because there the number of expected dark pions is less than 5 times its error in the baseline model. Like for LLDD (and LLLL) it confirms the similarity with baseline at low mass, but the larger differences at high mass.*

Number of expected dark pions in Run 2 in the DDDD category.
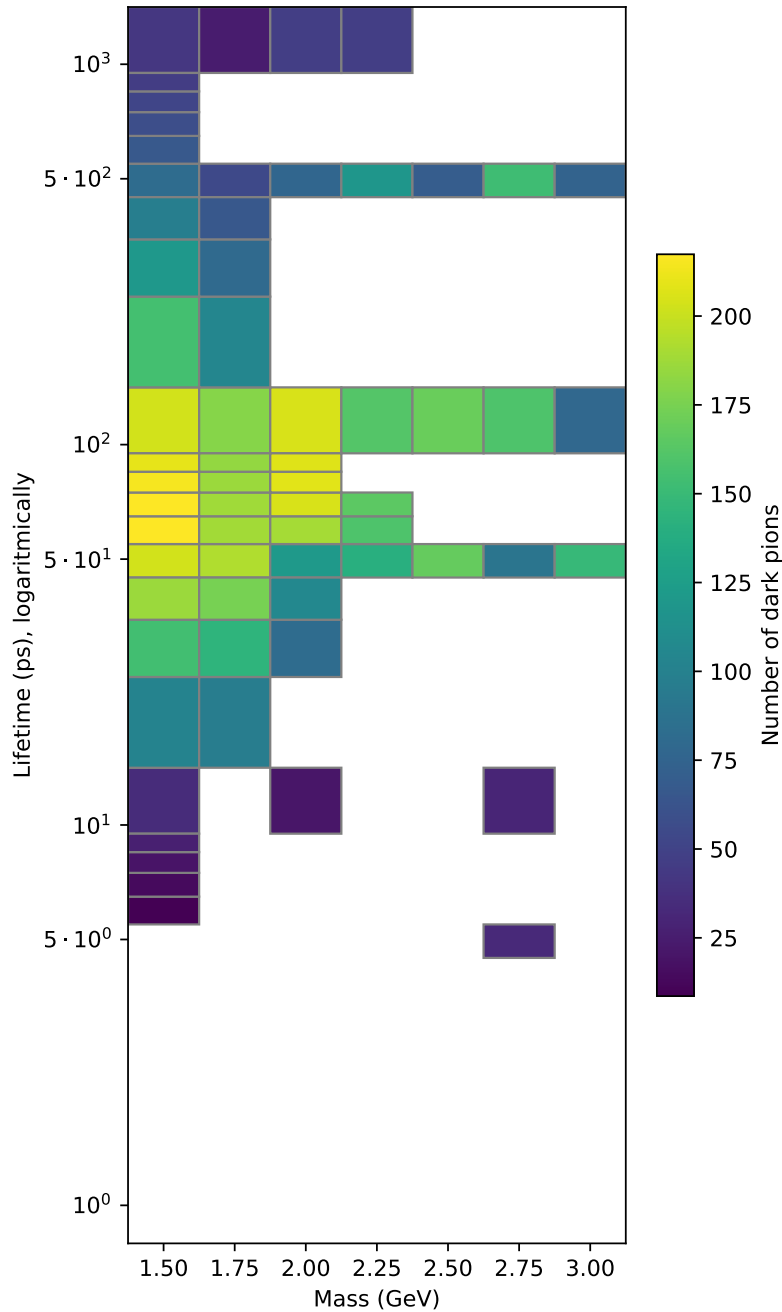
Figure A.10: *The expected number of dark pions in Run 2 passing the cuts in the DDDD category, after reweighting, for the dark rho scenario. The white cells did not pass the statistical criteria, or have less particles passing than 5 times their standard deviation. Like we saw for LLDD (and LLLL) there are many rejected points, but the others are well-behaved.*

A.3   Dark colour scenario

Below follow the results for the dark colour scenario, before and after reweighting. There is also the percentual difference plot.
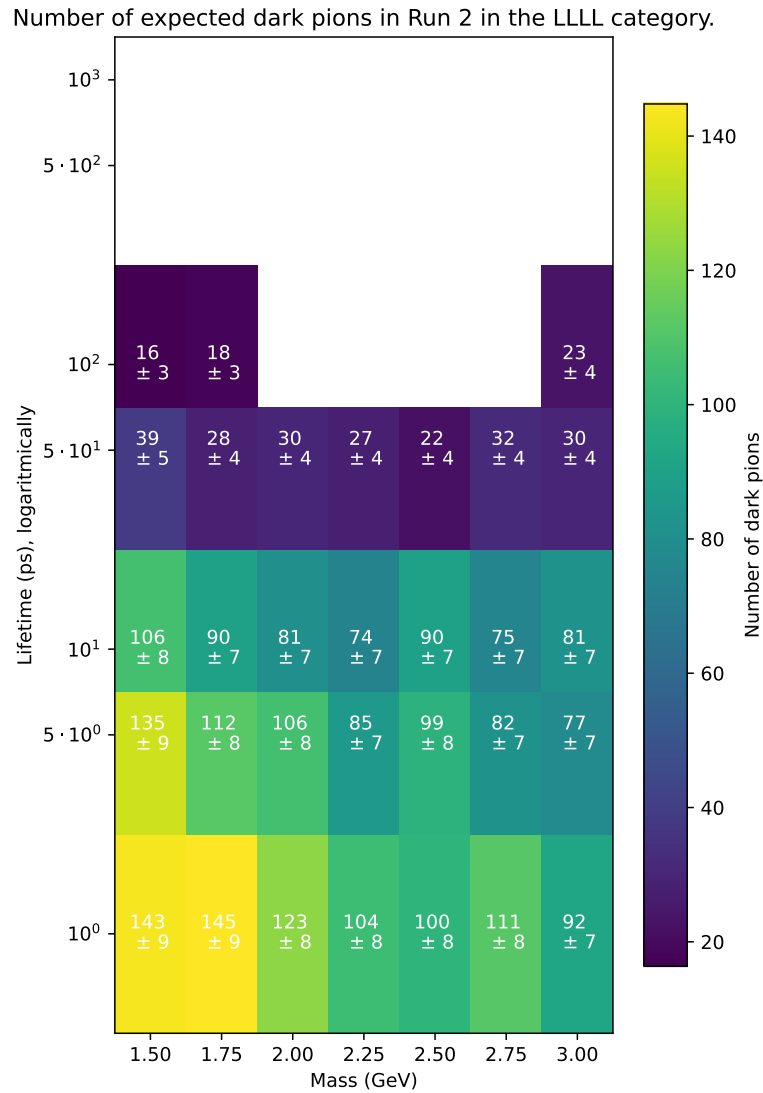
Figure A.11: *The expected number of dark pions in Run 2 passing the cuts in the LLLL category, for the dark colour scenario. The white cells have less particles passing than 5 times their standard deviation. This result is quite similar to that of the baseline model, like we saw for LLDD.*

Percentage of the difference in expected dark pions in the LLLL category.
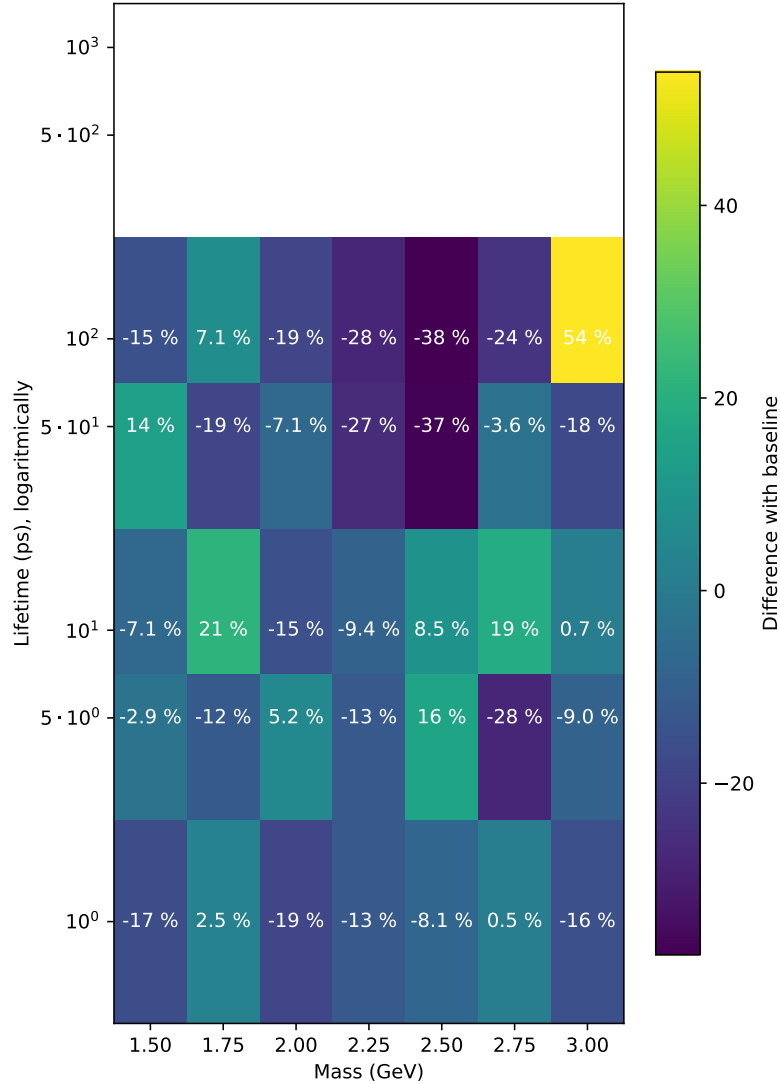
Figure A.12: *The percentual difference for the dark colour scenario in the LLLL category. The whitespaces indicate the points left out because there the number of expected dark pions is less than 5 times its error in the baseline model. No mass or lifetime dependence is visible, but perhaps there is a small overall decrease.*
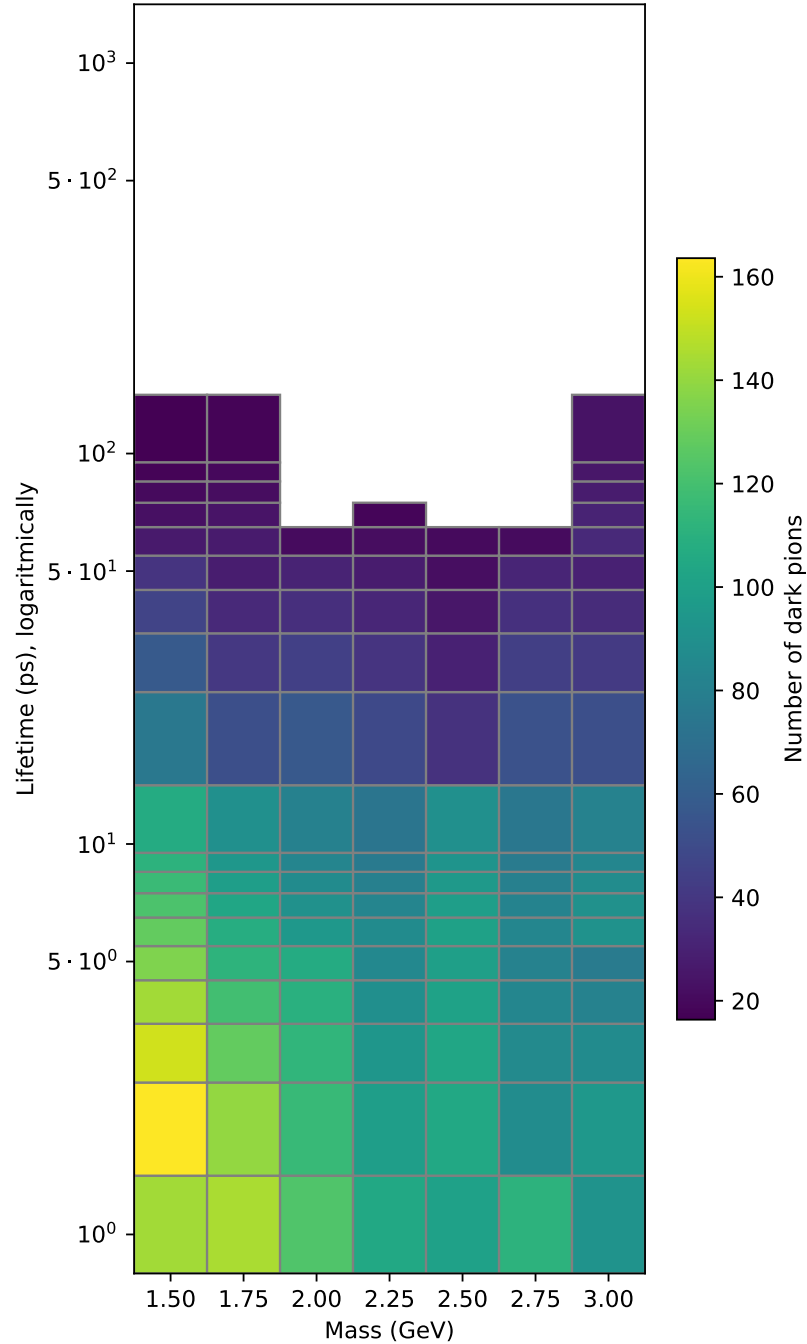
Figure A.13: *The expected number of dark pions in Run 2 passing the cuts in the LLLL category, after reweighting, for the dark colour scenario. The white cells did not pass the statistical criteria, or have less particles passing than 5 times their standard deviation. The reweighted results are well-behaved.*

Number of expected dark pions in Run 2 in the DDDD category.
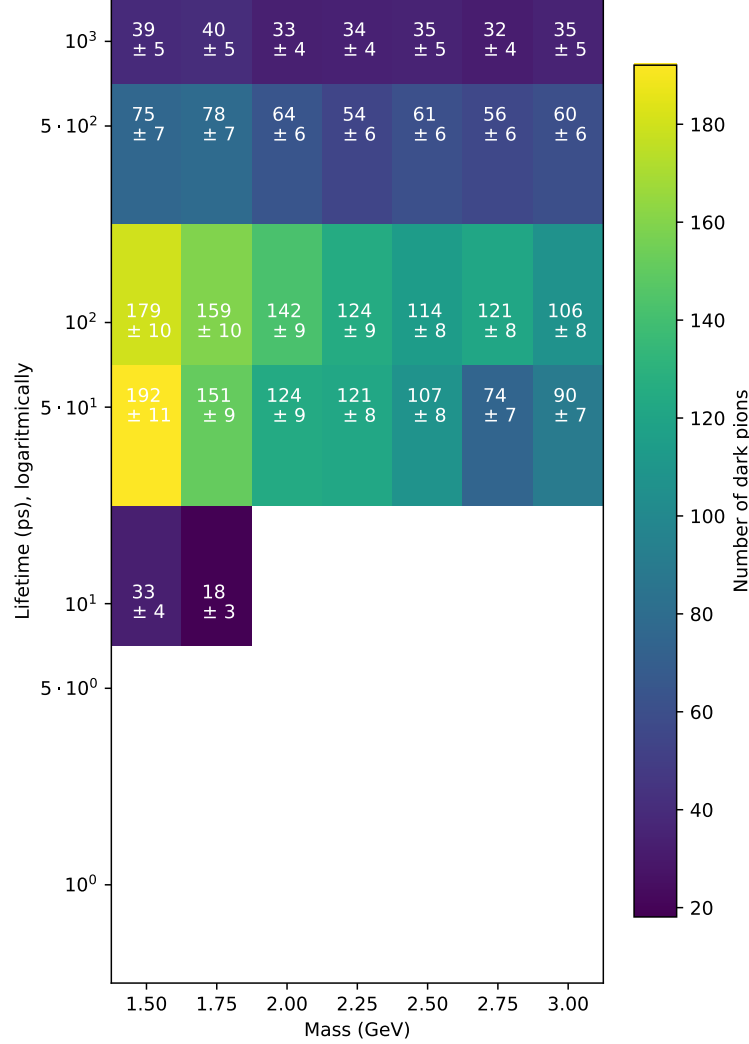
Figure A.14: *The expected number of dark pions in Run 2 passing the cuts in the DDDD category, for the dark colour scenario. The white cells have less particles passing than 5 times their standard deviation. This result is quite similar to that of the baseline model, like we saw for LLDD (and LLLL too).*

Percentage of the difference in expected dark pions in the DDDD category.
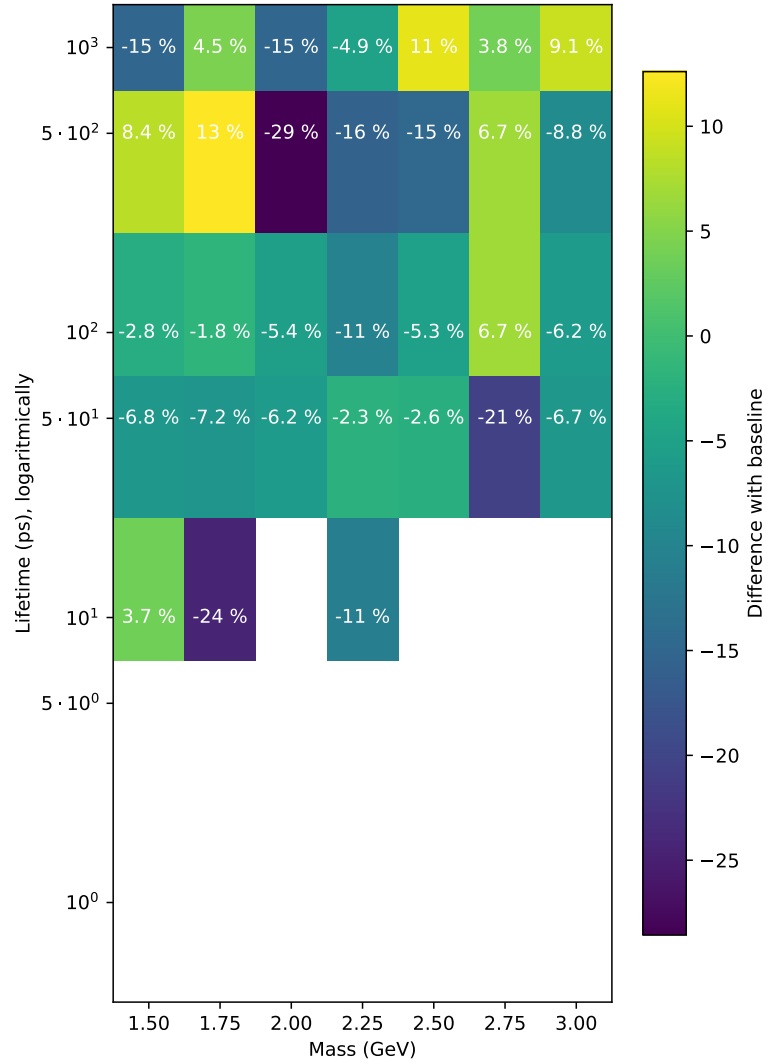
Figure A.15: *The percentual difference for the dark colour scenario in the DDDD category. The whitespaces indicate the points left out because there the number of expected dark pions is less than 5 times its error in the baseline model. Like for LLLL, no mass or lifetime dependence is visible, but there may be a small overall decrease.*

Number of expected dark pions in Run 2 in the DDDD category.
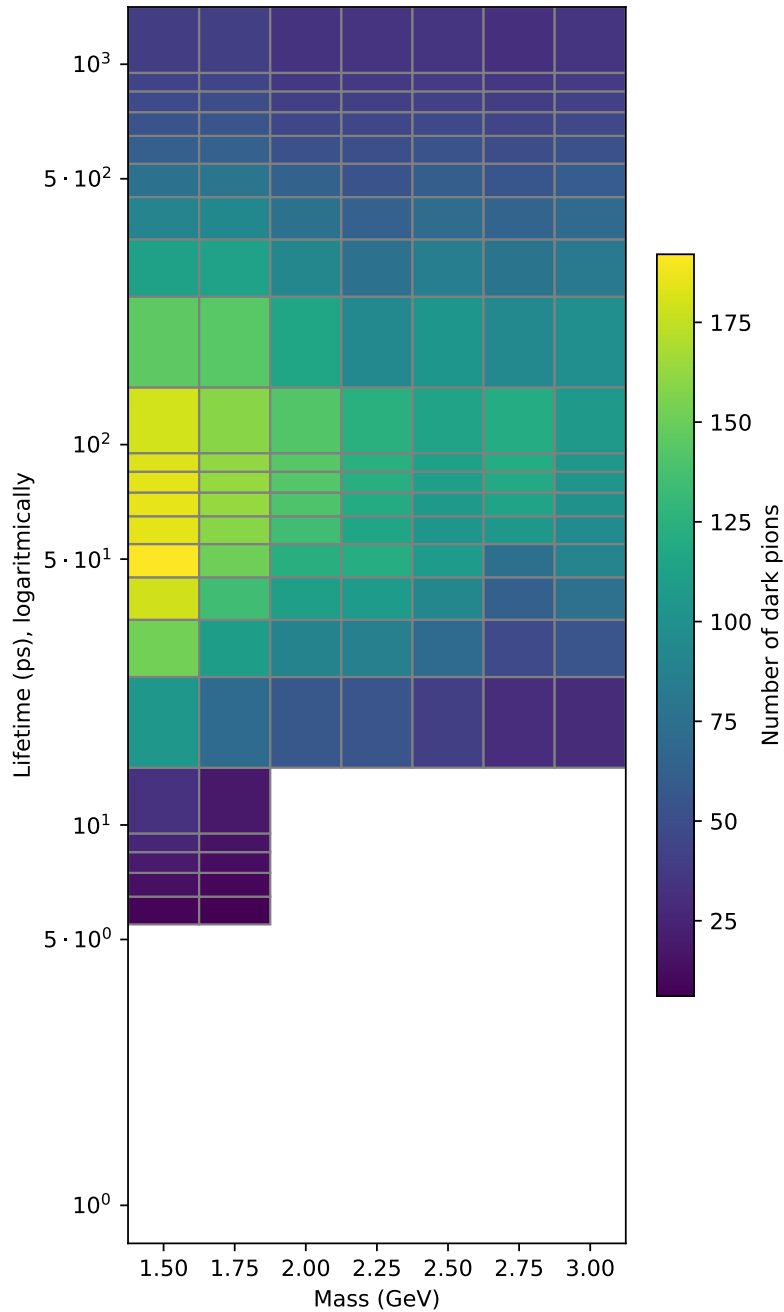
Figure A.16: *The expected number of dark pions in Run 2 passing the cuts in the DDDD category, after reweighting, for the dark colour scenario. The white cells did not pass the statistical criteria, or have less particles passing than 5 times their standard deviation. The reweighted results are well-behaved.*

A.4   Dark QCD scale scenario

Below follow the results for the dark QCD scale scenario, with $\tilde{\Lambda}_{\mathrm{QCD}} = 8$ GeV, before and after reweighting. There is also the percentual difference plot.
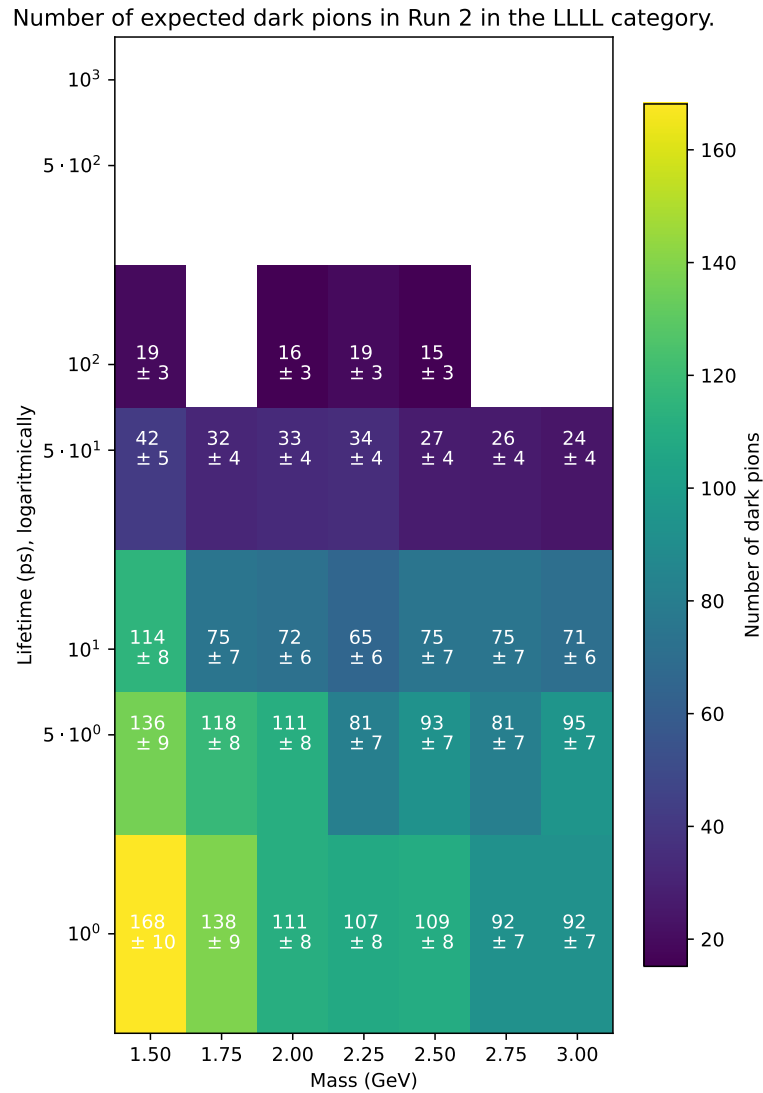
Figure A.17: *The expected number of dark pions in Run 2 passing the cuts in the LLLL category, for the $\tilde{\Lambda}_{\mathrm{QCD}} = 8$ GeV scenario. The white cells have less particles passing than 5 times their standard deviation. This result is very similar to that of the baseline model, like we saw for LLDD.*

Percentage of the difference in expected dark pions in the LLLL category.
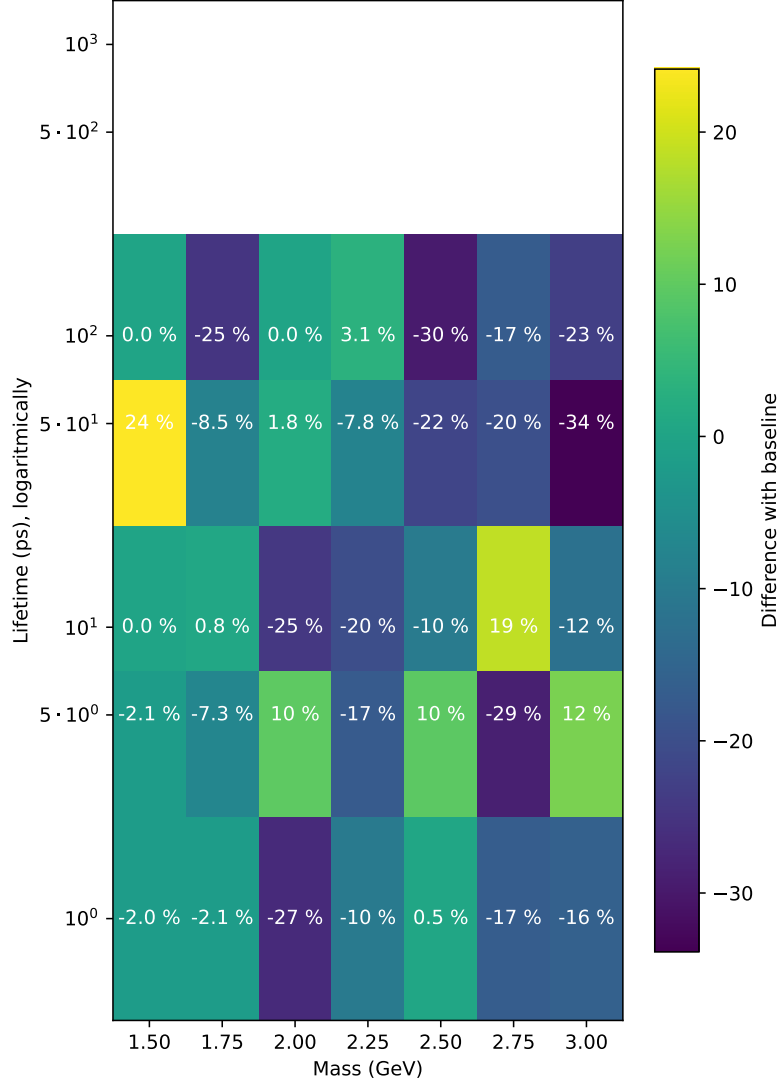
Figure A.18: *The percentual difference for the $\tilde{\Lambda}_{\mathrm{QCD}} = 8$ GeV scenario in the LLLL category. The whitespaces indicate the points left out because there the number of expected dark pions is less than 5 times its error in the baseline model. There is a small decrease visible, on average.*

Number of expected dark pions in Run 2 in the LLLL category.
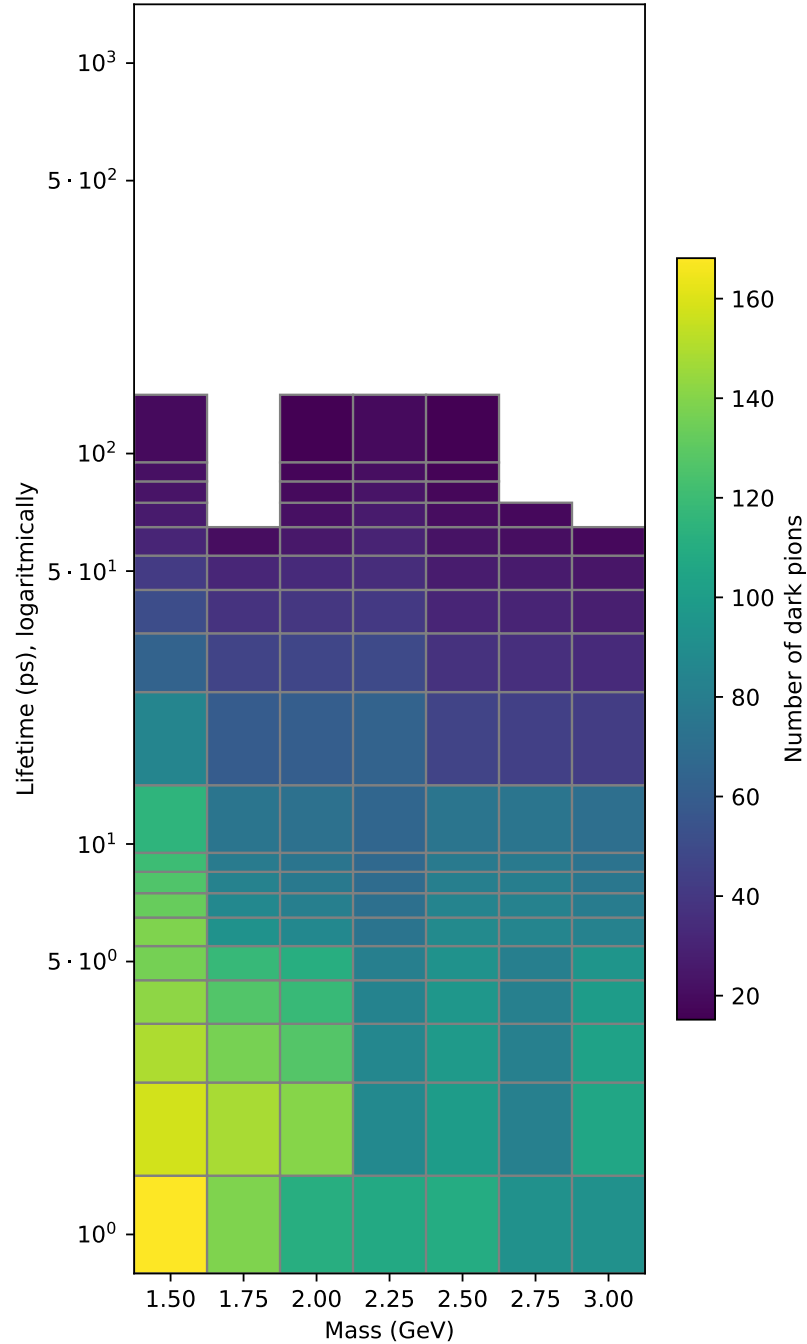
Figure A.19: *The expected number of dark pions in Run 2 passing the cuts in the LLLL category, after reweighting, for the $\tilde{\Lambda}_{\mathrm{QCD}} = 8$ GeV scenario. The white cells did not pass the statistical criteria, or have less particles passing than 5 times their standard deviation. The reweighted results are well-behaved.*

Number of expected dark pions in Run 2 in the DDDD category.
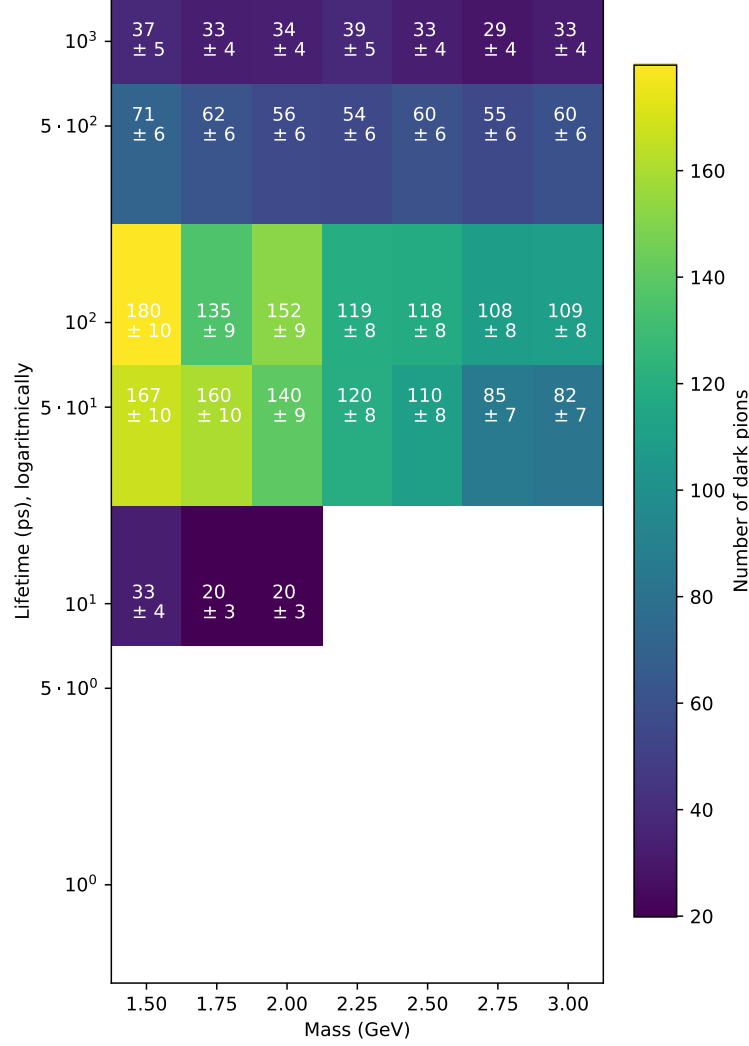
Figure A.20: *The expected number of dark pions in Run 2 passing the cuts in the DDDD category, for the $\tilde{\Lambda}_{\mathrm{QCD}} = 8$ GeV scenario. The white cells have less particles passing than 5 times their standard deviation. This result is very similar to that of the baseline model, like we saw for LLDD.*

Percentage of the difference in expected dark pions in the DDDD category.
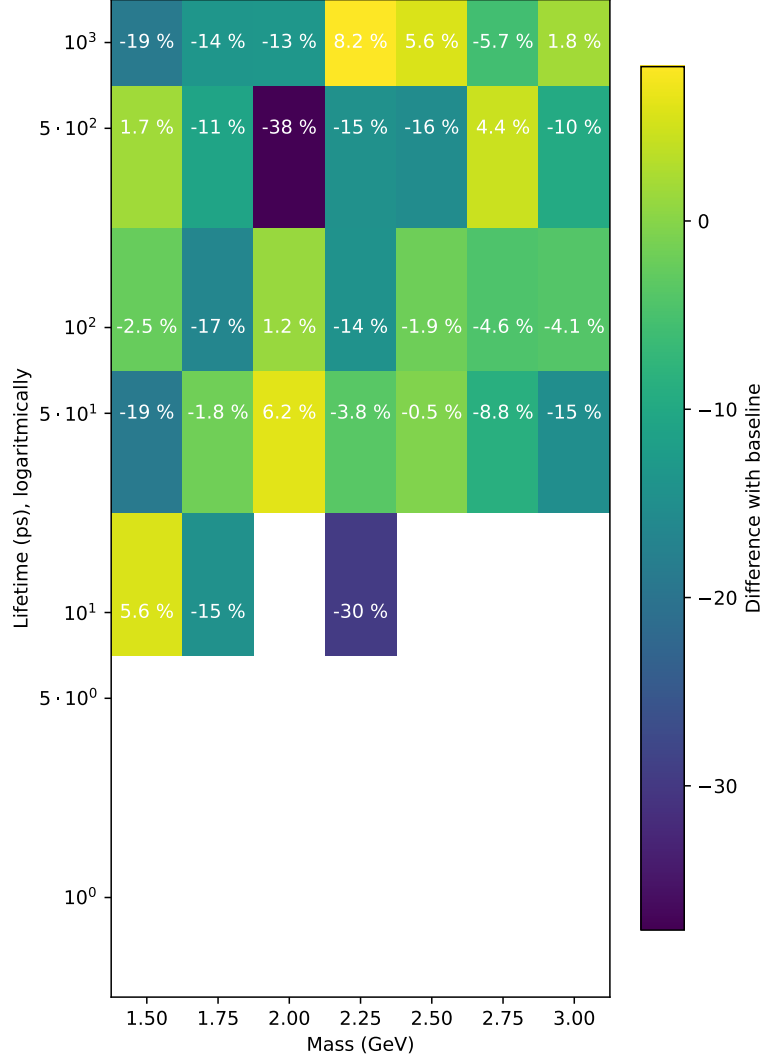
Figure A.21: *The percentual difference for the $\tilde{\Lambda}_{\mathrm{QCD}} = 8$ GeV scenario in the DDDD category. The whitespaces indicate the points left out because there the number of expected dark pions is less than 5 times its error in the baseline model. There is a small decrease visible, on average.*

Number of expected dark pions in Run 2 in the DDDD category.
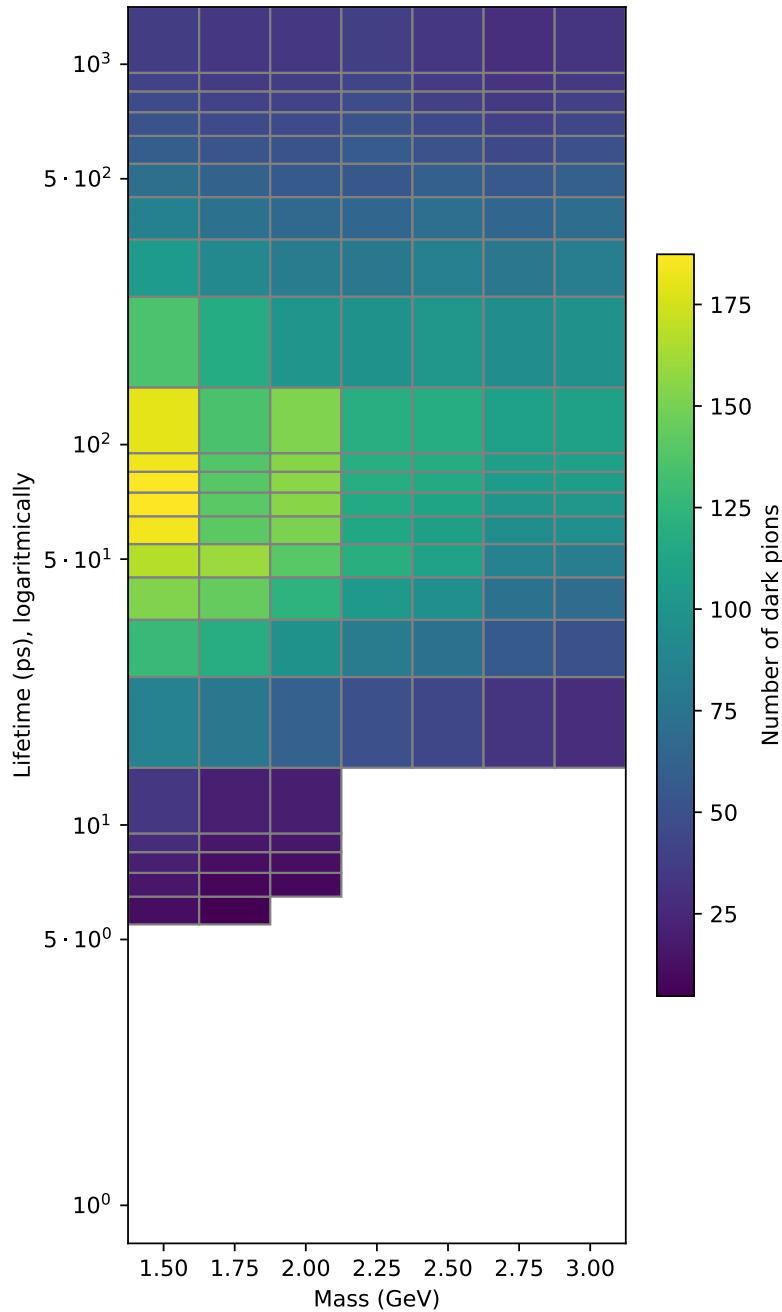
Figure A.22: *The expected number of dark pions in Run 2 passing the cuts in the DDDD category, after reweighting, for the $\tilde{\Lambda}_{\mathrm{QCD}} = 8$ GeV scenario. The white cells did not pass the statistical criteria, or have less particles passing than 5 times their standard deviation. The reweighted results are well-behaved.*

Below follow the results for the dark QCD scale scenario, with $\tilde{\Lambda}_{\text{QCD}} = 2$ GeV, before and after reweighting. There is also the percentual difference plot.
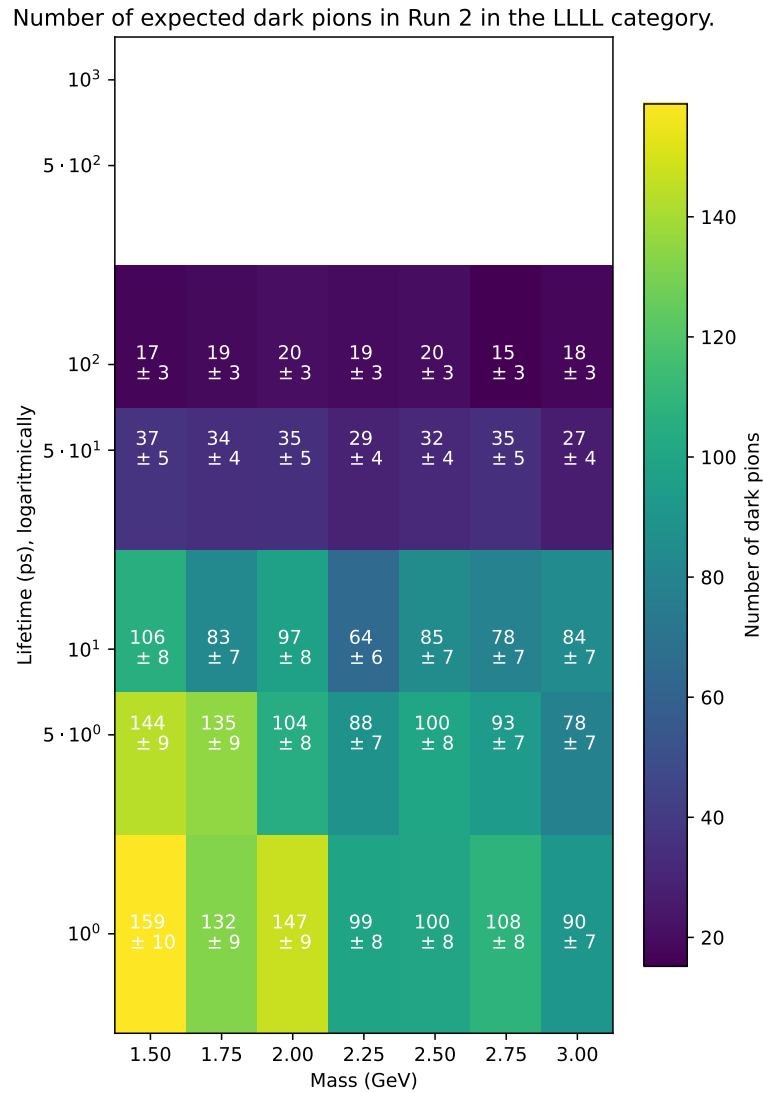
Figure A.23: *The expected number of dark pions in Run 2 passing the cuts in the LLLL category, for the $\tilde{\Lambda}_{\text{QCD}} = 2$ GeV scenario. The white cells have less particles passing than 5 times their standard deviation. This result is very similar to that of the baseline model, like we saw for LLDD.*

Percentage of the difference in expected dark pions in the LLLL category.
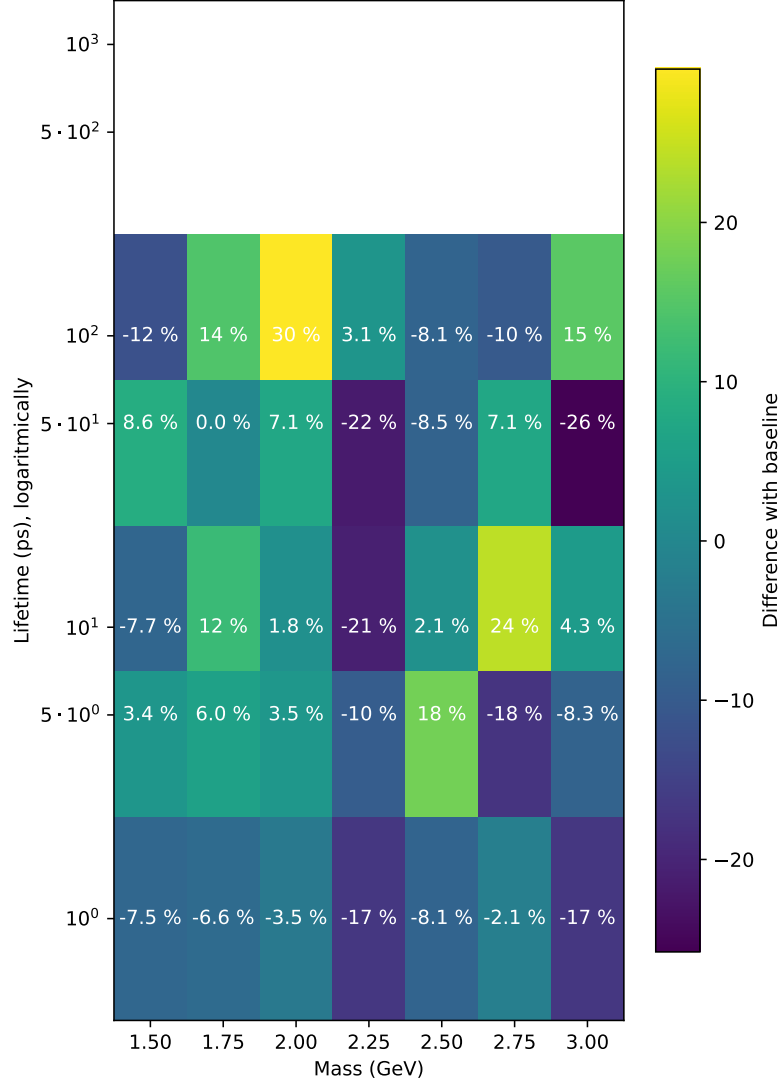
Figure A.24: *The percentual difference for the $\tilde{\Lambda}_{\mathrm{QCD}} = 2$ GeV scenario in the LLLL category. The whitespaces indicate the points left out because there the number of expected dark pions is less than 5 times its error in the baseline model. This time there is no average decrease visible.*

Number of expected dark pions in Run 2 in the LLLL category.
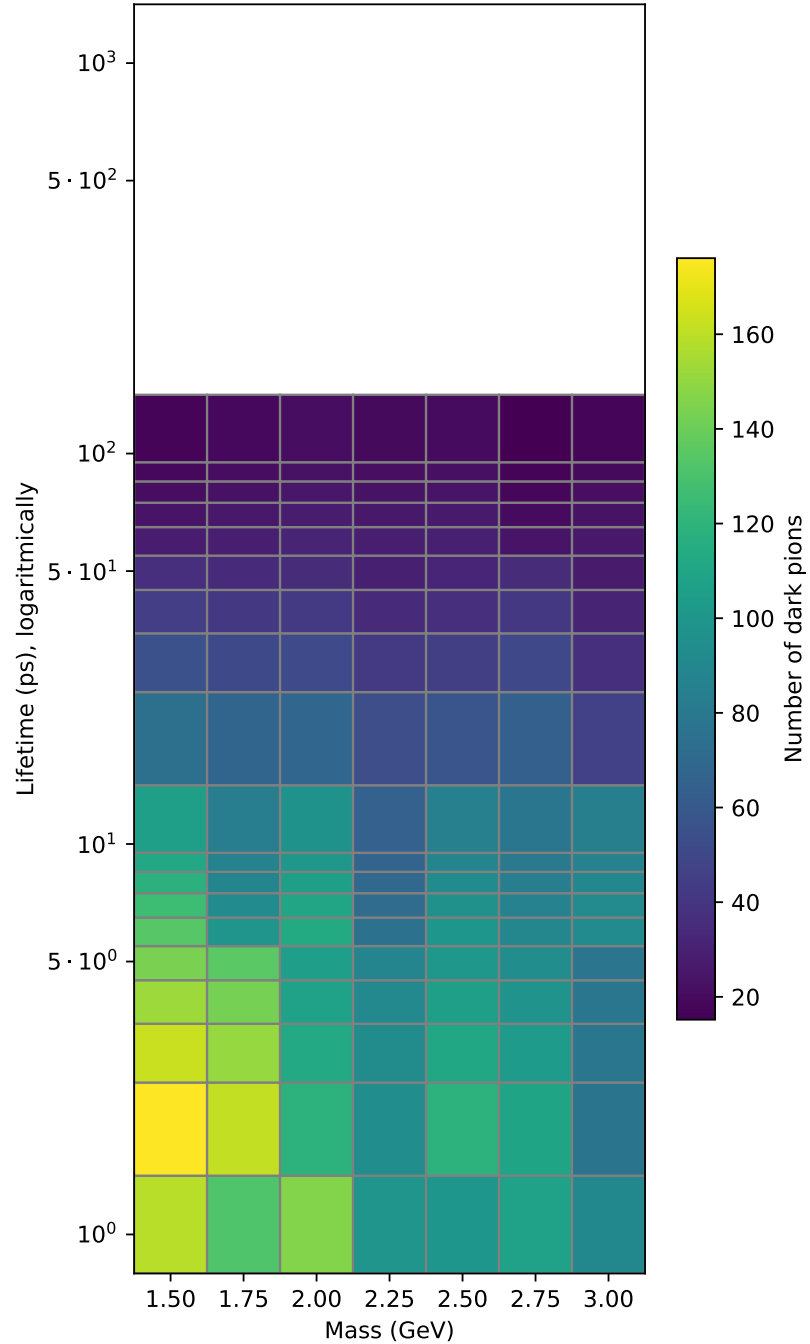
Figure A.25: *The expected number of dark pions in Run 2 passing the cuts in the LLLL category, after reweighting, for the $\tilde{\Lambda}_{\mathrm{QCD}} = 2$ GeV scenario. The white cells did not pass the statistical criteria, or have less particles passing than 5 times their standard deviation. The reweighted results are well-behaved.*

Number of expected dark pions in Run 2 in the DDDD category.
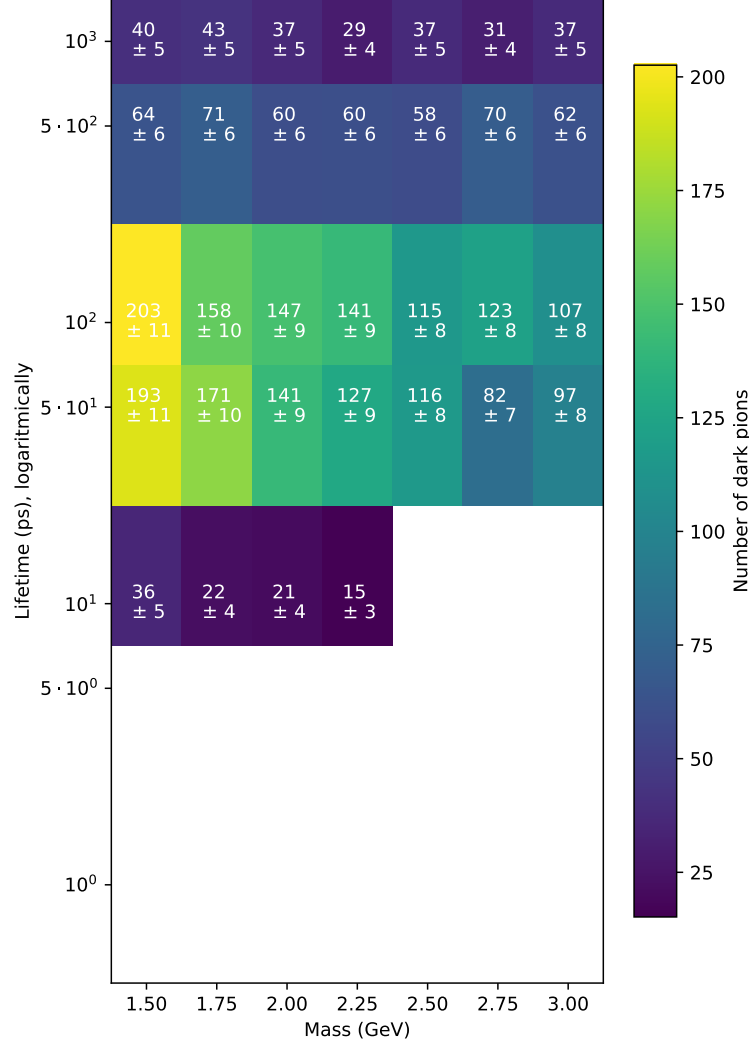
Figure A.26: *The expected number of dark pions in Run 2 passing the cuts in the DDDD category, for the $\tilde{\Lambda}_{QCD} = 2$ GeV scenario. The white cells have less particles passing than 5 times their standard deviation. This result is very similar to that of the baseline model, like we saw for LLDD.*

Percentage of the difference in expected dark pions in the DDDD category.
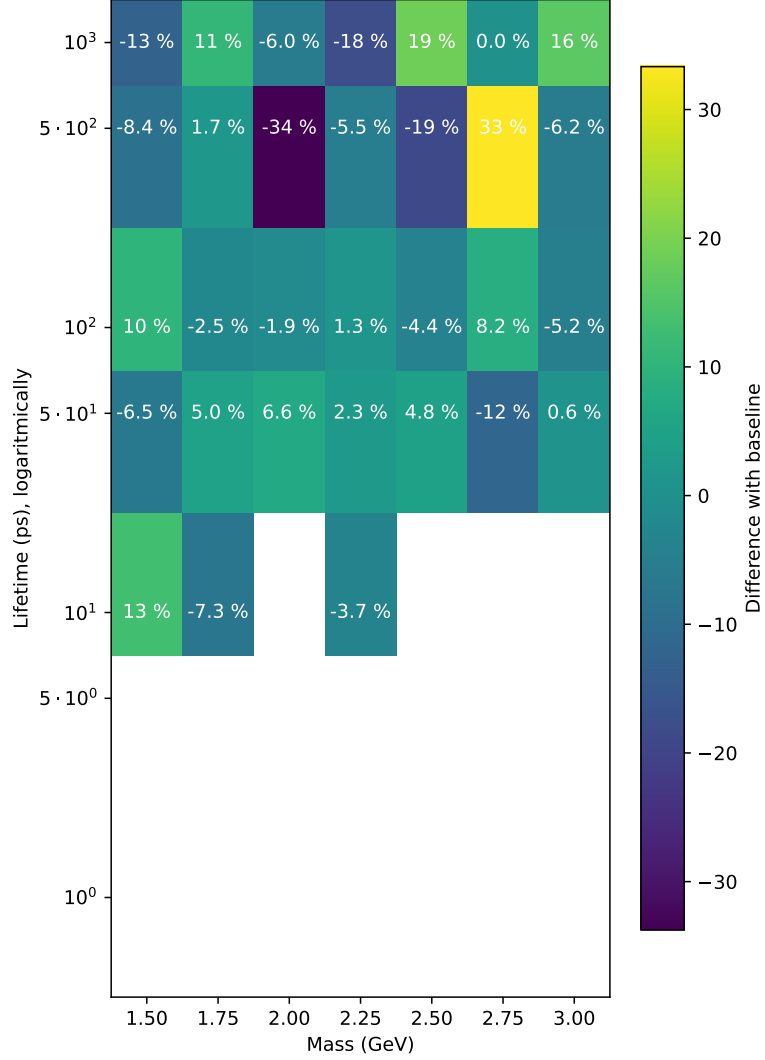
Figure A.27: *The percentual difference for the $\tilde{\Lambda}_{\mathrm{QCD}} = 2$ GeV scenario in the DDDD category. The whitespaces indicate the points left out because there the number of expected dark pions is less than 5 times its error in the baseline model. This time there is no average decrease visible.*

Number of expected dark pions in Run 2 in the DDDD category.
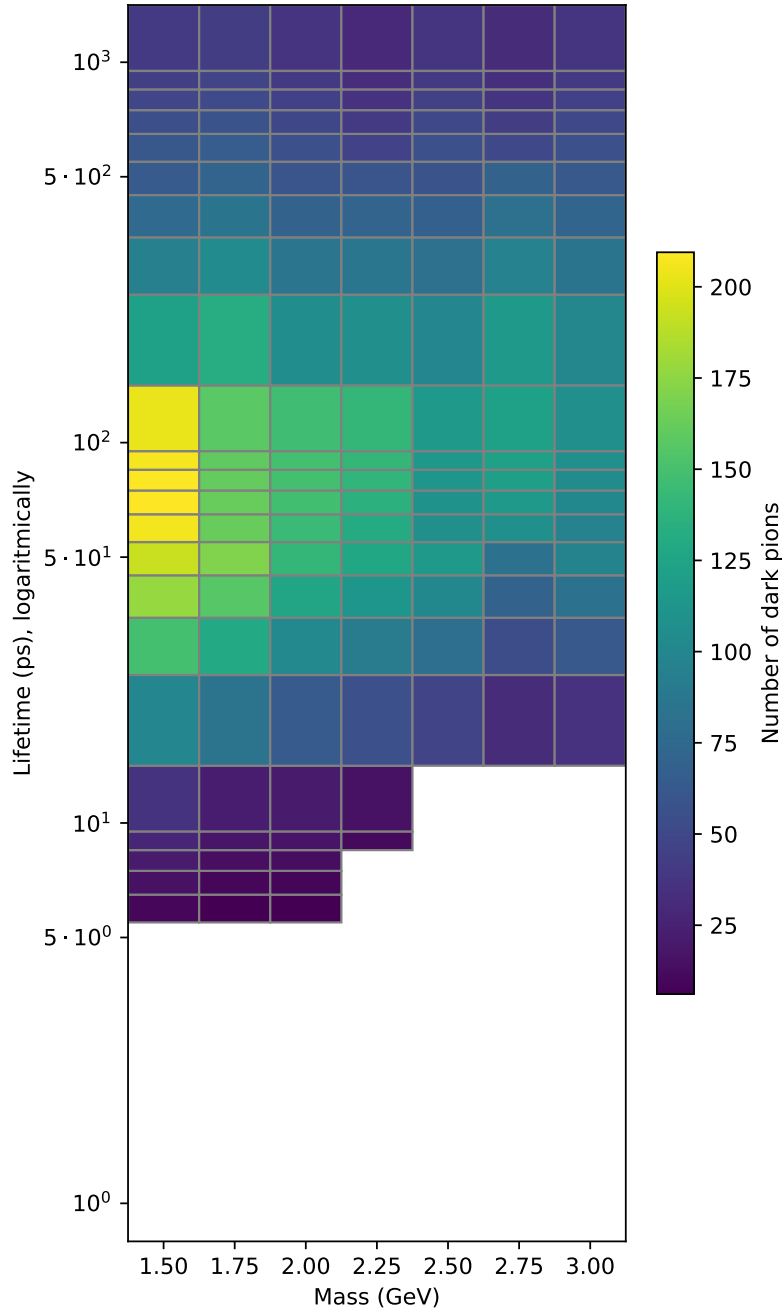
Figure A.28: *The expected number of dark pions in Run 2 passing the cuts in the DDDD category, after reweighting, for the $\tilde{\Lambda}_{\text{QCD}} = 2$ GeV scenario. The white cells did not pass the statistical criteria, or have less particles passing than 5 times their standard deviation. The reweighted results are well-behaved.*

A.5 Higgs mass scenario

Below follow the results for the 500 GeV Higgs mass scenario. There is also the percentual difference plot.
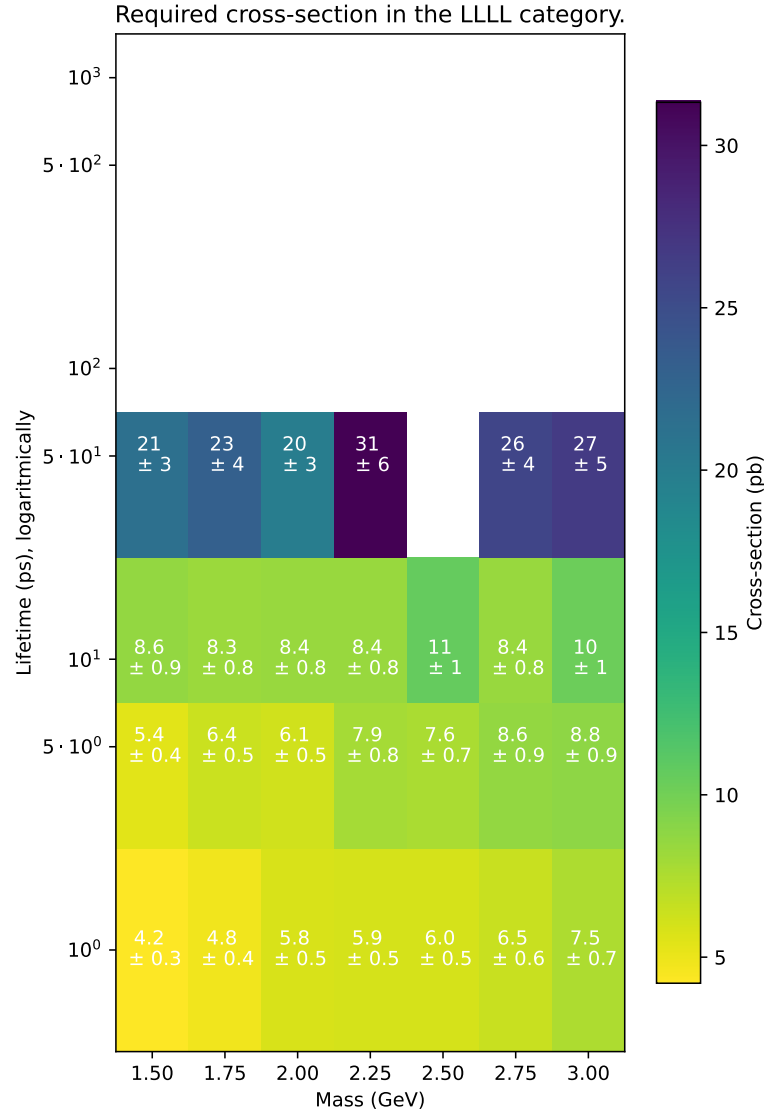
Figure A.29: *The required cross-section of the Higgs-like boson to have 50 dark pions in Run 2 for the 500 GeV Higgs mass scenario in the LLLL category. The white cells are left out because there the number of dark pions passing from the simulation is less than 5 times its error. The lifetime and mass dependence is similar to LLDD and the baseline model.*

Figure A.30: *The percentual difference for the 500 GeV Higgs mass scenario in the LLLL category. The whitespaces indicate the points left out because there the number of dark pions passing from the simulation is less than 5 times its error in the baseline model. Generally we see an increase of required cross-section in this scenario (larger than in LLDD), but no dependence on lifetime.*

Required cross-section in the DDDD category.
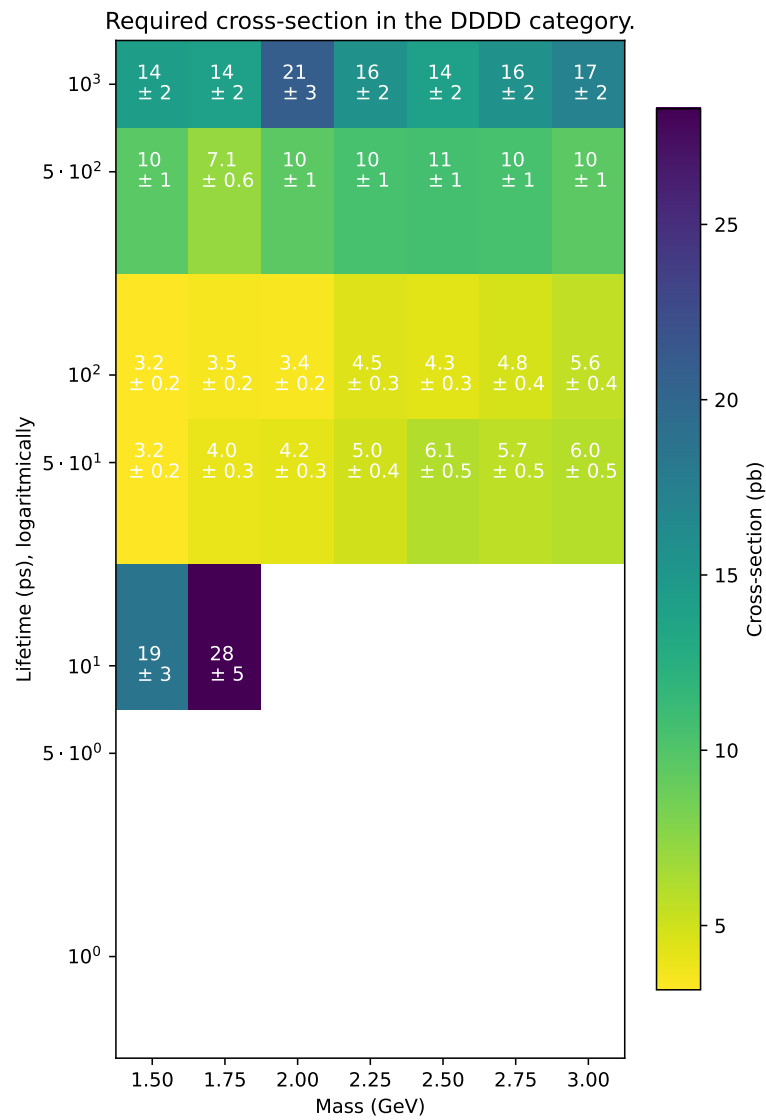
Figure A.31: *The required cross-section of the Higgs-like boson to have 50 dark pions in Run 2 for the 500 GeV Higgs mass scenario in the DDDD category. The white cells are left out because there the number of dark pions passing from the simulation is less than 5 times its error. The lifetime and mass dependence is similar to the baseline model still.*

Percentage of the difference in cross-section in the DDDD category.
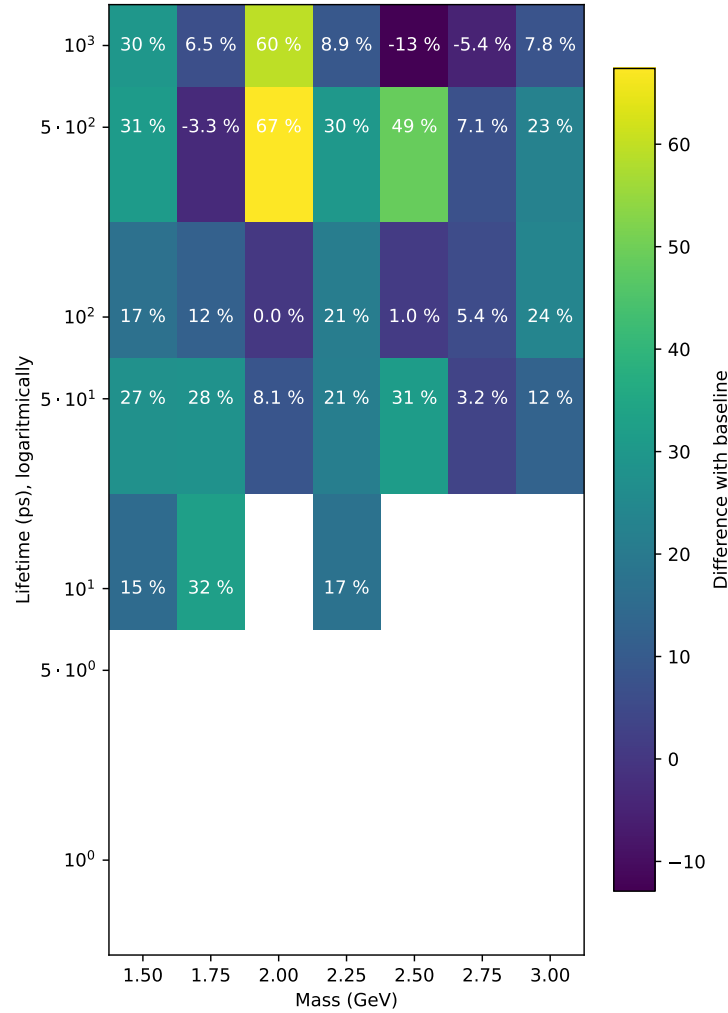
Figure A.32: *The percentual difference for the 500 GeV Higgs mass scenario in the DDDD category. The whitespaces indicate the points left out because there the number of dark pions passing from the simulation is less than 5 times its error in the baseline model. There are now not only increases but also decreases of required cross-section. It seems like there is no dependence on lifetime.*

Below follow the results for the 50 GeV Higgs mass scenario. There is also the percentual difference plot.
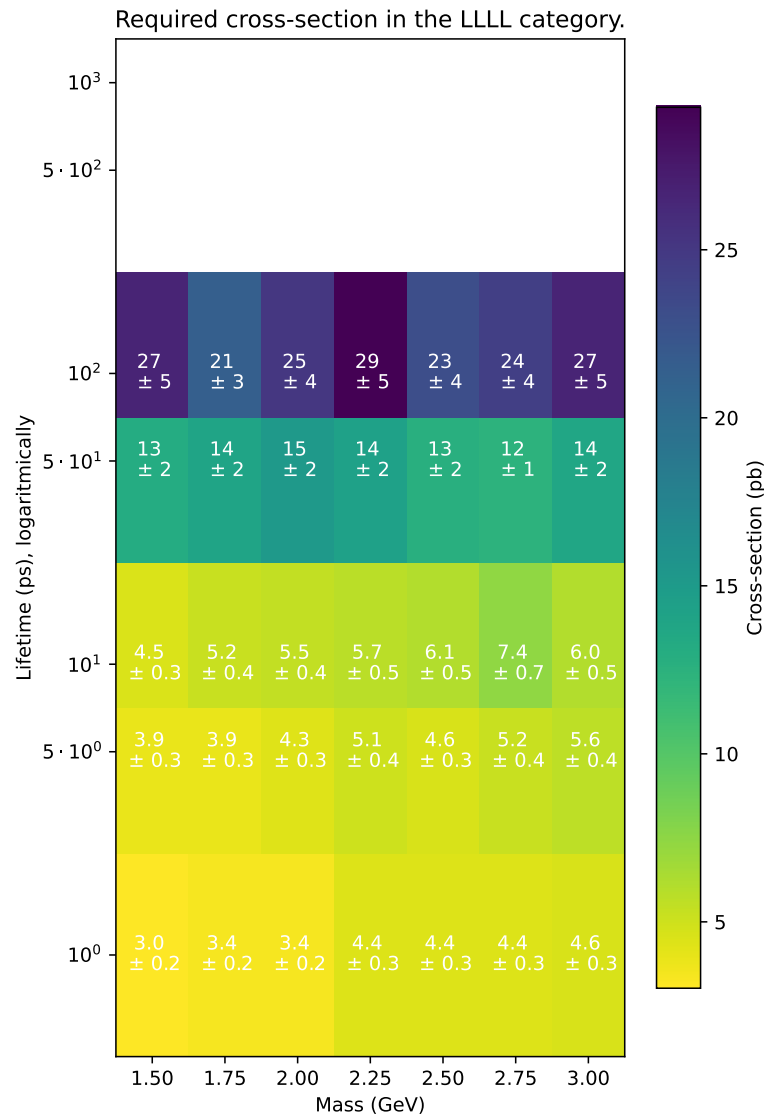
Figure A.33: *The required cross-section of the Higgs-like boson to have 50 dark pions in Run 2 for the 50 GeV Higgs mass scenario in the LLLL category. The white cells are left out because there the number of dark pions passing from the simulation is less than 5 times its error. The lifetime and mass dependence is similar to LLDD and the baseline model.*

Percentage of the difference in cross-section in the LLLL category.
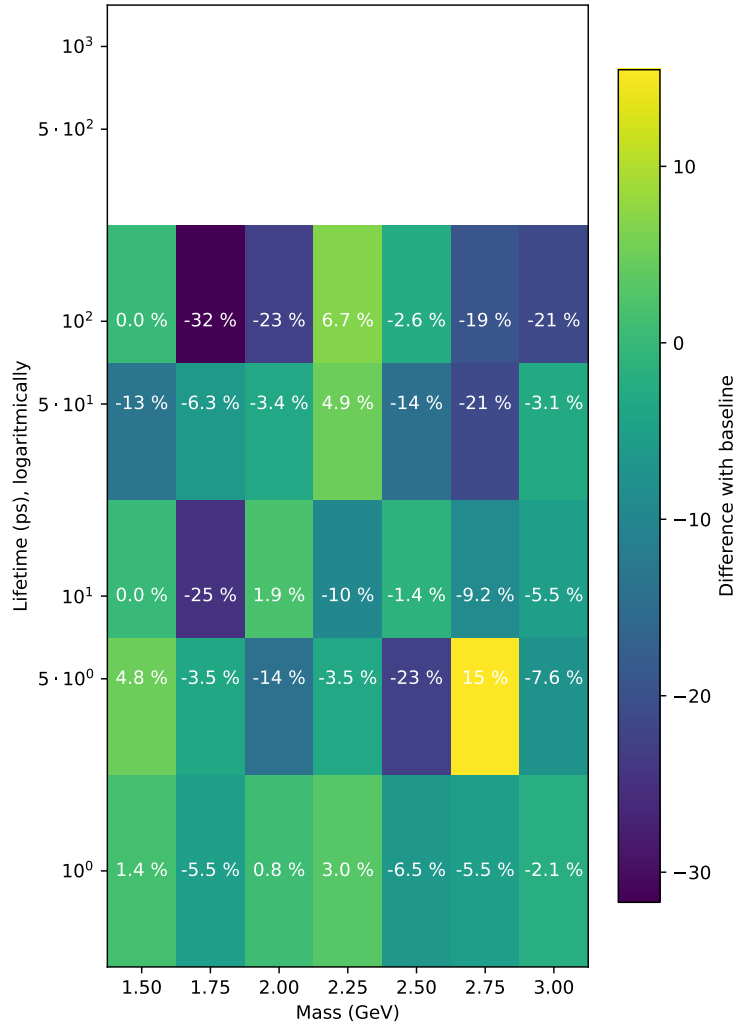
Figure A.34: *The percentual difference for the 50 GeV Higgs mass scenario in the LLLL category. The whitespaces indicate the points left out because there the number of dark pions passing from the simulation is less than 5 times its error in the baseline model. Compared to LLDD, there is no clear dependence on lifetime and there seems to be a small overall decrease in cross-section.*
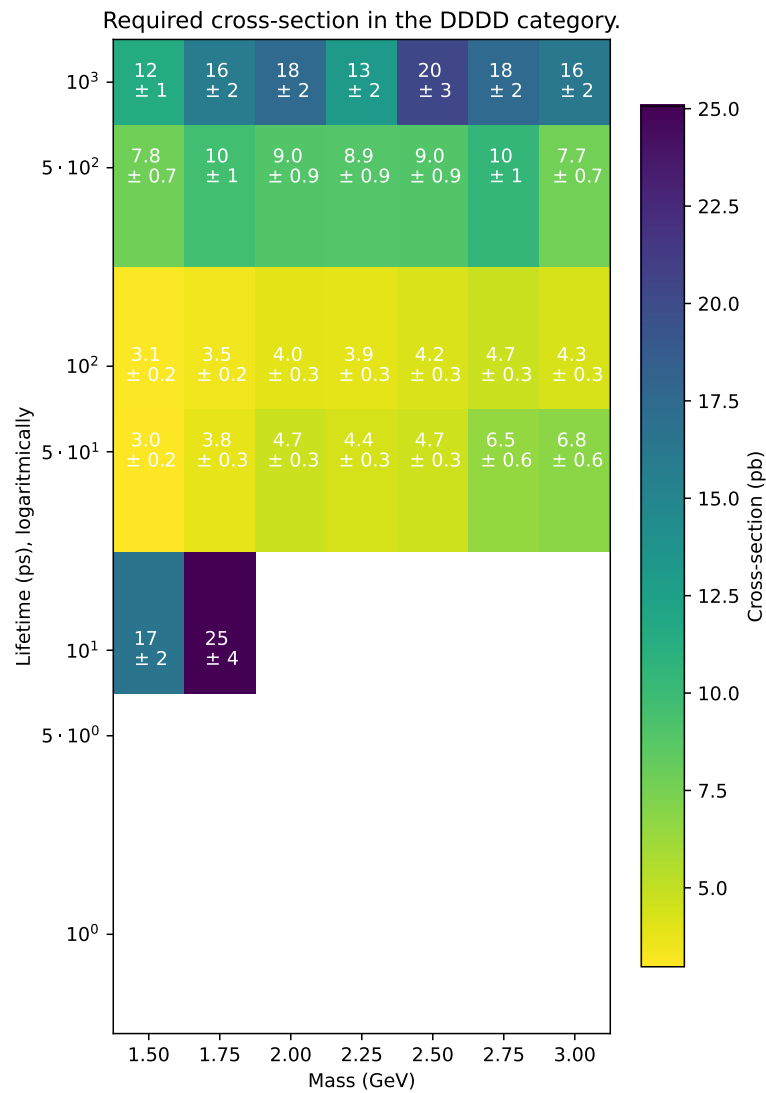
Figure A.35: *The required cross-section of the Higgs-like boson to have 50 dark pions in Run 2 for the 50 GeV Higgs mass scenario in the DDDD category. The white cells are left out because there the number of dark pions passing from the simulation is less than 5 times its error. The lifetime and mass dependence is similar to the baseline model still.*

Percentage of the difference in cross-section in the DDDD category.
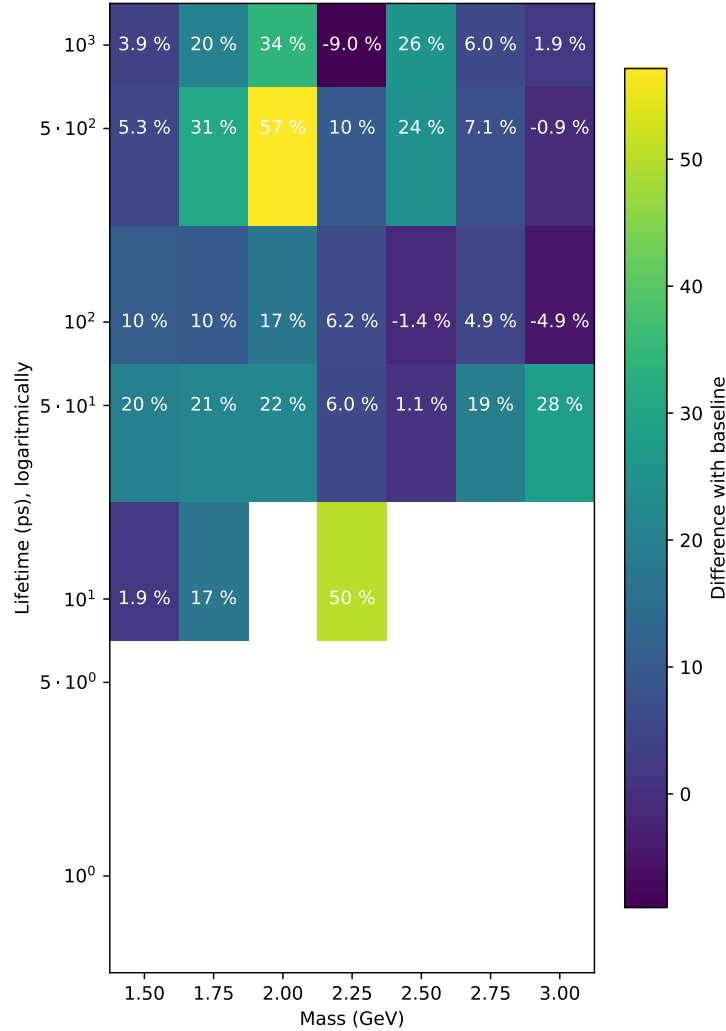
Figure A.36: *The percentual difference for the 50 GeV Higgs mass scenario in the DDDD category. The whitespaces indicate the points left out because there the number of dark pions passing from the simulation is less than 5 times its error in the baseline model. This result is similar to the 500 GeV mass one but has smaller outliers. It seems like there is no dependence on lifetime again.*

Below follow the results for the 1250 GeV Higgs mass scenario. There is also the percentual difference plot.
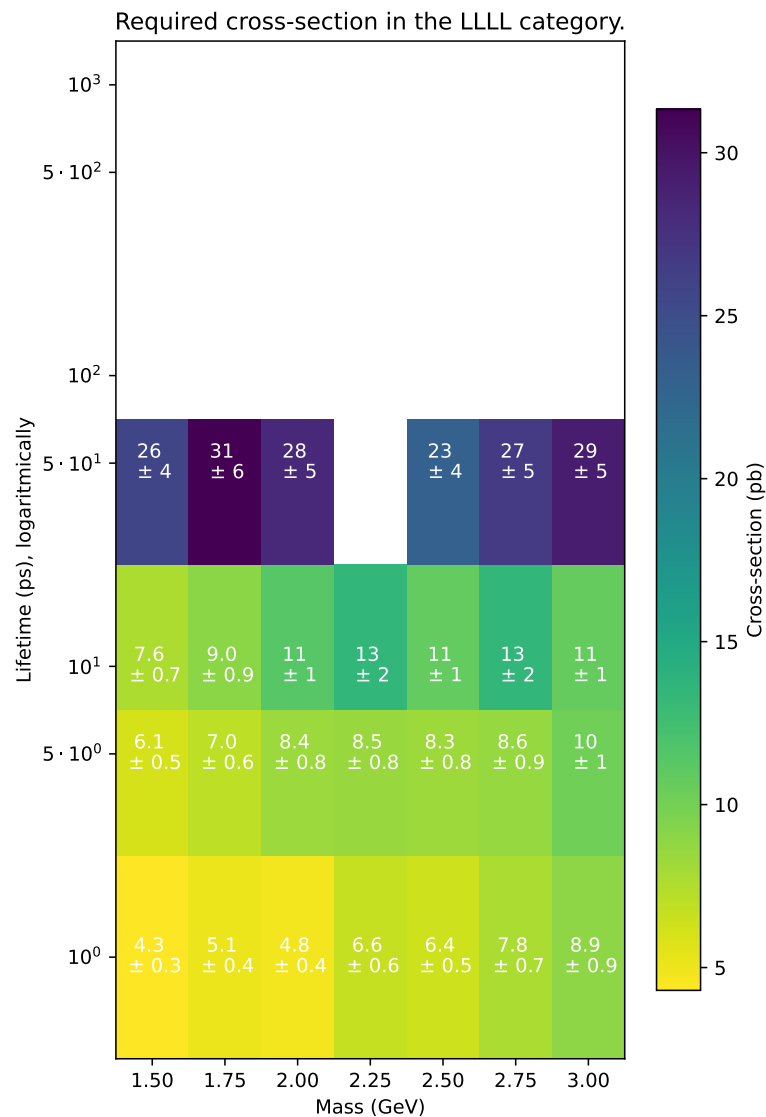
Figure A.37: *The required cross-section of the Higgs-like boson to have 50 dark pions in Run 2 for the 1250 GeV Higgs mass scenario in the LLLL category. The white cells are left out because there the number of dark pions passing from the simulation is less than 5 times its error. This plot is very similar to the 500 GeV mass LLLL result.*

Figure A.38: *The percentual difference for the 1250 GeV Higgs mass scenario in the LLLL category. The whitespaces indicate the points left out because there the number of dark pions passing from the simulation is less than 5 times its error in the baseline model. This plot is very similar to the 500 GeV mass LLLL result, but has higher percentages.*
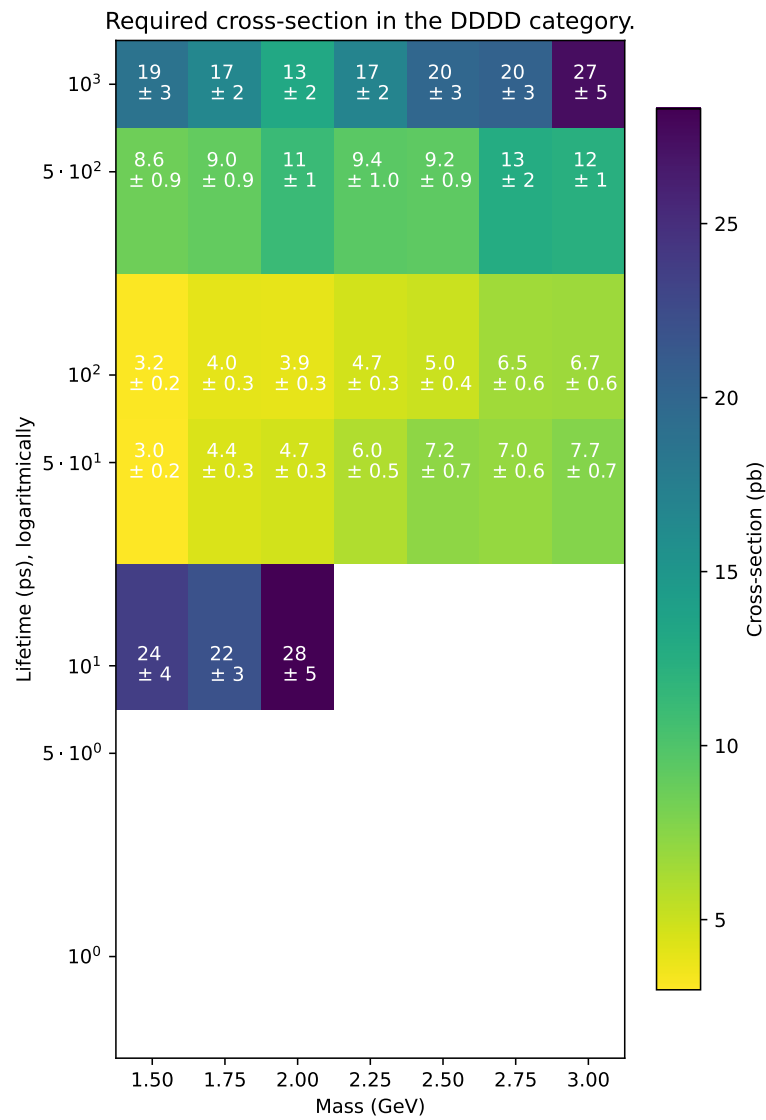
Figure A.39: *The required cross-section of the Higgs-like boson to have 50 dark pions in Run 2 for the 1250 GeV Higgs mass scenario in the DDDD category. The white cells are left out because there the number of dark pions passing from the simulation is less than 5 times its error. This plot is very similar to the 500 GeV mass DDDD result.*
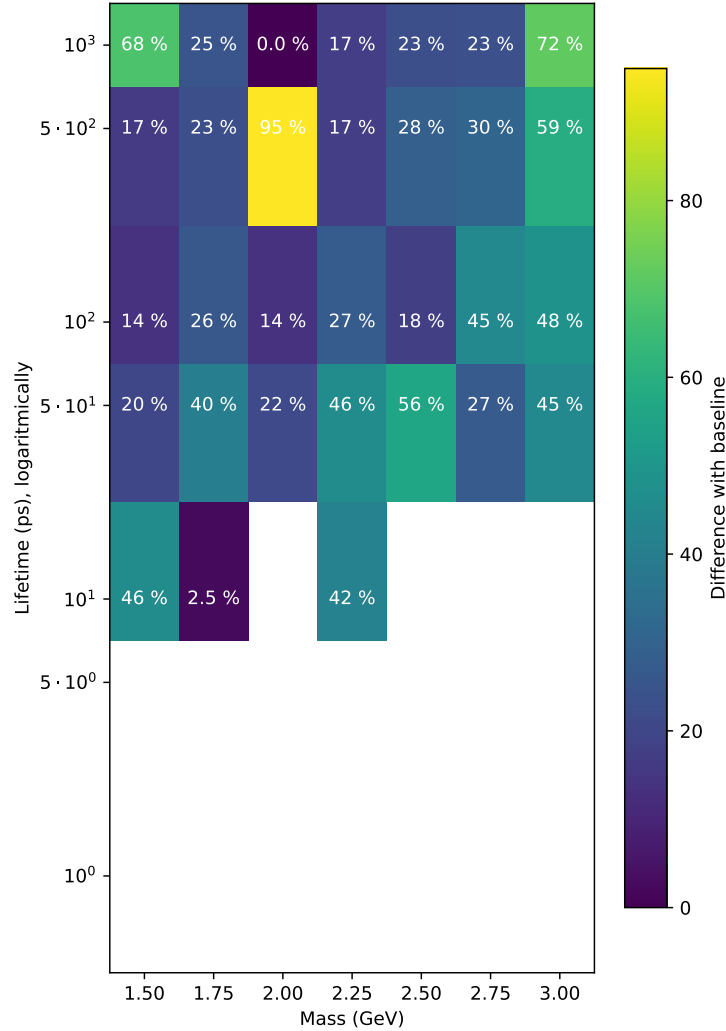
Figure A.40: *The percentual difference for the 1250 GeV Higgs mass scenario in the DDDD category. The whitespaces indicate the points left out because there the number of dark pions passing from the simulation is less than 5 times its error in the baseline model. This plot is very similar to the 500 GeV mass DDDD result, but has higher percentages.*

Indication of total sensitivity

This appendix contains the figures of the sum of the expected number of particles in Run 2 in each category, for all scenarios (except for the Higgs mass scenarios, where we have the required cross-section for the sum of the number of particles passing from the simulation). These give us an indication of the total sensitivity of the LHCb detector.

These figures look somewhat similar to the LLDD results for each category, with the most particles passing at the smallest mass and lifetime. This is to be expected as both LLLL and LLDD peak there, and about the same number of particles is added by LLLL and DDDD to LLDD. The transitions between 10 and 50 ps, and 50 and 100 ps are less sharp though, as a lot of extra particles are added by DDDD there. Between 100 and 500 ps it is extra sharp now though, as LLDD only adds a significant amount of particles up to 100 ps and afterwards mostly just the DDDD numbers are left.

Overall, these results show that LHCb can cover lifetimes from $\mathcal{O}(1)$ to $\mathcal{O}(100)$ ps very well, with at least around 100 particles expected there.
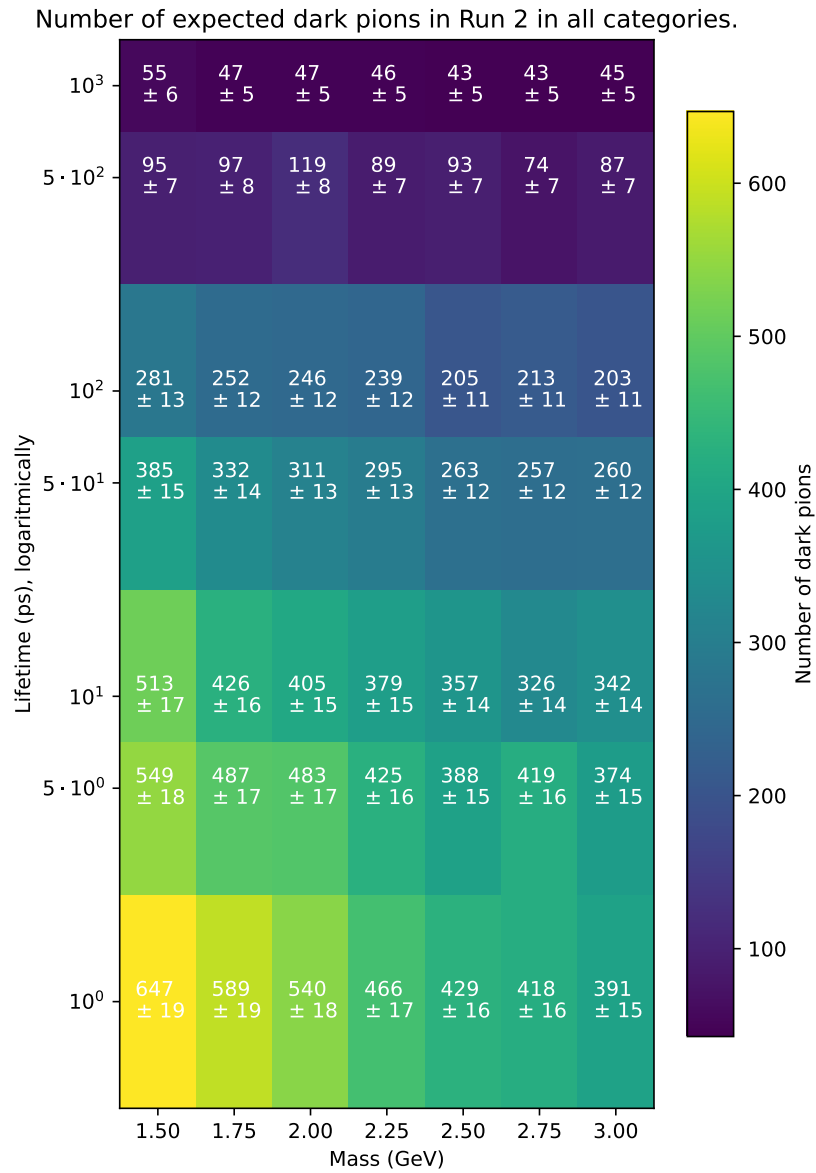
Figure B.1: *The combined number of expected particles in Run 2 for each category, for the baseline model.*
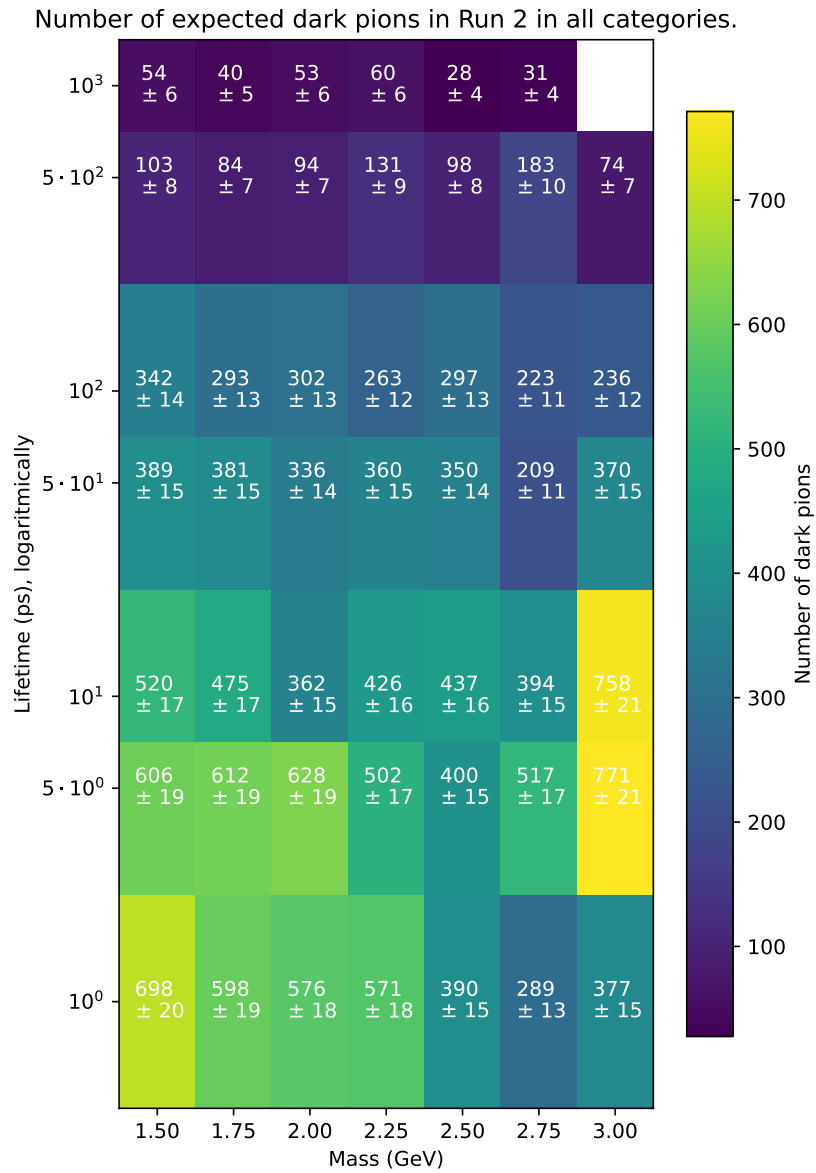
Figure B.2: *The combined number of expected particles in Run 2 for each category, for the dark rho scenario.*
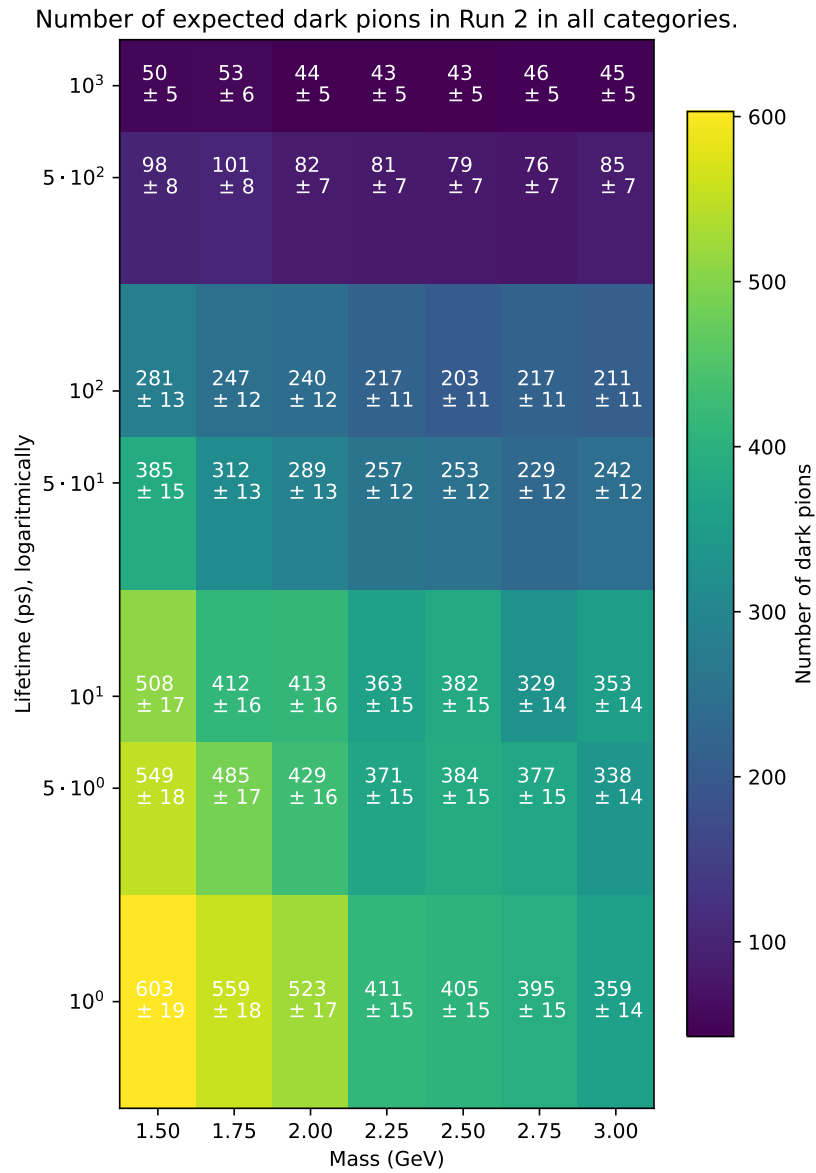
***Figure B.3:** The combined number of expected particles in Run 2 for each category, for the dark colour scenario.*
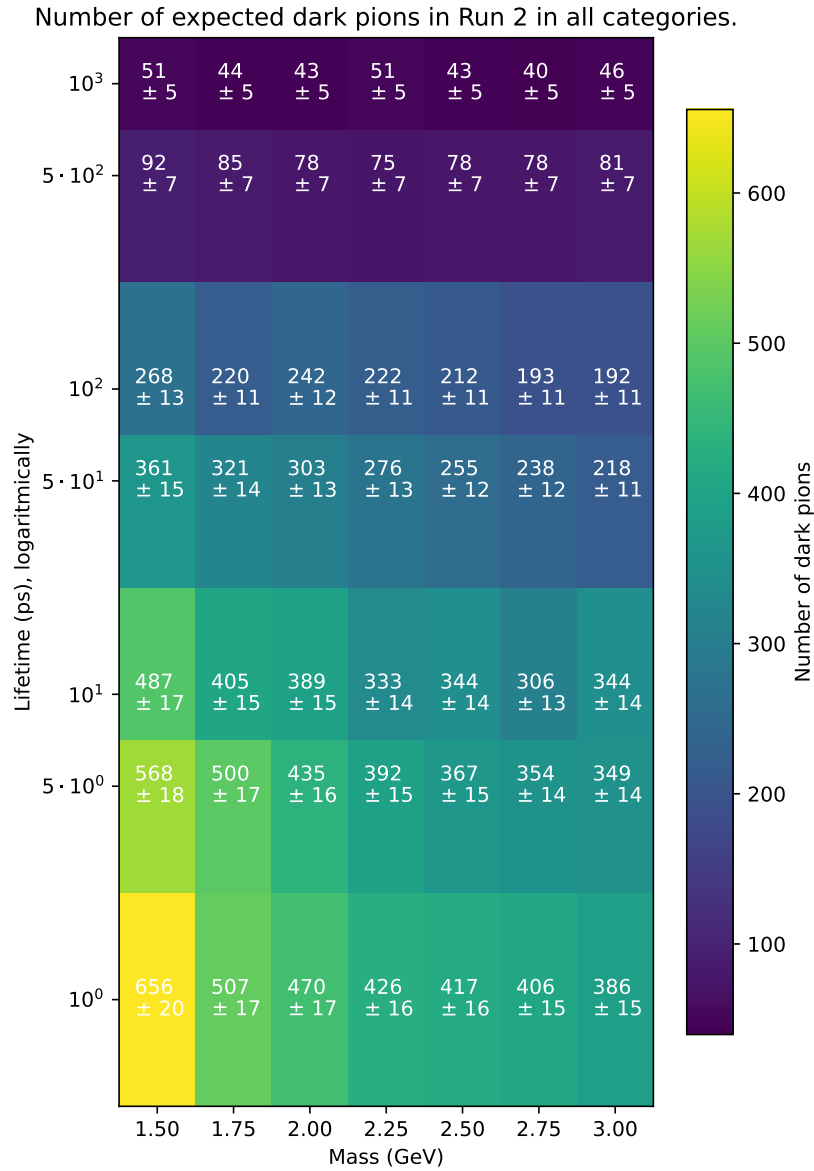
Figure B.4: *The combined number of expected particles in Run 2 for each category, for the dark QCD scale scenario, with $\tilde{\Lambda}_{\text{QCD}} = 8$ GeV.*
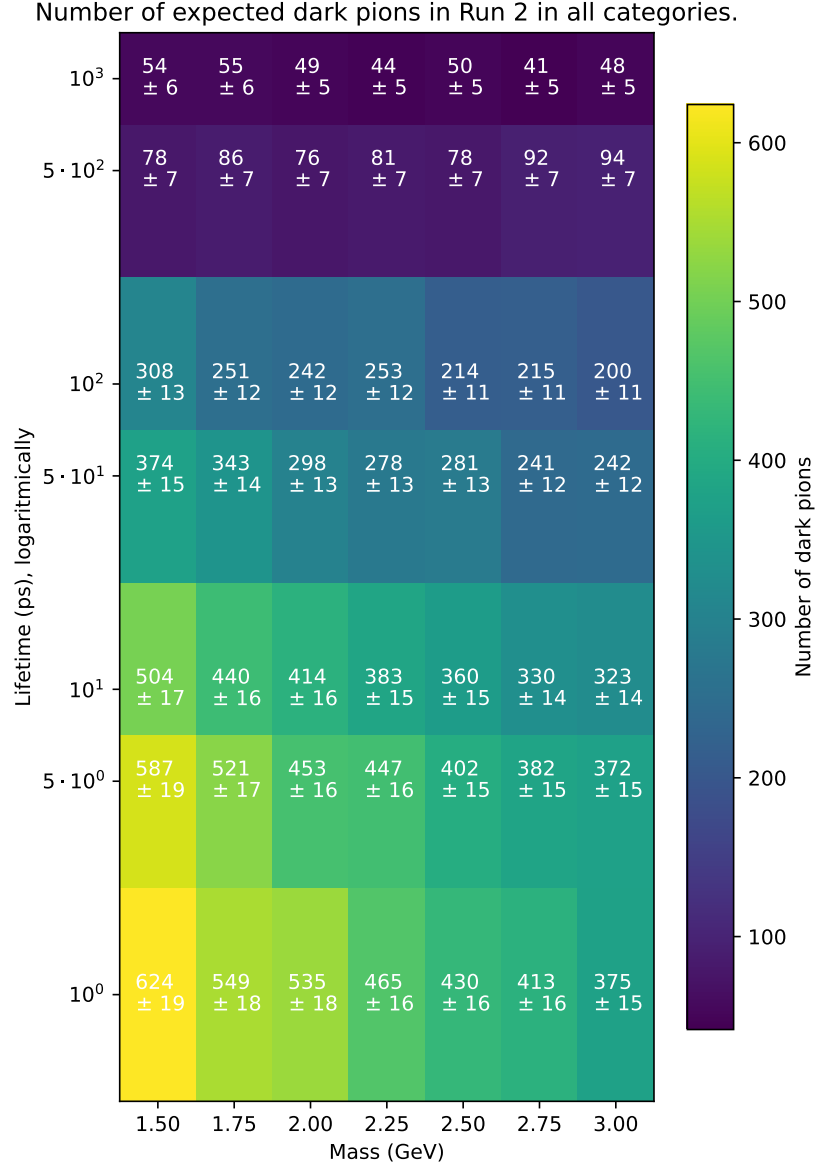
Figure B.5: *The combined number of expected particles in Run 2 for each category, for the dark QCD scale scenario, with $\tilde{\Lambda}_{\mathrm{QCD}} = 2$ GeV.*
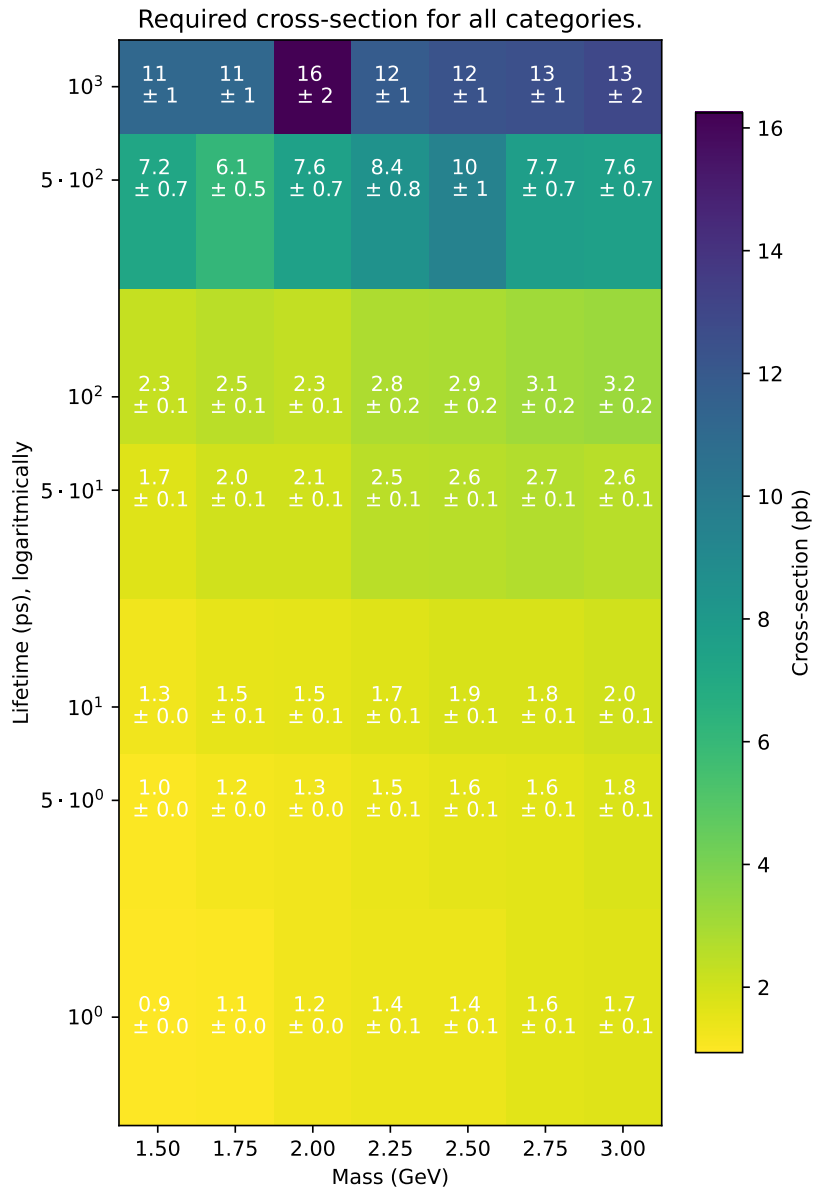
Figure B.6: *The required cross-section for the combined number of particles passing in the simulation for each category, for the Higgs mass scenario, with 500 GeV mass.*
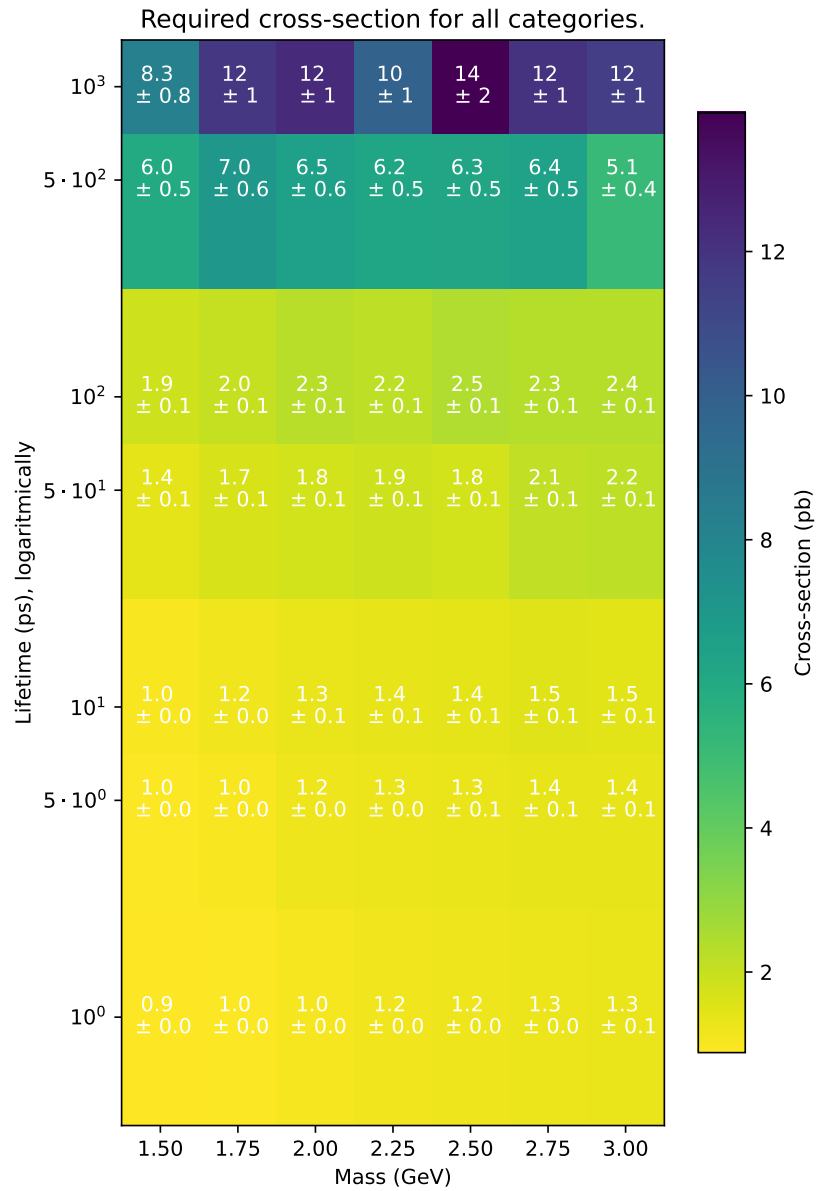
Figure B.7: *The required cross-section for the combined number of particles passing in the simulation for each category, for the Higgs mass scenario, with 50 GeV mass.*
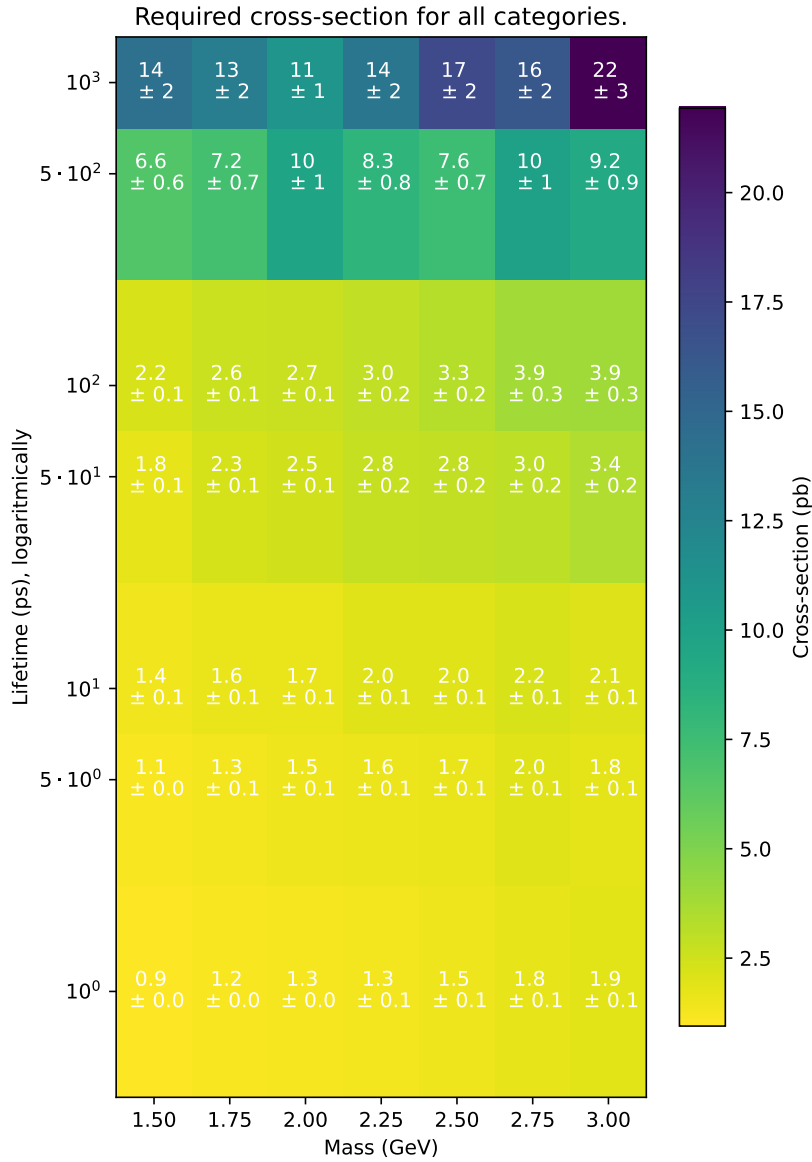
Figure B.8: *The required cross-section for the combined number of particles passing in the simulation for each category, for the Higgs mass scenario, with 1250 GeV mass.*